The function of the *ASYMMETRIC LEAVES1* gene in *Arabidopsis* organ development

Ross N. Barley

Doctor of Philosophy

University of Edinburgh

2001

Contents

Acknowledgements

This project could not have been achieved without the help and advice of many people. Firstly I thank the members of the Hudson and Goodrich labs, past and present, for their help and encouragement in the workplace. Many thanks to Andrew and Richard in particular for all their assistance, direction, advice, enthusiasm and wit. A big thank you to all the friends I have been fortunate enough to make during my time in Edinburgh, Jess certainly deserves a mention. The people who I especially devote this to are my mother and father, and Emma, without whose love during this time there would have been no hope of completion, confidence, and importantly, sanity.

Publication

The major findings of this thesis appear in the following publication, which is bound inside the back cover:

Mary E. Byrne, Ross Barley, Mark Curtis, Juana Maria Arroyo, Maitreya Dunham, Andrew Hudson and Robert A. Martienssen. (2000). *Asymmetric leaves1* mediates leaf patterning and stem cell function in *Arabidopsis*. *Nature* **408**, 967-971.

Abstract

Much of a plants architecture is formed postembryonically by shoot apical meristems (SAMs). SAMs produce lateral organs such as leaves from their flanks whilst maintaining a pool of undifferentiated cells centrally. *knox* genes are expressed in the SAM but are downregulated in organ founder cells at the time of initiation. The *knox* genes are implicated in maintaining division or preventing differentiation of SAM cells. Loss-of-function mutations in *knox* genes are associated with defects in meristem maintenance. Gain-of-function mutations resulting in ectopic *knox* expression disrupt normal organ development.

PHANTASTICA (*PHAN*) in *Antirrhinum* and *ROUGHSHEATH2* (*RS2*) in maize encode MYB transcription factors that accumulate in initiating organs and negatively regulate *knox* genes. *phan* mutants show variable defects in leaf patterning, affecting both proximodistal and dorsoventral axes whilst *rs2* mutations resemble dominant mutations in *knox* genes. A homologous protein is encoded by *AtPHAN* in *Arabidopsis*. *asymmetric leaves1* (*as1*) is a recessive mutation in *Arabidopsis* that disrupts development of cotyledons, leaves, and floral organs and shares lobing characteristics with transgenic plants misexpressing *knox* genes. *AtPHAN* was found to correspond to *as1* by PCR analysis and complementation.

AS1 was found to be expressed in initiating organs throughout *Arabidopsis* development in a domain complementary to *knox* genes. Molecular and genetic epistasis experiments showed that *AS1* negatively regulates the *knox* genes *KNAT1* and *KNAT2* in organs. In turn the *knox* gene *SHOOTMERISTEMLESS* downregulates *AS1* expression in the meristem. This genetic pathway defines a mechanism for distinguishing between organ founder cells and meristem cells at the shoot apex and demonstrates that genes expressed in organ primordia interact with meristem genes in regulating morphogenesis.

Introduction

Arabidopsis thaliana as a model plant system

Arabidopsis thaliana is an annual cruciferous weed related to mustards and cabbages. It has been the object of genetic and molecular studies for over 50 years (Martienssen and McCombie, 2001) and the complete 125 Mb genome sequence was published last year (Arabidopsis Genome Initiative, 2000). As a result, *Arabidopsis* has been used as an ideal model plant to study developmental genetics. The field of research investigating mechanisms of gene regulation at the growing shoot tip has continued to expand and a more detailed picture is beginning to emerge. Development of the aerial parts of higher plants depends on the activity of meristems, regions that are situated at the apex of the shoot above the most recently formed leaf and are able to continuously initiate new organs at their flanks. Meristems have a dual role in acting as both a self-perpetuating stem cell system and as a 'factory' for the production of organs. This piece of work describes attempts to further investigate the control of plant organogenesis using *Arabidopsis*. First a brief overview of *Arabidopsis* development is given followed by a review, including classic and recent evidence, of genetic control of the shoot apical meristem and organ initiation.

Embryogenesis

The basic body plan of the mature *Arabidopsis* plant is generated during embryogenesis (Jürgens *et al.*, 1991; Mayer *et al.*, 1991). This includes production of both shoot and root meristems, cotyledons, radicle and hypocotyl, that result in the establishment of the apical-basal axis of the plant and also formation of the radial pattern elements of epidermis, ground tissue and vasculature. Stages of embryogenesis have been defined according to the number of cells derived from an early apical cell, which gives rise to all the embryo except for the root, and according to the shape of the developing embryo. These stages are: zygote, two-terminal cell, quadrant, octant, dermatogen, globular, transition, heart, torpedo, walking-stick and upturned-U (Figure 1.1).

During the transition stage of embryo development, the two cotyledon primordia become apparent through cell divisions at the embryo apex. These divisions are rapid and lead to the heart-stage embryo. During heart-stage, the enlarging cotyledon primordia and cell divisions and cell elongation in the hypocotyl and radicle (root primordium) cause the embryo to assume an elongate shape known as the torpedo stage. At this stage provascular tissue starts to differentiate at the base of the cotyledons.

The shoot and root meristems, ultimately responsible for the postembryonic architecture of the plant both have their origins in embryogenesis. However the timing of their initiation differs - the root meristem is formed by the mid-heart stage and the shoot meristem arises later, during the torpedo-stage of development. The shoot meristem is derived from a subset of cells of the upper half of the globular-stage embryo (Bowman, 1994). During transition from the heart-stage to the torpedo-stage embryo, three distinct layers of cells overlying a core of provascular cells become recognisable in the apical hemisphere of the developing embryo between the enlarging cotyledons (Barton and Poethig, 1993). The upper two layers, L1 and L2, form the tunica and the lower L3 layers form the corpus of the shoot meristem. During the torpedo-stage embryo, the cell division patterns of the shoot meristem are characteristic of a tunica-corpus organisation (Barton and Poethig, 1993) - this is described later in *The Shoot Apical Meristem*.

Later stages of embryogenesis are characterised by cell differentiation and an increase in embryo size. An increase in cotyledon size, primarily due to cell division, results in the cotyledons bending back over the rest of the embryo in the walking-stick stage. Further cell expansion results in the embryo forcing into the surrounding endosperm and cotyledons fully bending over, forming the upturned-U embryo. Continued cell expansion throughout the embryo causes it to occupy most of the embryo sac, crushing the endosperm and absorbing it (Mansfield and Briarty, 1992).

Figure 1.1 Stages of *Arabidopsis* embryogenesis
(**A**) One-cell embryo after the first division of the zygote, which forms the apical and basal cells. (**B**) Two-cell embryo. (**C**) Eight-cell embryo. (**D**) Early globular stage. (**E**) Early heart stage. (**F**) Late heart stage. (**G**) Torpedo stage. (**H**) Mature upturned-U embryo. Diagram from West and Harada, 1993.

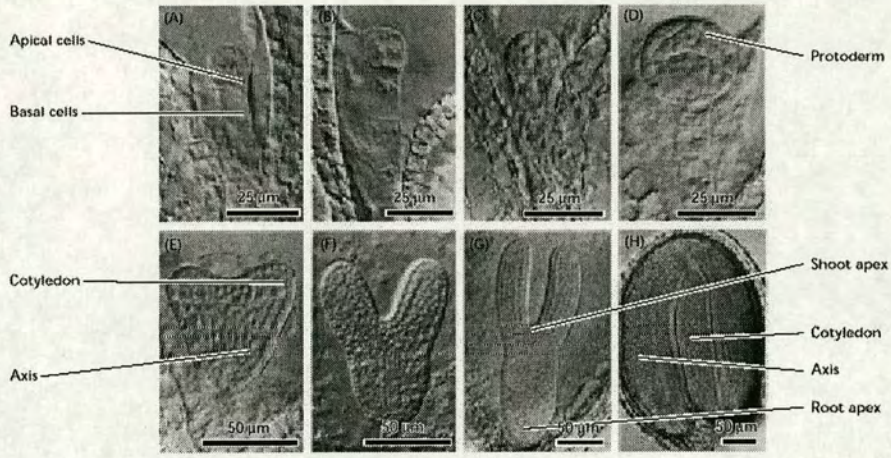

By maturity, a single layer of endosperm remains within the outer seed coat, or testa, which is derived from the two integuments. In the mature embryo the shoot apical meristem consists of approximately 60-80 cells in total (Bowman, 1994). The time from fertilisation through to desiccation of the seed varies with genotype and environmental conditions. The mature desiccated embryo is induced under favourable conditions to germinate and postembryonic growth begins.

Vegetative Development

After germination of the seed, the vegetative shoot apical meristem (SAM) of *Arabidopsis* produces rosette leaves in a phyllotactic spiral. Typically by day 4 postgermination, the first two leaf primordia develop in a plane 90° from that of the cotyledons. Initially the leaf primordia form as approximately radially symmetric structures on opposite sides of the SAM and are ~35 μm in size (Bowman, 1994). Between days 5 and 6 postgermination, the primordia of the first pair of leaves enlarge to approximately 105 μm and begin to adopt a dorsoventral asymmetry. Trichomes, unicellular hairs of unknown function, become apparent on the distal adaxial leaf surface. Paired leafy appendages, the stipules, enlarge at the base of the primordia. At this stage the meristem appears fairly flat in shape. By day 7 postgermination, the SAM begins to enlarge, becoming a radially symmetric structure of approximately 450 cells. Leaves 3 and 4 initiate in the phyllotactic spiral, which can be either clockwise or anti-clockwise. Growth conditions affect the number of rosette leaves formed by the plant before entering the reproductive phase. Low growth temperature and short days retard the transition to flowering and generate an increase in the number of rosette leaves formed (Bowman, 1994). A varying leaf number is also found between different *Arabidopsis* ecotypes. The rosette leaf number may be as low as 5-8 for early flowering ecotypes under long days and more than 30 for late flowering ecotypes.

Development of the leaf itself is marked by cell division and elongation. In the first pair of leaves, the differentiation of the mesophyll tissue into palisade and spongy mesophyll is evident by day 6 postgermination. Dorsoventral differences continue

to emerge, by day 8 a distinct layer of palisade mesophyll cells exists beneath the adaxial epidermis of the leaf. A few vacuolated cells are restricted to the epidermis and cells between the developing vascular bundle and abaxial epidermis. Trichomes also continue emerging from the adaxial epidermis. A developmental gradient exists across the proximodistal axis of a 9 day old leaf. Whilst in the proximal part of the leaf, cells are largely still mitotic (small, undifferentiated and still dividing), more distal cells are differentiating and undergoing expansion. The transition from the mitotic phase to the expansion phase is marked by the appearance of vacuoles. From day 9 through day 20, cell expansion is the most important parameter in terms of increasing leaf size. Lateral expansion of the lamina continues until day 18, although the increase in thickness of the lamina continues until day 20.

At the transition to reproductive growth, the vegetative SAM becomes an inflorescence meristem and produces the primary inflorescence shoot. The vegetative meristem is apparently converted directly into an inflorescence meristem. Only the identity of the lateral structures formed on the flanks of the meristem appears to differ - cauline leaves and flowers replace rosette leaves. After the inflorescence meristem has produced the first few flower primordia, increased elongation of the internodes between the uppermost leaves and between flowers gives rise to the inflorescence shoot, which is also termed a bolt. The basal positions on the primary inflorescence shoot are occupied by a small number of cauline (stem) leaves and the apical positions by a potentially indeterminate number of flowers formed by the inflorescence meristem. Secondary inflorescence meristems that develop in the axil of each cauline leaf of the primary inflorescence shoot reiterate the same pattern of development. Similarly, tertiary inflorescence shoots arise in the axils of the cauline leaves on the secondary inflorescence shoots. Further inflorescence meristems develop in a basipetal manner in the axils of the rosette leaves. The rosette leaves, cauline leaves and flowers of *Arabidopsis* all arise in the same phyllotactic spiral.

Floral Development

Flowers derive from determinate floral meristems produced on the flanks of the inflorescence meristem. Floral organ primordia develop in a well defined pattern, sequentially from the floral meristem. Four concentric whorls of organs initiate, each organ type occupying a different whorl, separated by short internodes. A whorl of sepals initiate first followed by petals, stamens and finally carpels. While both the vegetative and inflorescence meristems are indeterminate, the floral meristem is determinate in that it forms a fixed number of whorls of organs. The reproductive organs of the flower, the stamens and carpels occupy the last two whorls initiated.

Each flower normally consists of fifteen floral organs that arise sequentially on the flanks of the floral meristem in a well defined pattern. The *Arabidopsis* flower has a calyx of four sepals and a corolla of four petals, the positions of which are alternate and interior to those of the sepals. Four medial, long stamens and two lateral, short stamens comprise the androecium. The anthers of the stamens dehisce longitudinally and mediate self-fertilisation. In the centre of the flower the gynoecium consists of two fused carpels, its two locules separated by a false septum. Ovules arise from placental tissue either side of the septum. Following the specification of floral organ identity, each primordium follows a developmental program specific to organ-type, with differentiation into both organ-specific cell types and common cell types.

The Shoot Apical Meristem

Stem cells in the centre of the shoot meristem are the source from which all tissues of the growing shoot are ultimately derived. Maintenance of a functional meristem requires a co-ordination between stem cell divisions and loss of cells by differentiation and incorporation into stem and lateral organs. In *Arabidopsis* cells of the tunica, the L1 and L2, divide nearly exclusively anticlinally, except when organ primordia are initiated by periclinal divisions in the L2 (Vaughan, 1955). The progeny of a cell in the L1 will therefore remain in this meristem layer and may eventually differentiate as an epidermal cell. Cells of the underlying L2 will form one or more subepidermal cell layers, and cells that will give rise to the gametes. Below these tunica layers, cell divisions are not oriented and the L3, or corpus, will give rise to the pith and the vascular system through random cell divisions that are anticlinal and periclinal.

This definition of a meristem comprising separate clonal cell layers is suggestive of shoot development functioning as a result of cell-lineage-dependent mechanisms. However, studies using genetic mosaics have shown that a cell's clonal origin does not ultimately determine its fate. Cells in layers of the SAM do not possess fixed developmental fates and all three layers contribute to organ formation and growth of the stem (Dermen, 1953). This suggests that communication between cell layers that specify positional cues is required for the co-ordination of cell proliferation and cell fate specification.

A classification of the apical meristem into distinct zones based upon cell size, cell division rates and density of histological staining also exists - Figure 1.2 (Vaughan, 1955; Steeves and Sussex, 1989; Laufs *et al.*, 1998a). In this organisation, the shoot meristem is divided during embryogenesis into a central zone at the summit of the convex dome, and a surrounding flanking region, or peripheral zone. These zones comprise all three clonal layers and differ in cell division rates; infrequent in the central zone and relatively high in the flanking peripheral zone. The cells of the peripheral zone also stain more deeply than

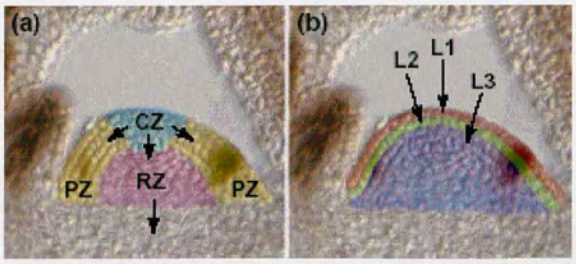

Figure 1.2 The *Arabidopsis* Shoot Apical Meristem (SAM)

(**a**) shows the central zone (CZ - blue) that harbours pluripotent stem cells and replenishes both the peripheral zone (PZ - yellow) and the rib zone (RZ - pink) as indicated by arrows. Lateral organs are produced from cells recruited from the PZ, whereas the bulk of the stem is derived from cells recruited from the RZ (arrow). (**b**) shows the three clonally distinct layers of the SAM; L1 - red, L2 - green, and L3 - violet. Expression of the *FILAMENTOUS FLOWER* (*FIL*) gene in (**a**) and (**b**) demarcates lateral organ initiation in the PZ and abaxial domains of leaf primordia - diagram taken from Bowman and Eshed (2000).

those of the central zone. The central zone harbours the pluripotent stem cells responsible for maintaining both the peripheral zone and underlying 'rib' zone that gives rise to the pith of the stem. In addition to the stem, all lateral organs and floral meristems are formed exclusively from cells in the peripheral zone. Therefore one interpretation of meristem maintenance is that all organs are inhibited from initiating within the central zone.

In the apical meristem, cells are interconnected via plasmodesmata, cytoplasmically continuous (symplastic) channels that exchange small molecules. Restriction of small potential morphogens or transcriptional regulators may be confined to certain cells that fall within the boundaries of either central or peripheral zones (Gisel *et al.*, 1999). Signalling within and between symplastic fields in *Arabidopsis* could be used to co-ordinate morphogenetic events and meristem maintenance.

Functional Domains of Shoot Apical Meristems

Discussion of SAM organisation in terms of physical properties is perhaps limited to an extent. In recent years an increasing number of genes have been isolated in various angiosperms that control the establishment and maintenance of the SAM. Gene expression patterns have revealed new functional domains that exist in the SAM as well as marking existing domains. The complexity of SAM organisation is still being revealed and many questions remain. What are the genes and gene products? How do they interact with each other? What are the genetic pathways that regulate SAM maintenance and replenishment? How is organ formation regulated and what communication is there between the SAM and initiating organ primordia? Many of these regulatory genes encode putative transcription factors that are expressed in subdomains of the SAM. Once initiated during embryogenesis, their expression domains often persist with little or no spatial change throughout all developmental stages. However, because a cell changes its position in the meristem during growth, it may adopt a new and different gene expression profile. This indicates that within meristems, cell fate is position-dependent rather than lineage-dependent.

During the life of a plant, cell loss in the peripheral zone of the meristem due to organ initiation is compensated by divisions of stem cells in the central zone and cell displacement in the periphery. The first insights into the mechanisms that control this process came from studies of mutations that disrupt meristem organisation. Loss-of-function mutations in the *CLAVATA* (*CLV*)*1*, *2* or *3* genes of *Arabidopsis* cause an accumulation of undifferentiated cells in the centre of shoot and floral meristems, resulting in a size increase of the meristem, fasciation of the shoot, and the initiation of supernumerous floral organs (Leyser and Furner, 1992; Clark *et al.*, 1993; Clark *et al.*, 1995; Kayes and Clark, 1998). The extra organs produced reflect an increased peripheral zone, a direct effect of the enlarged central zone. Floral meristems of *clv* mutants maintain more stem cells and produce extra carpels that form large club-shaped siliques. Genetic analysis using double mutants suggested that the *CLV1*, *2*, and *3* gene products function in the same pathway to restrict stem cell fate or division in the meristem (Clark *et al.*, 1995; Kayes and Clark, 1998).

The cloning of all three *CLV* genes enabled analysis of their expression patterns and function in controlling stem cell fate in the *Arabidopsis* meristem. *CLV3* mRNA is found primarily in the L1 and L2 layer of the central zone of shoot and floral meristems, marking the presumed position of pluripotent stem cells (Fletcher *et al.*, 1999), whilst *CLV1* RNA is mostly located in the underlying L3 (Clark *et al.*, 1997). *CLV2* is found in a larger domain of expression that includes all shoot tissues (Jeong *et al.*, 1999). Both the *CLV1* and *CLV2* genes encode leucine-rich repeat (LRR) transmembrane proteins and *CLV1* has a cytoplasmic kinase domain (Clark *et al.*, 1997; Jeong *et al.*, 1999). *CLV3* encodes a small protein that is likely to be secreted (Fletcher *et al.*, 1999), and biochemical experiments showed that *CLV3* acts as a ligand that binds and thereby activates a heterodimeric receptor kinase consisting of *CLV1* and *CLV2* (Jeong *et al.*, 1999). Therefore, *CLV3* might act as a signal, secreted from outer meristem cell layers, that binds to a receptor complex consisting of *CLV1* and *CLV2* in deeper cell layers. The receptor complex, which localises to the plasma membrane, may then trigger a signal transduction

cascade, but what are the ultimate targets and how do they regulate meristem organisation?

The *WUSCHEL* (*WUS*) gene of *Arabidopsis* promotes stem cell fate and is expressed in the L3 layer of shoot and floral meristems (Mayer *et al.*, 1998). *wus* mutants fail to initiate or maintain an active stem cell population in meristems - cells in the central zone differentiate prematurely and meristems are not maintained. Mutations in *WUS* therefore have opposite effects to *clv* mutations suggesting that *WUS* promotes stem cell fate in the central zone of the meristem. *WUS* encodes a homeodomain transcription factor that becomes restricted to a small group of cells directly beneath the stem cell zone at an early stage of embryo development. Its expression persists in this domain in meristems throughout development (Mayer *et al.*, 1998). Ectopic *WUS* expression in transgenic *Arabidopsis* leads to accumulation of stem cells as in *clv* mutants (Schoof *et al.*, 2000) suggesting that *CLV* genes might act to repress *WUS*. Double mutants of *wus* and *clv* resemble *wus* single mutants (Laux *et al.*, 1996; Schoof *et al.*, 2000) raising the possibility that *WUS* might also promote *CLV* expression.

Ectopic expression of *WUS* induces *CLV3* expression, indicating that *WUS* acts to promote *CLV3* expression (Schoof *et al.*, 2000 - see Figure 1.3). An interpretation of the *clv* phenotype is that these mutants fail to repress *WUS* activity; indeed *WUS* RNA is seen to expand laterally and apically in *clv* mutant meristems. By contrast, ectopic *CLV3* expression reduces the size of the *WUS*-dependent stem cell population. These findings suggest that CLV signalling represses *WUS* expression. It is unclear how the *WUS* gene promotes stem cell fate if it is not expressed in stem cells. The *WUS* gene product or perhaps a downstream target of *WUS* may act non-cell autonomously possibly moving apically through plasmodesmata. This current model begins to explain how a balance may be maintained between stem cell proliferation and stem cell loss due to peripheral zone displacement supplying organ production. Whilst this research is beginning

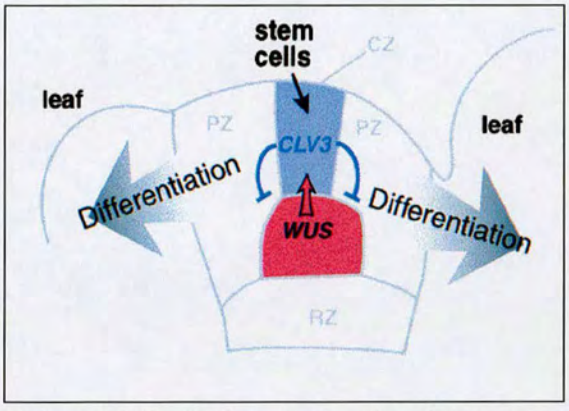

Figure 1.3 Model for stem cell maintenance
Stem cell identity in the central zone, marked by *CLV3* expression (blue), is specified by signalling (red arrow) from an underlying organising centre (red) requiring *WUS* activity. Stem cells are able to restrict *WUS* activity via CLV signalling (dark blue). This regulatory feedback loop maintains the size of the stem cell population in the SAM whilst cells that pass beyond the domain of *CLV* expression become incorporated into organs. **CZ**, central zone; **PZ**, peripheral zone; **RZ**, rib zone - diagram taken from Schoof *et al.* (2000).

to answer some of the questions of how the meristem is maintained and replenished, obvious questions remain. Presumably, communication through genetic pathways is likely to exist between the sites of organ initiation, the organ founder cells, and the stem cell population in order to maintain normal growth. However, such regulating factors have yet to be identified in *Arabidopsis*.

In *Arabidopsis*, a gene that is a requirement for SAM maintenance, *SHOOTMERISTEMLESS* (*STM*), encodes a homeodomain containing protein (Long *et al.*, 1996). *STM* belongs to a wider family of homeobox genes in plants that are collectively termed *knox* genes, of which the class I *knox* genes appear to be exclusively expressed in shoot meristems (Reiser *et al.*, 2000). In an *stm* mutant seedling, partly-fused cotyledons are produced and there is a lack of a meristem capable of normal postembryonic growth except for occasional ectopic organ production (Barton and Poethig, 1993; Endrizzi *et al*, 1996). Similarly, recessive mutations in the maize *knox* gene *KNOTTED1* are also defective in meristem maintenance (Vollbrecht *et al.*, 1991; Kerstetter *et al.*, 1997). *STM* RNA is first expressed in one cell at the apex of late-globular stage embryos and becomes restricted to cells of the presumptive SAM (Barton and Poethig; 1993; Long and Barton, 1998). Expression of *STM* persists throughout vegetative and floral meristems, in both central and peripheral zones, although it is not present in the initial cells of newly initiating organ primordia.

The expression pattern of *STM* suggests that its role may be to inhibit differentiation and therefore organ production, and/or to implement SAM-specific gene expression and maintenance. One interpretation of the *stm* phenotype suggests that, in the absence of *STM* activity, a meristem is never formed. This would suggest that *STM* is necessary for the implementation of a SAM-specific program of development through the activation of several SAM-specific genes. However, in *stm* mutant apices SAM-specific *CLV1* and *WUS* expression is initiated normally (Long and Barton, 1998). Alternatively, *STM* may be necessary to prevent precocious determination of the meristem after initiation, since the meristems of weak *stm* alleles terminate prematurely (Clark *et al.*, 1996). However,

there is evidence that suggests *STM* is necessary to prevent organ fate in the SAM. Partly fused cotyledons are observed in *stm* mutant apices and, in weak *stm* mutants ectopic leaves are formed, suggesting that meristem cells are actively recruited into organs (Long *et al.*, Endrizzi *et al.*, Clark *et al.*; 1996). Similarly, most *Arabidopsis pinhead* (also known as *zwille* [*zll*]) mutant embryos fail to establish a functional SAM and instead differentiate a leaf-like organ in its place (Endrizzi *et al.*, 1996; Moussian *et al.*, 1998). *pnh* mutant embryos fail to maintain *STM* expression suggesting that loss of *STM* expression results in a change from meristematic to organ cell fate (Lynn *et al.*, 1999). Ectopic leaves and carpels are also observed with loss-of-function mutations in the *KNOTTED1* gene of maize (Kerstetter *et al.*, 1997). Together these findings suggest that *STM* may function by preventing incorporation of cells in the meristem centre into differentiating organ primordia and that this role may account for all defects observed in *stm* mutants.

Currently, evidence for interactions of *STM* are not very clear. *STM* may act as a positive regulator of *WUS* based on double mutant phenotypes (Endrizzi *et al.*, 1996). In relation to this *clv* mutations are seen to enhance meristem activity in *stm* mutants (Clark *et al.*, 1996). However, in *clv stm* double mutants an embryonic SAM is not restored suggesting that the *CLV* genes may only be required to limit the size of the stem cell population which in *stm* mutants never forms initially.

Meristem and Organ Boundaries

The molecular mechanisms that regulate organ separation are thought to involve genes that are expressed at the boundary of the SAM and organ founder cells during development. The *Arabidopsis UNUSUAL FLORAL ORGANS* (*UFO*) gene is expressed in embryonic, vegetative, inflorescence and floral meristem where it is found at low levels in the centre of the SAM and at higher levels towards the periphery of the SAM (Lee *et al.*, 1997; Long and Barton, 1998). The *ufo* mutant phenotype suggests that, in addition to a role in controlling floral meristem identity, *UFO* has a role in specifying the boundaries between floral organs (Wilkinson and

Haughn, 1995; Levin and Meyerowitz, 1998). In embryos, *UFO* expression appears to be dependent upon *STM*, defining a link between meristem and boundary genes (Long and Barton, 1998).

The *CUP SHAPED COTYLEDON1,* and *2* (*CUC1*, and *2*) genes of *Arabidopsis* both encode NAC-domain proteins that are also expressed in the presumptive SAM during embryogenesis (Aida *et al.*, 1999; Takada *et al.*, 2001). *CUC2* is expressed later in development between the vegetative meristem and leaf primordia, between the inflorescence meristem and floral meristems, and between floral organ primordia (Ishida *et al.*, 2000), *CUC1* is also expressed at the boundaries between floral organ primordia (Takada *et al.*, 2001). *CUC1* and *CUC2* are functionally redundant - *cuc1 cuc2* double mutant seedlings completely lack an embryonic SAM and the two cotyledons are completely fused along both edges to form a cup-shaped structure (Aida *et al.*, 1997). These observations indicate that *CUC1* and *CUC2* are required for embryonic SAM development and for specifying non-organ cell fates that keep cotyledons and floral organs from fusing with each other. *CUC1* and *CUC2* are thought to promote transcriptional activation of *STM* since accumulation of *STM* RNA does not occur in *cuc1 cuc2* double mutant embryos (Aida *et al.*, 1999). In addition, ectopic *CUC1* expression also induces *STM* expression ectopically (Takada *et al.*, 2001). This suggests that *CUC1* and *CUC2* function upstream of *STM* and regulate SAM formation during embryogenesis.

Organ Initiation

The shoot apical meristem initiates organs from its flanks throughout the life of the plant. The SAM comprises stem cells at its centre and daughter cells at its periphery from which organ founder cells are recruited. Clonal analysis in tobacco demonstrated that all the major parts of the leaf (midrib, lamina and petiole) are specified from organ founder cells at some point after organ initiation (Poethig and Sussex, 1985). Organ founder cells divide rapidly initiating the outgrowth of organ

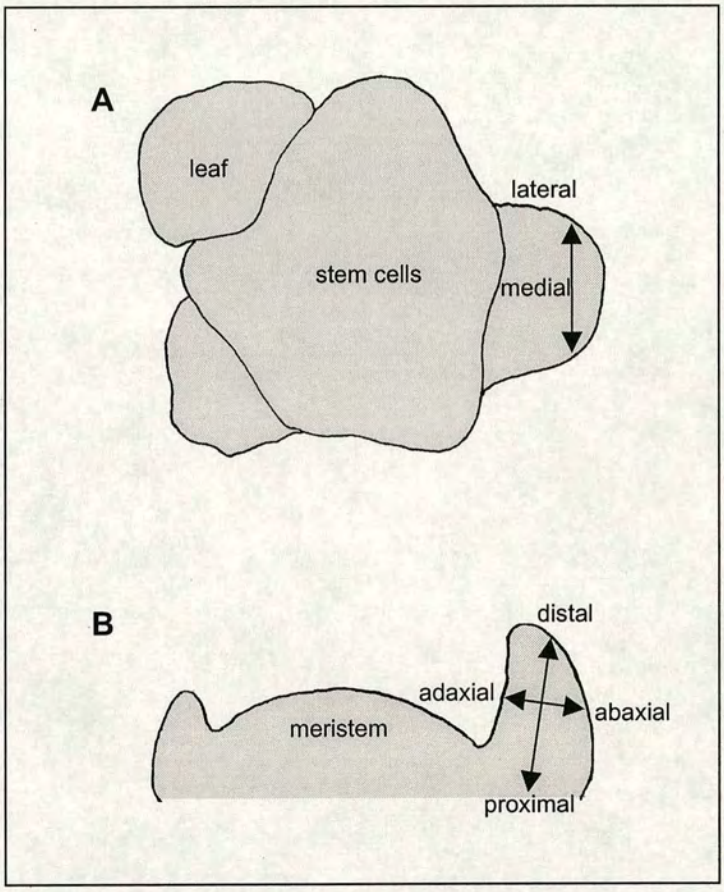

Figure 1.4 Axes of leaf growth
In (**A**) a graphical representation of a transverse section through a shoot meristem. Initiating leaf primordia are shown. An arrow indicates the mediolateral (medial/lateral) axis of a leaf primordium. In the longitudinal section (**B**) arrows indicate the proximodistal (proximal/distal) and the dorsoventral (adaxial/abaxial) axes of the leaf. Redrawn from Clark (2001).

primordia with polarity established along the proximodistal, dorsoventral and mediolateral axes (Martienssen and Dolan, 1998; Hudson, 2000 - see Figure 1.4).

Following cotyledon formation in *Arabidopsis*, leaf primordia emerge in a spiral phyllotaxis with each new leaf primordium initiated in a predictable regular pattern and within defined time intervals. The time interval between the initiation of two successive leaves is termed a plastochron and is useful as a guide for following the progression of leaf development. In addition the plastochron index describes the position of leaf primordia in relation to the meristem. A Plastochron 1 (P1) leaf is visible as a bump on the flank of the meristem. A P2 leaf is the next oldest leaf and so on, whereas a P0 leaf is not yet morphologically distinct from the rest of the meristem, but its position within the meristem can be predicted on the basis of the regular pattern of leaf initiation.

The molecular nature of the mechanisms that control phyllotaxis is not well understood. Recent studies suggest that organ positioning is regulated by the plant hormone auxin, which is thought to be synthesised in young apical tissues and transported downwards by a polar transport system (Reinhardt *et al.*, 2000; Vernoux *et al.*, 2000). In tomato apices, inhibition of auxin transport is able to specifically block primordia initiation but not meristem maintenance or stem growth (Reinhardt *et al.*, 2000). This phenotype is also observed in inflorescences of the *Arabidopsis pin1-1* mutant that has a defect in auxin transport caused by the inactivation of a putative membrane efflux carrier for auxin (Galweiler *et al.*, 1998). Furthermore, application of auxin to either pin-like tomato or *Arabidopsis* apices was observed to be sufficient for initiation of primordia at the site of application, at least in the radial dimension (Reinhardt *et al.*, 2000). Therefore, localised auxin concentration peaks may determine the sites of primordia initiation.

The first morphological sign of proximodistal axis formation is initiation of a primordium growing away from the SAM and stem axis and, therefore, the proximodistal axis appears to be specified in organ founder cells within the meristem. Unequal growth of the adaxial and abaxial sides of the primordium

(growth is faster on the abaxial side) causes the primordium to curve over the meristem. Later, growth is faster on the adaxial side of the primordium causing it to curve away from the meristem (Long and Barton, 2000). Polar differentiation then occurs along all axes to evolve the final flattened morphology of the leaf structure (reviewed by Harper and Freeling; 1996).

Alteration in cell division activity within the peripheral zone of the meristem leads to organ initiation. Periclinal cell divisions in the L2 of the presumptive primordium region are considered more important than an increase in cell division frequency in this process (Lyndon, 1982). Cell divisions could be completely suppressed in apical meristems of wheat, however characteristic bulges were still initiated on the flanks of the meristem that were typical of organ primordia, suggesting that their initiation did not require new cell divisions (Haber, 1962). Similarly, maize *crinkly4* and *tangled-1* mutants with compromised epidermal cell differentiation or altered division patterns of other cell layers are also capable of normal leaf initiation and morphogenesis (Becraft *et al.*, 1996; Smith *et al.*, 1996). Recent studies concerning the role of expansins suggests cell wall loosening in the L1 epidermal layer may be a major factor in the initiation of organs (Fleming *et al.*, 1997; Reinhardt *et al.*, 1998).

Genetic studies of early events in organ initiation have centred largely upon the monocot maize and dicots such as *Antirrhinum* and *Arabidopsis*. In grasses such as maize, the leaf emanates from founder cells that emerge from much of the SAM circumference. In maize, the *narrow sheath* mutation results in deletion of the leaf margins that is caused by failure to recruit the corresponding founder cells (Scanlon *et al.*, 1996; Scanlon and Freeling, 1997; Scanlon *et al.*, 2000). Therefore the *narrow sheath* mutant phenotype suggests that the lateral domains of maize leaves are specified within the SAM prior to leaf initiation.

A number of mutations in *Arabidopsis* are known that affect the size and shape of leaves without altering overall pattern. *ROTUNDIFOLIA* and *ANGUSTIFOLIA* are late acting and affect leaf shape as a result of changes in cell elongation (Tsuge

et al., 1996; Kim *et al.*, 1998). Similarly, although the *APETALA2* (*AP2*)-like *AINTEGUMENTA* gene encodes a transcription factor that is expressed in early leaf and other organ primordia throughout the plant, its role appears to be in maintenance of a proliferative cell state during organ development rather than control of initiation (Elliott *et al.*, 1996; Krizek, 1999; Mizukami and Fischer, 2000). *AP2* is also expressed in organ primordia throughout development although *ap2* mutants only show floral homeotic transformations of sepals and petals into stamens and carpels (Jofuku *et al.*, 1994). The *mgoun* (*mgo1* and *mgo2*) mutants of *Arabidopsis* produce a reduced number of leaves and floral organs and accumulate more cells in the peripheral zone of the SAM where organs form suggesting that the *MGOUN* genes may promote organ fate (Laufs *et al.*, 1998b).

The mechanism by which stem cell and founder cell derivatives are distinguished is obscure at present but is likely to involve the highly conserved *knox* genes. Perhaps the earliest known marker for organ initiation is the downregulation of *knox* transcripts from the flanks of the SAM (Reiser *et al.*, 2000). Although the negative regulation of these gene products may not be necessary for leaf formation itself to occur, changes in organ morphology as a result of *knox* misregulation are dramatic. In both maize and *Arabidopsis*, *knox* genes are normally expressed in the SAM and are downregulated in founder cells and leaf primordia (Jackson *et al.*, 1994; Long *et al.*, 1996). Recent research has implicated that transcriptional regulators are required to repress *knox* expression in lateral organs. *ROUGH SHEATH2* (*RS2*) in maize and *PHANTASTICA* (*PHAN*) in *Antirrhinum* are negative regulators of *knox* gene expression in leaves (Waites *et al.*, 1998; Timmermans *et al.*, 1999; Tsiantis *et al.*, 1999a). Ectopic expression of the *knox* genes *rs1*, *knotted1* and *liguleless3* can be detected only from P1 in *rs2* mutant leaf primordia (Schneeberger *et al.*, 1998). Therefore, in maize other factors such as *NARROWSHEATH* or *LEAFBLADELESS* may be required to repress *knox* genes earlier in organ development (Scanlon *et al.*, 1996; Timmermans *et al.*, 1998). *RS2* and *PHAN* encode MYB domain proteins that are closely related in sequence and are expressed in initiating leaf primordia. Loss-of-function mutations in *RS2* conditions proximal to distal transformations similar to

ectopic *knox* expression in maize leaves (Schneeberger *et al.*, 1998). *phan* mutants however display variable phenotypes with leaves becoming progressively more needle-like later in development (Waites and Hudson, 1995). These radial structures were observed to be completely ventralised and suggest perturbation of the dorsoventral axis although it is unclear if these phenotypes are conditioned by the effects of ectopic *knox* gene expression. A *PHAN*-like *MYB* gene is also found in *Arabidopsis*, *AtPHAN*, and might therefore have a similar role in the regulation of *knox* gene expression as its homologous counterparts in maize and *Antirrhinum* (Timmermans *et al.*, 1999).

Loss-of-function mutations (e.g. *stm*) implicate class I *knox* genes in determination of cell fate and patterning in the meristem (Reiser *et al.*, 2000). Also gain-of-function mutations or ectopic expression of *knox* genes result in profoundly altered organ morphologies. In *Arabidopsis*, two *knox* genes (*KNAT1* and *KNAT2* [also known as *ATK1*]), for *knotted*-like from *Arabidopsis thaliana*) are expressed in the SAM but excluded from young leaf primordia (Lincoln *et al.*, 1994; Dockx *et al.*, 1995). Leaves of plants that overexpress *KNAT1* display deep leaf lobing that initiates in the position of serrations, and also occasional ectopic meristems that form adaxially at the base of the lobes (Lincoln *et al.*, 1994; Chuck *et al.*, 1996). In tobacco, ectopic expression of *knox* genes driven by a constitutive promoter result in leaf phenotypes such as rumpling, reduced lamina, and formation of ectopic shoots on leaves (Sinha *et al.*, 1993). These transformations have in some cases been interpreted to disrupt patterning along the proximodistal axis of the leaf. The resulting leaves are highly dissected or lobed and show distal displacement of stipules that are normally found at the base of the leaf to regions between the lobes. Similar phenotypes have previously been observed in the *asymmetric leaves1* and *2* (*as1* and *2*) mutants of *Arabidopsis* (Rédei and Hirono, 1964; Tsukaya *et al.*, 1997).

Dorsoventral Patterning

Leaves are the major photosynthetic organs of plants and are suitably flattened perpendicular to their dorsoventral axis to efficiently utilise the sun's energy. Surgical experiments first demonstrated that interaction between the SAM and the developing leaf primordium is required to establish the dorsoventral axis and lateral outgrowth of the leaf (Sussex, 1954; Sussex, 1955, Snow and Snow, 1959). When incisions were made that separated incipient leaf primordia from the SAM, radial organs developed. Lateral organ development however was shown to be unaffected by disruption of central cells of the SAM which suggests that any interaction occurs between cells of the SAM periphery and the organ primordium. The *phan* mutant of *Antirrhinum* was the first mutant affected in dorsoventral patterning to be described in detail (Waites and Hudson, 1995). Grown at a restrictive temperature, the lower leaves of *phan* mutants form patches of abaxial tissue on the adaxial surface with ectopic lamina outgrowths at their boundaries (Waites and Hudson, 1995). Later *phan* leaves are radial and completely abaxialised. On the basis of these phenotypes, Waites and Hudson proposed that lamina outgrowth requires the juxtaposition of adaxial and abaxial domains and mutations that cause the loss of either domain therefore result in bladeless organs. In this respect *phan* mutants are unable to specify adaxial cell types and develop radial leaves that display abaxial cell types.

Similarly, in *Arabidopsis* the *phabulosa* (*phb-1d*) mutant forms adaxially radial leaves (McConnell and Barton, 1998). The *phb-1d* mutation is dominant and therefore the mutant phenotype might result in the constitutive activation of a gene sufficient for dorsal identity. However, *phb-1d* does not correspond to a mutation in *AtPHAN* since recombination between the loci on chromosome 2 was observed (Andrew Hudson, pers. communication). Recently, *PHB* was shown to encode a protein of unknown function containing a sterol/lipid binding domain and a DNA-binding motif (McConnell *et al.*, 2001). Therefore *PHB* may act as a receptor for an adaxialising signal (McConnell *et al.*, 2001). *PHB* is expressed throughout the P0 leaf primordium and becomes preferentially localised to the

adaxial leaf domain by the P2 stage suggesting that when first specified, the leaf primordium lacks molecular evidence of polarity (McConnell *et al.*, 2001).

Recent evidence suggests that organ primordia also promote SAM activity. *PHAN* is expressed throughout organ initials and early primordia and importantly is absent from meristem cells (Waites *et al.*, 1998). *phan* mutant meristems become quiescent at restrictive temperatures (Waites and Hudson, 1995). This appears to demonstrate that organ founder cells or primordia produce a *PHAN*-dependent signal required to maintain SAM activity (Waites *et al.*, 1998). Interestingly, in *phb-1d* mutants, axillary meristems are formed at the abaxial boundary between ectopic adaxial tissues and the stem (McConnell and Barton, 1998). This evidence suggests that adaxial organ identity might be necessary for normal axillary meristem formation.

A link between adaxial organ identity and meristem function is also suggested by mutations in two closely related genes, *PNH*, and *ARGONAUTE* (*AGO*) that encode proteins related to the eukaryotic translation factor eIF2C (Bohmert *et al.*, 1997; Moussian *et al.*, 1998). Although the genes encode members of the same family, *AGO* is expressed ubiquitously and *PNH* in vascular tissues and the adaxial side of leaves and the SAM (Moussian *et al.*, 1998; Lynn *et al.*, 1999). *PNH* is expressed throughout the P0 leaf primordium however adaxial accumulation of transcript occurs by the P2 stage (Lynn *et al.*, 1999). Although *AGO* is not specifically expressed in the adaxial domain of leaves its overexpression causes abaxial cells to assume adaxial fate, indicating that *AGO* is sufficient for adaxial fate. Interestingly, the *pnh/ago* double mutant embryos do not express STM protein, suggesting that *PNH/AGO* are required cell-autonomously for *STM* expression in the SAM or that *PNH/AGO* dependent adaxial fate is necessary for *STM* expression non-cell-autonomously (Lynn *et al.*, 1999). Evidence for this is observed in *phb-1d* ectopic axillary meristems whose formation is associated with upregulation of an *STM* reporter (Lynn *et al.*, 1999). However, it is not known yet whether this is a direct cause of *PNH/AGO* adaxial function in adjacent radial organs.

The *YABBY* gene family of *Arabidopsis* comprises at least six family members that are also involved in dorsoventral development. *YABBY* genes encode a zinc finger and a helix-loop-helix motif and are predicted to be transcriptional regulators (Bowman and Smyth, 1999; Sawa *et al.*, 1999; Siegfried *et al.*, 1999). Largely because of redundancy, mutations in *YABBY* genes cause relatively mild abaxial patterning defects. Initially *YABBY* gene expression occurs throughout the incipient organ primordium before becoming abaxially localised by P2 stage. This expression pattern and predicted function is consistent with a role for *YABBY* genes in specifying abaxial leaf identity. Consistent with this view, in *phb-1d* mutants, expression of the *YABBY* gene *FILAMENTOUS FLOWER* is altered but remains correlated with abaxial domains indicating that *YABBY* genes act after polarity is established (Siegfried *et al.*, 1999). Polar expression of the adaxialising *PHB* and *PNH* genes is also observed by the P2 stage suggesting that the leaf primordium has become a polarised entity with adaxial and abaxial transcripts separated into the appropriate domains.

Project Aims

This work aimed to identify a possible function in leaf development for *AtPHAN*, the *Arabidopsis* homologue of the *PHANTASTICA* and *ROUGHSHEATH2* genes. A major goal of the project was to identify a loss-of-function *AtPHAN* allele and to utilise this mutation to deduce a role for the gene in normal development. It was hoped to identify whether *AtPHAN* is expressed in similar patterns to its homologues in other species, to determine if it is involved in regulation of *Arabidopsis knox* genes and if so to determine whether this affects morphogenesis along organ axes.

2 Materials and Methods

2.1 Plant material

2.2 DNA manipulation

2.3 *In situ* hybridisation

2.4 *Arabidopsis* transformation and GUS staining

2.5 Image analysis

Materials and Methods

2.1 Plant material

Arabidopsis thaliana stock lines

The following lines were supplied by the *Arabidopsis* Biological Resource Center (ABRC), Ohio, USA:

CS6239 - *apetela2* - *ap2-5* - Col background

CS146 - *asymmetric leaves1* - *as1-1* - L*er*-0 / Col-2 mixed background

CS8066 - *clavata3* - *clv3-2* - L*er* background

CS3283 - *magnifica* - *mag* - En background

CS8154 - *shootmeristemless* - *stm-1* - L*er* background

CS8137 - *shootmeristemless* - *stm-2* - L*er* background

CS6235 - *terminal flower1 – tfl1-11* - Col background

CS6294 - *unusual floral organs* - *ufo-2* - L*er* background

CS6295 - *unusual floral organs* - *ufo-6* - L*er* background

The following lines were supplied by Nottingham Arabidopsis Stock Centre (NASC), UK:

N908 - wild type - Col-3 ecotype

cup-shaped cotyledons1 and *2* - *cuc1*; *cuc2*/+ - a gift from Mitsuhiro Aida, NIST, Japan.

35S::KNAT1 (3B) - a gift from Sarah Hake, PGEC - University of Berkeley, California.

wuschel - *wus-1* - a gift from Heiko Schoof, Tubingen.

zwille - *zll-3* - a gift from Heiko Schoof, Tubingen.

STM::GUS - a gift from Kathryn Barton, University of Wisconsin.

KNAT1::GUS - a gift from Sarah Hake, PGEC - University of Berkeley, California.

KNAT2::GUS - a gift from J. Dockx, University of Utrecht, The Netherlands.

Plant growth conditions

Seeds were vernalised at 4°C for 3-4 days following imbibition and grown in Levington M3 potting compost. Plants were grown in greenhouses or growth rooms at an average temperature of 20°C. Growth rooms supplied light from metal halide lamps, which also supplemented daylight in greenhouses.

For genetic crosses, pollination was carried out by emasculating flowers to be used as the female (pollen acceptor) and transferring pollen from the male (pollen donor) using fine pointed watchmaker's forceps to hold stamen filaments and brush pollen onto receiving stigmas.

2.2 DNA manipulation

Escherichia coli strains and plasmid vectors

DH5α Φ80d*lacZ*ΔM15, *recA*1, *endA*1, *gry*A96, *thi*-1, *hsdR*17(r_k- m_k+), *supE*44, *relA*1, *deoR*, Δ(*lacZYA-argF*)U169

The above strain was used as a plasmid host, allowing detection of recombinant plasmids through alpha-complementation. Two plasmid vectors were used principally for subcloning DNA inserts, pBluescript (Stratagene) and pGEM-T (Promega) which both contain a selectable ampicillin resistance marker. A polylinker within the coding region of *LacZ* enabled the cloning of DNA inserts, disrupting expression of the amino-terminal region of the β-galactosidase enzyme and preventing complementation of the bacterial host's *LacZ*ΔM15 mutation (an N-terminal deletion). Active β-galactosidase catalyses the removal of a galactose residue from the colourless X-Gal (5-bromo-4-chloro-3-indolyl-β-D-galactoside) converting it to a blue derivative. White colonies of *E. coli* hosting recombinant plasmids were therefore distinguishable from their blue non-recombinant counterparts on X-Gal coated agar plates. Another advantageous property of these plasmids was in production of probes for *in situ* hybridisation. Cloning of a gene in either orientation ensured the insert was flanked by a bacteriophage promoter facilitating *in vitro* transcription of antisense RNA probes. Bacteriophage M13 sequencing primer binding sites of both vectors were conveniently placed for amplification of PCR products and for sequencing.

Gel electrophoresis

For the resolution of small amounts of DNA, meniscus gels were poured on thin rectangular (15 cm x 6 cm) glass plates underlying a comb of required size to form the wells. 30 ml of 0.7% agarose (w/v) in 0.5 x TBE was used for each gel with 10 µg/ml of ethidium bromide for subsequent visualisation. Larger sized gels were used if subsequent Southern blotting was required. Gels were allowed to set and were equilibrated in an electrophoresis gel tank containing 0.5 x TBE. Before

loading into the wells, DNA samples were mixed with 0.1 volumes of loading buffer (0.25% (w/v) bromophenol blue, 0.25% (w/v) xylene cyanol, 15% (w/v) Ficoll type 400). DNA was subjected to a potential gradient of 10 V/cm for approximately 45 minutes to size fractionate the samples, after which gels were analysed on a UV transilluminator (UVT-28MP, E.A.S.Y., Herolab).

Arabidopsis genomic DNA extraction

4-5 mature *Arabidopsis* rosette leaves per plant were collected in foil packets and frozen in liquid nitrogen. A pestle and mortar was prechilled with a little liquid nitrogen and the frozen material ground to a fine powder using a fine glass coverslip as abrasive. The resulting green powder was mixed with 1 ml of DNA extraction buffer (3 x SSC, 0.1 M EDTA, 0.1 M sodiumdiethyldithiocarbamate, 2% [w/v] SDS) and 1 ml of the mixture transferred to an Eppendorf tube containing 0.5 ml of chloroform. Following good vortexing and centrifugation at 15800 x g for 5 minutes the supernatant was removed to a clean tube and an equal volume of phenol/chloroform added, vortexed well, and spun. 0.75 ml of supernatant was recovered to a fresh tube containing 0.75 ml of ethanol and mixed before being spun at 15800 x g for 5 minutes. Supernatant was carefully removed from the resulting pellet and the pellet dissolved in 50 µl TE (100 mM Tris-HCl pH 8.0, 50 mM EDTA) containing RNase A at a concentration of 100 µg/ml and incubated overnight at 4°C for digestion of RNA.

The DNA solution was vortexed and spun to pellet any insoluble material and supernatant transferred to a new tube, mixed with 7 µl of 5 M NaCl and 57 µl of CTAB solution (50 mM Tris pH 8.0, 10 mM EDTA, 2% (w/v) hexadecyltrimethylammoniumbromide). Tubes were inverted several times to mix the contents and spun to pellet DNA. Supernatant was removed from the pellet and 1 ml 0.15 M NaCl / 70% (v/v) ethanol vortexed with the pellet to wash it. Further spins and changes of wash were carried out over several hours to

completely remove CTAB. The pellet was finally dissolved in 50 µl of TE and stored at -20°C until needed.

Preparation of plasmid DNA from bacterial culture

3 ml of overnight bacterial culture was centrifuged at 4600 x g in a benchtop mini centrifuge for 2 minutes. The supernatant was discarded and the pelleted bacterial cells taken through lysis and DNA purification in spincolumns using a QIAprep Miniprep Kit (Qiagen) as for the manufacturer's instructions. Final elutions from the spincolumns were typically in a volume of 30 µl distilled H_2O.

Measuring DNA concentration

To quantitate amounts of DNA recovered from purification procedures, DNA was diluted 1:100 in a total volume of 1 ml and the absorbance measured in a UV spectrophotometer. Using a cuvette with a 1 cm light path, the absorbance at 260 nm was used to estimate concentration using the following calculation.

1 OD_{260} Unit = 50µg/ml for double-stranded DNA

Restriction endonuclease digestion of DNA

1-5 µg of plasmid DNA was digested in a total volume of 25 µl comprising 2.5 µl of 10 x manufacturer's enzyme buffer and 1.5 µl of restriction endonuclease (15-18 units). The digest was incubated for a minimum of 1 hour at 37°C.

Isolation of DNA fragments from agarose gels

Electrophoresed DNA fragments of a required size were detected by UV visualisation and excised carefully from agarose gels by cutting with a clean scalpel. The sliced gel fragment was transferred to an Eppendorf tube for weighing. Further purification procedures were performed using spincolumns of a

QIAquick™ Gel Extraction Kit (Qiagen) according to the manufacturer's instructions. Final elutions from spincolumns were typically in a volume of 30 µl of distilled H_2O.

Dephosphorylation of vector ends

To a completed digest of vector DNA in 7 µl was added 0.9 µl of 10 x dephosphorylation buffer and 1 µl (1 unit) Shrimp Alkaline Phosphatase (Roche Diagnostics). Shrimp Alkaline Phosphatase catalyses the hydrolysis of phosphate groups from either 5' protruding or 5' recessive ends following digestion of vector DNA. The dephosphorylation reaction was incubated for 10 minutes at 37°C and the alkaline phosphatase inactivated at 65°C for 15 minutes.

Ligations

Ligation of insert DNA into target vectors was carried out by calculating a 3:1 molar ratio of insert DNA to vector DNA in a total volume of 5 µl containing 0.5 µl of 10 x manufacturer's ligation buffer and 2.5 units of T4 DNA ligase (Roche Diagnostics). Reactions were incubated overnight at 15°C. A range of molar ratios was tested following unsuccessful ligation attempts. Ligations into the pGEM-T vector were performed according to the manufacturer's instructions (Promega) using the ligation buffer supplied.

Bacterial transformation by heat-shock

1 ml of an overnight culture of DH5α was used to inoculate 100 ml of L-broth and the subculture grown at 37°C until the absorbance at 550 nm was 0.45. The culture was cooled on ice for 15 minutes, transferred into 50 ml Falcon tubes and centrifuged at 6500 x g at 4°C for 10 minutes to spin down the cells. The pellet was resuspended in 4 ml of ice cold TFB1 (30 mM potassium acetate, 100 mM rubidium chloride, 10mM calcium chloride, 50 mM manganese chloride, 15% [v/v]

glycerol, pH 5.8 using acetic acid) and spun as before. The pellet was then resuspended in 4 ml ice cold TFB2 (10 mM MOPS, 75 mM calcium chloride, 10 mM rubidium chloride, 15% [v/v] glycerol, pH 6.5 using KOH). Cells were aliquoted on ice and snap frozen in liquid nitrogen. Competent cell aliquots were stored at -70°C until required.

For each transformation a 100 µl aliquot of cells was thawed on ice for approximately 15 minutes. The cells were typically mixed with 10 ng of plasmid DNA by gentle pipetting and incubated on ice for a further 20 minutes. Cells were heat-shocked at 42°C for 90 seconds and transferred back to ice for several minutes. 1 ml of 2 x YT was added to the cells which were then incubated at 37°C for 1 hour. Cells were spun at 4600 x g for 2 minutes and resuspended in a reduced volume of approximately 200 µl of supernatant. Cell suspensions were then spread on LB agar (LB containing 1.5% Bacto agar) plates containing appropriate antibiotic concentrations for selection of transformants and incubated at 37°C overnight.

Bacterial transformation by electroporation

A litre of LB was inoculated with 1 ml of a freshly grown overnight culture. Cells were grown at 37°C for 3-4 hours until the absorbance at 600 nm reached 0.5-0.7. Cells were chilled on ice for 25 minutes and centrifuged at 6500 x g for 15 minutes. Supernatant was removed and the cells resuspended in 1 litre of ice-cold sterile 10% (v/v) glycerol and centrifuged as before. This was repeated three times, reducing the resuspension volume from 500 ml to 20 ml then finally to 2-3 ml. Aliquots of 40 µl were snap frozen in liquid nitrogen and stored at -80°C for up to six months.

For each transformation, 1-2 µl of DNA containing 10 ng of plasmid DNA was carefully mixed with 40 µl of cells thawed on ice. Cells were then transferred to

chilled electroporation cuvettes (gap width 1 mm) and pulsed at 200 Ω / 1.8 kV. Immediately cells were resuspended in 1 ml of SOC and transferred to an Eppendorf for incubation at 37°C for 60 minutes. Cells were then plated as above.

Ethanol precipitation of DNA

0.1 volume of 3 M sodium acetate (pH 5.5) and 2.5 volumes of ethanol was added to the DNA solution which was then incubated at -20°C for 30 minutes. The solution was centrifuged at 15800 x g for 10 minutes and the resulting pellet washed with 70 % (v/v) ethanol and air dried. The DNA was dissolved in an appropriate volume of TE or H_2O.

Phenol/chloroform extraction

Phenol was presaturated with 10 mM Tris-HCl pH 8.0, mixed with an equal volume of chloroform and centrifuged to separate the mixture into organic and aqueous layers. An equal volume of phenol/chloroform was added to the DNA solution, vortexed well to mix and centrifuged to extract proteins. The upper aqueous layer containing the DNA was removed to a clean tube.

Polymerase Chain Reaction (PCR)

All PCR reactions were performed with a Rapidcycler™ (Idaho Technology) which heats and cools samples sealed inside thin walled glass capillary tubes using air. In typical reactions, 100 ng of genomic DNA or 100 fg of plasmid DNA was used as a template. PCR buffer (50 mM Tris-HCl pH 8.3, 0.25 mg/ml crystalline BSA, 3 mM $MgCl_2$, 0.5% Ficoll 400 and 1 mM tartrazine) was used in reactions with 200 µM of each dNTP (deoxynucleoside 5' triphosphate), 0.2 µM each primer and 0.4 units of *Taq* DNA polymerase (Roche Biochemicals) in a total volume of 20 µl. Typically the reaction was predenatured at 94°C for 30 seconds followed by 35

cycles of three temperatures - 94°C to denature DNA, 45°C for annealing primers and 72°C to extend products of the reaction. Extension times allowed one second per 50 bp for products less than 500 bp, or one second per 25 bp for products greater than 2 kbp. A final extension at 72°C for 2 minutes was typically performed. The annealing temperature reflected calculated primer melting temperatures and often required optimisation to obtain specificity. Products were run on agarose gels to visualise DNA bands or purified using a QIAquick™ PCR Purification Kit (Qiagen) as for the manufacturer's instructions.

Southern analysis

Southern blotting

Following electrophoresis the gel was prepared for blotting onto nylon. Firstly the gel was gently agitated in 0.25 M HCl for 10 minutes. The acid causes the DNA to be nicked and allows the transfer of larger DNA fragments from the gel. The gel was then rinsed briefly with H_2O and then gently agitated in denaturing solution (1.5 M NaCl, 0.5 M NaOH) for 20 minutes and then neutralising solution (1.5 M NaCl, 0.5 M Tris-HCl pH 7.2, 1 mM EDTA) for a further 20 minutes. The gel was placed on Saranwrap and a Hybond-N nylon filter (0.45 µm, Amersham) cut to size, pre-soaked in neutralising solution and placed flat on the gel. Whatman 3MM paper and paper towels were stacked on top of the filter and a flat heavy object rested on top to gently press the whole apparatus. The gel was left overnight or for a sufficient period to allow transfer of DNA to the nylon filter. The filter was removed and soaked briefly in 2 x SSC (100 mM NaCl, 10 mM Na citrate) and air dried before crosslinking of DNA to the filter using 0.4 J cm^{-2} of UV (254 nm) light in a transilluminator.

Oligolabelling of DNA

25-50 ng of DNA in a total volume of 15.5 µl of H_20 was incubated at 100°C for 10 minutes to separate strands and cooled briefly on ice. To the DNA was added 6 µl of oligolabelling buffer (250 mM Tris-HCl pH 8.0, 25 mM $MgCl_2$, 5 mM β-mercaptoethanol, 2 mM each of dATP, dGTP, dTTP, 1 M HEPES pH 6.0, 1 mg/ml random hexamers), 1 µl of BSA (10 mg/ml), 2 µl (1.5 units) of DNA polymerase I (Klenow fragment) and 3 µl of 10 µCi/µl of radiolabelled (α^{32}P) dCTP (Amersham). The labelling reaction was incubated at 37°C for 45 minutes.

For separation of labelled probe from unincorporated labelled nucleotide, 30 µl of 5% (w/v) blue dextran and 0.5% (w/v) orange G was added to the labelling reaction to visually identify labelled probe. This was passed through a column of Sephadex G50 (Pharmacia) in TE, in a 1 ml syringe plugged with filter paper, and eluted with addition of further TE. The blue dextran co-eluted with labelled probe followed by co-elution of orange G with unincorporated radiolabelled nucleotide.

Hybridisation

Filters were pre-hybridised in prewarmed buffer (0.5% (w/v) skimmed milk powder, 1% (w/v) SDS, 4 x SSC) for 15 minutes at 65°C. The labelled probe was denatured by boiling at 100°C for 5 minutes and then added to fresh prewarmed hybridisation buffer and the filter was gently agitated overnight at 65°C.

Washing probed filters

Filters were removed from hybridisation solution and washed to remove background signal. This was done by agitating in wash buffer (2 x SSC, 0.5% (w/v) SDS) for 15-60 minutes at 65°C ('high' stringency) with several changes of wash. Filters were air dried on paper towels, enclosed in Saran wrap and placed

in autoradiography cassettes adjacent to X-ray film. Exposure times were of varied lengths. X-ray film was developed using an automatic developing unit.

Automated DNA sequencing

Cycle sequencing using dye-labelled terminators was performed using the ABI Prism™ Dye Terminator Cycle Sequencing Ready Reaction kits with AmpliTaq DNA Polymerase, FS (Perkin-Elmer). DNA template was purified using a QIAprep Miniprep Kit (Qiagen). For each sequencing reaction, 500 ng of DNA, 4 µl of terminator ready reaction mix and 1.6 pmole of primer was mixed in a thin walled plastic 250 µl tube and placed in a Rapidcycler™ (Idaho Technology) performing the following cycle; 25 cycles of 96°C for 30 seconds, 50°C for 15 seconds and 60°C for 4 minutes, with maximum thermal ramp throughout. Extension products of the reaction were ethanol precipitated to remove unincorporated terminators. For this 10 µl of reaction was mixed with 1 µl of 3 M sodium acetate, 25 µl of ethanol and incubated on ice for 10 minutes. Samples were centrifuged at 15800 x g for 10 minutes, washed with 70% (v/v) ethanol and vacuum dried.

Loading buffer was 5 volumes of deionized formamide to 1 volume of 25 mM EDTA pH 8.0 containing 50 mg/ml of Blue dextran. The sample was dissolved in 6-9 µl of loading buffer, heated for 2 minutes to denature and loaded onto an ABI Prism 377 sequencing gel (Perkin-Elmer). Sequencing data was analysed using the GCG9 or GCG10 (University of Wisconsin) software packages.

Oligonucleotides

The following transposon-specific primers were used in an attempt to isolate dSpm insertions in the *AtPHAN* gene (*see Results 1.2*):

5' dspm11: GGTGCAGCAAAACCCACACTTTTACTTC

5' (nested) dspm5: CGGGATCCGACACTCTTTAATTAACTGACACTC

or

3' dspm1: CTTATTTCAGTAAGAGTGTGGGGTTTTGG

3' (nested) dspm8: GTTTTGGCCGACACTCCTTACC

in combination with the following *AtPHAN*-specific primers:

5' MAD2F: TGTGGTCTAATCGTGTACGTCGTCTGG

5' (nested) MADF: GTGTGATGGAAGTTGCTCTTGAGTTTGGGA

or

3' MAD2R: GTTGCAGCTGACTAAATCAACATCAAGCTT

3' (nested) MADR: TAC AAA GCT GAG GCA AGG AAC CCA AAA GTC

For hybridisation of specific products an 1892 bp fragment of *AtPHAN* was amplified using MAD2F v MAD2R and radiolabelled with ^{32}P.

The following primers were used to amplify the *AtPHAN* and *CLF* genes in *as1* mutants (*see Results 1.3*):

5' MAD2F (5' TGTGGTCTAATCGTGTACGTCGTCTGG 3')

3' MAD2F (5' GTTGCAGCTGACTAAATCAACATCAAGCTT 3')

which amplified a 1892 bp *AtPHAN* genomic DNA fragment.

CLF F (5' TCCGGCTGAGAAACCAGCTCCATGGTGTC 3')

CLF R (5' AGCCAATCTTCCTCGAGATACAGTTTCACCC 3')

which amplified a 706 bp *CLF* genomic DNA fragment.

2.3 *In situ* hybridisation

The expression of *AS1* and other genes was deduced by mRNA *in situ* hybridisation. The tissue preparation and detection protocols followed were based on those described previously (Long and Barton, 1998; http://www.wisc.edu/genetics/CATG/barton/index.html). Antisense RNA probes were hybridised to sections of plant apices at various stages of development.

AS1 probe

A PCR fragment was amplified from a genomic *AS1* clone using the following primers and cloned downstream of the *T7* promoter in pGEM-T:

Forward primer: 5' GTGTGATGGAAGTTGCTCTTGAGTTTGGGA 3'

Reverse primer: 5' TACAAAGCTGAGGCAAGGAACCCAAAAGTC 3'

These span *AS1* genomic DNA nucleotide positions -444 to +1245 relative to the translation start.

A linear PCR fragment was amplified from the plasmid template using the following primers and the probe transcribed from it using *T7* RNA polymerase (Roche Diagnostics).

Forward primer: 5' GGGAGTATCGAGAGTGTGTTCTTGTCAGAGCTTG 3'

Reverse primer: 5' GTTTTCCCAGTCACGAC 3' (the M13 universal sequencing primer in the polylinker of pGEM-T).

STM probe

The plasmid p*MeriHB1* containing *STM* cDNA sequence downstream of the *T3* promoter (a gift from Kathryn Barton and Jeff Long) was linearised with *Xho* I. The template was purified using phenol/chloroform extraction and ethanol precipitation to remove the restriction enzyme and RNase. Transcription was performed with *T3* RNA polymerase (Roche Diagnostics).

KNAT1 probe

A PCR fragment was amplified from first-strand cDNA that had been made from *Arabidopsis* plants (*35S::KNAT1* [3B]) over-expressing the *KNAT1* gene using the following primers and cloned downstream of the *T7* promoter in pGEM-T (Promega):

Forward primer: 5' CATAGATGAGTCGTCTAGTCG 3'

Reverse primer: 5' CATGTCACAGTATGCTTCCATG 3'

These span *KNAT1* cDNA nucleotide positions -210 to +612 relative to the translation start.

A linear PCR fragment was amplified using the forward primer against the M13 universal sequencing primer and the probe transcribed from it using *T7* RNA polymerase (Roche Diagnostics).

Fixation, dehydration and embedding of plant material

Apices and siliques were fixed so that tissue morphology and RNA position would remain intact and final observations would reflect transcript expression *in vivo*. Crosslinking occurs during fixation such that nucleic acids, proteins and macromolecules form a three-dimensional array. All steps involving paraformaldehyde were performed in a fume hood. Histoclear used for solubilising wax was from Cellpath.

Day 1

Siliques (containing embryos), seedlings and inflorescence apices were harvested using a clean scalpel and immediately placed in fixative in glass bottles. The fixative was made by dissolving 4% (w/v) paraformaldehyde in 1 x PBS (130 mM NaCl, 7 mM Na_2HPO_4, 3 mM NaH_2PO_4) that had been adjusted to pH 11.0 and heated to 60-70°C. The fixative was subsequently cooled on ice. When cooled to approximately 4°C the fixative was adjusted to pH 7.0 with H_2SO_4 and 4% (v/v)

DMSO, 0.1% (w/v) Tween and 0.1% (w/v) Triton X-100 added. Samples in fixative were vacuum infiltrated twice for 15 minutes each. Fixative was then replaced and samples gently agitated overnight at 4°C.

Day 2

The samples were then treated as follows.

All steps were at 4°C with agitation.

1 x PBS wash - 30 minutes.

1 x PBS wash - 30 minutes.

30% (v/v) ethanol - 60 minutes.

40% (v/v) ethanol - 60 minutes.

50% (v/v) ethanol - 60 minutes.

60% (v/v) ethanol - 60 minutes.

70% (v/v) ethanol - 60 minutes.

85% (v/v) ethanol - 60 minutes.

95% (v/v) ethanol / 0.1% (w/v) eosin overnight. Eosin stains tissues red making them more visible in embedding wax.

Day 3

All steps were at room temperature with agitation.

100% ethanol - 30 minutes.

100% ethanol - 30 minutes.

100% ethanol - 60 minutes.

100% ethanol - 60 minutes.

25% (v/v) histoclear / 75% (v/v) ethanol - 60 minutes.

50% (v/v) histoclear / 50% (v/v) ethanol - 60 minutes.

75% (v/v) histoclear / 25% (v/v) ethanol - 60 minutes.

100% histoclear - 60 minutes.

100% histoclear - 60 minutes.

100% histoclear / 1/4 volume paraplast chips overnight (without shaking).

Day 4

Samples were moved to 42°C until paraplast chips melted completely. A further 1/4 volume of paraplast chips was added to the samples and left until they melted, then the samples were moved to 60°C for several hours. The wax / histoclear mix was then replaced with freshly melted wax.

Days 5-7

The wax was changed in the morning and evening for three days.

Day 8

Wax and tissue were set in Dispomoulds by placing them on a horizontal metal block on ice to solidify the wax. Wax blocks were stored at 4°C until required.

Sectioning

Wax blocks were trimmed to have a slightly trapezoidal face and mounted onto metal stubs with a little molten wax. The stubs were secured onto a Leica RM2025 microtome so that they faced the blade with the longest side of the trapezoidal block at the bottom. Ribbons of sections were cut 7-8 µm thick, handled with brushes and cut to manageable lengths with a clean razor blade. Ribbons were floated, shiny side down on top of several drops of DEPC treated water upon ProbeOn Plus slides (Fisher Biotechnology) at 42°C. The slides used were ribonuclease free and have an evenly charged surface to which the tissue can adhere. After several minutes, water was carefully drained from the flattened

ribbon with paper towels. Slides were incubated overnight at 42°C to allow tissue to adhere. The slides were kept at 4°C until required.

In vitro transcription

Linearised plasmid or a PCR fragment was used as template for *in vitro* transcription. *T7* or *T3* RNA polymerase was used according to the DNA template. Each transcription reaction was in a total volume of 25 µl containing 1-2 µg of template DNA, 1 x RNA polymerase buffer (supplied with the RNA polymerase), 12.5 nM final concentrations of ATP, GTP and CTP, 2.5 nM final concentration of digoxygenin-labelled UTP, 20 units of RNAse inhibitor and 20 units of RNA polymerase. All components were supplied by Roche Diagnostics.

Reactions were mixed and incubated at 37°C for 60 minutes. To remove DNA templates they were then made up to a total volume of 100 µl containing 5 units of DNase and 100 µg of tRNA. The reactions were incubated at 37°C for 10 minutes. The RNA probe was precipitated by adding an equal volume of 3.8 M ammonium acetate and 2 volumes of ethanol and incubating at -80°C for 10-15 minutes. RNA was pelleted by spinning for 10 minutes at 15800 x g, washed with 70% (v/v) ethanol and air dried.

Carbonate hydrolysis was used to break long RNA probes into fragments of typically 75-150 bp in length using the following formula:

Time (minutes) = Li - Lf / K Li Lf

Li = initial length of probe (kb)

Lf = final length of probe (kb)

K = 0.11 kbp / minute

RNA pellets were dissolved in 100 µl of H_2O, an equal volume of 2 x carbonate buffer (80 mM $NaHCO_3$, 120 mM Na_2CO_3) was added and incubated at 60°C for

the required amount of time. Carbonate hydrolysis reactions were neutralised by adding 10 µl of 10% acetic acid and then RNA precipitated with ethanol. Finally probes were dissolved in 50 µl of 50% formamide and stored at -80°C until needed.

To check incorporation of the dig-UTP label, 0.5 µl of probe was spotted onto a nylon filter adjacent to labelled (100 µg/ml) and unlabelled (200 µg/ml) control RNA (Roche Diagnostics) and UV crosslinked. The filter was wetted briefly in buffer 1 (100 mM Tris pH 7.5, 150 mM NaCl) and incubated in buffer 2 (1% [w/v] blocking reagent [Roche Diagnostics] in buffer 1) for 30 minutes to block. The filter was then washed briefly in buffer 1 and incubated in buffer 1 containing anti-Dig antibody (1:5000 dilution of 0.75 U/ml stock). The filter was then washed twice in buffer 1 for 15 minutes each wash. The pH was raised by a brief immersion of the filter in buffer 5 (100 mM Tris pH 9.5, 100 mM NaCl, 50 mM $MgCl_2$) and the filter incubated for 10-15 minutes in the substrate solution Western Blue (Promega). The intensity of purple/brown probe spots relative to the controls gave an indication of the success of *in vitro* transcription.

Section pretreatment

All solutions were made up free of RNAse using baked glassware and stirbars and autoclaving before use. Slides were placed in a stainless steel sliderack (Raymond Lamb) and transferred in and out of plastic containers holding the solutions. For most washes, 300 ml of solution was sufficient to fully immerse the sliderack. The pretreatments include a protease digestion step which permeabilises the tissue increasing the accessibility of probe and antibody. An acetylation step serves to neutralise positive charges and reduce non-specific binding of probe. All steps were at room temperature unless indicated otherwise.

Firstly slides were deparaffinised and dehydrated by the following steps (the first 3 were in glass containers):

Histoclear - 10 minutes.

Histoclear - 10 minutes.

100% ethanol - 2 minutes.

100% ethanol - 2 minutes.

95% (v/v) ethanol - 2 minutes.

90% (v/v) ethanol - 2 minutes.

80% (v/v) ethanol - 2 minutes.

60% (v/v) ethanol - 2 minutes.

30% (v/v) ethanol - 2 minutes.

H_2O - 2 minutes.

2 x SSC - 15-20 minutes.

100 mM Tris-HCl pH 8.0 / 50 mM EDTA (prewarmed) with 1 µg/ml of proteinase K added just before slides - 30 minutes at 37°C.

2 mg/ml glycine (pH 7.0) in 1 x PBS - 2 minutes.

1 x PBS - 2 minutes.

1 x PBS - 2 minutes.

4% (w/v) paraformaldehyde pH 7.0 (made freshly) - 10 minutes.

1 x PBS - 5 minutes.

1 x PBS - 5 minutes.

0.1 M triethanolamine (made fresh to pH 8.0) with 4 ml acetic anhydride in 800 ml. The acetic anhydride was dispensed a few minutes before the slide rack was added, and elevated in the solution above a stirbar - 10 minutes with stirring.

1 x PBS - 5 minutes.

1 x PBS - 5 minutes.

30% (v/v) ethanol - 30 seconds.

60% (v/v) ethanol - 30 seconds.

80% (v/v) ethanol - 30 seconds.

90% (v/v) ethanol - 30 seconds.

95% (v/v) ethanol - 30 seconds.

100% ethanol - 30 seconds.

100% ethanol - 30 seconds.

Slides were then stored in a container above a small amount of ethanol for up to several hours at 4°C.

Probe hybridisation

Slides were removed from the rack and air dried until completely dry. For each pair of slides, 4 µl of the probe (*see in vitro* transcription) was added to 50% (v/v) formamide to a volume of 40 µl and heated at 80°C for 2 minutes, immediately replaced on ice, spun and returned to ice. The probe was then added to 160 µl of hybridisation solution (50% (v/v) formamide, 12.5% (w/v) dextran sulphate, 10 mM Tris-HCl pH 8.0, 300 mM NaCl, 10 mM $NaPO_4$ pH 6.8, 5 mM EDTA, 1 x Denhardt's [0.02% polyvinylpyrrolidone, 0.02% Ficoll, 0.02% BSA fraction V], 1 mg/ml tRNA). The hybridisation solution was warmed to reduce the viscosity for dispensing. The probe/hybridisation solution mix was carefully mixed without generating bubbles and 200 µl added to each slide pair. The mix was added to one slide and the other slide gradually lowered onto it and sandwiched together ensuring that probe had covered all the sections. This method only applied to Probe-On Plus slides (Fisher Biotechnology). Sandwiched slide pairs were elevated on glass rods above wet paper towels in a tightly sealed plastic container and hybridised overnight at 55°C.

Posthybridisation treatment and immunological detection

0.2 x SSC (10 mM NaCl, 1 mM Na citrate) was preheated to 55°C and NTE (500 mM NaCl, 10 mM Tris-HCl pH 7.5, 1mM EDTA) was preheated to 37°C before use.

Slide pairs were separated in 0.2 x SSC and briefly rinsed before being placed in a rack and given the following washes with gentle agitation:

0.2 x SSC - 60 minutes at 55°C.

0.2 x SSC - 60 minutes at 55°C.

NTE - 5 minutes at 37°C.

NTE - 5 minutes at 37°C.

NTE / RNAse A (20 µg/ml) - 30 minutes at 37°C.

NTE - 5 minutes at 37°C.

NTE - 5 minutes at 37°C.

0.2 x SSC - 60 minutes at 55°C.

PBS - 5 minutes at room temperature.

Slides were removed from the rack, placed on the bottom of a large plastic container and immersed in buffer 1 (100 mM Tris pH 7.5, 150 mM NaCl) containing 1% (w/v) blocking reagent (Roche Diagnostics), using just enough solution to cover the slides. They were on a gently rocking platform for 45 minutes. Blocking solution was replaced with 1% (w/v) BSA (Sigma) in buffer 3 (100 mM Tris pH 7.5, 150 mM NaCl, 0.3% Triton X-100) and replaced on a rocking platform for 45 minutes.

Anti-digoxygenin-AP antibody (FAB fragments, Roche Diagnostics) was diluted to a concentration of 1:1250 in 1% BSA in buffer 3 and a puddle of the solution was made in a petri-dish. Slides were sandwiched together and capillary action used to draw up the antibody solution onto the sections. The sandwiched slides were drained on paper towels and the antibody solution drawn up again carefully without generating air bubbles. Sandwiched slides were then elevated above wet paper towels in a plastic container for 2 hours at room temperature.

Slides were drained on paper towels once more, separated and replaced in a rack. Slides were given 4 washes in 1% BSA in buffer 3 at room temperature with gentle agitation for 15 minutes each. They were then given a 10 minute wash with gentle agitation in buffer 5 (100 mM Tris pH 9.5, 100 mM NaCl, 50 mM $MgCl_2$) and a further rinse in a beaker of fresh buffer 5 to ensure detergent was washed off. A petri dish was prepared containing a puddle of Western Blue (Promega) with Levamisole (Sigma) to a final concentration of 1 mM. Slides were sandwiched and the substrate solution was drawn up and then drained on paper towels. Further substrate solution was drawn up without trapping air bubbles and the sandwiched slides were elevated above glass rods in a tightly sealed plastic container lined with wet paper towels. The slides were transferred to darkness at room temperature for 1-2 days to develop.

The enzyme reaction was stopped by washing in H_2O and a 2 minute wash in 70% (v/v) ethanol removed background. Counterstaining of the cell walls was carried out in 0.1% (w/v) Calcafluor White (Sigma) for 2 minutes. Sections were rinsed briefly in H_2O and allowed to air dry before being mounted with Entellan (Merk).

2.4 *Arabidopsis* transformation and GUS staining

AtPHAN complementation construct

The ~6 kb genomic DNA *Bam*H I fragment containing the *AtPHAN* gene was subcloned into the *Bam*H I site of pGreen (John Innes Centre), a binary vector containing a selection for kanamycin in *E. coli* and a cassette for BASTA (phosphinotricin) resistance in plants. The resulting construct, pGreen-*AtPHAN* was transformed into *Agrobacterium* strain AGL1 which contains the helper plasmid pJICSa-Rep that carries RepA required for pGreen function. Transformed plants were identified by spraying 100 mg/L phosphinotricin, 0.5 ml/L Silwet L-77 onto seedlings with 2-4 leaves and repeating 3-4 days later.

AS1::GUS reporter construct

An *AS1* promoter fragment was amplified from genomic DNA template using the following primers that introduced a *Hind* III site ~2.7kb upstream of the start codon and a *Bam*H I site adjacent to the start codon:

PROM5F (GGTTGATCAGAAGCTTGGACCAAAATGG)

CODE5R (CGTTGTCTCTCTTGGATCCCCTACTCCTCC)

The resulting PCR fragment was cloned into the pGEM-T vector using ampicillin for selection. The kanamycin selectable binary vector pBI121 was linearised with *Hind* III and *Bam*H I and ligated to the 2.7 kb *Hind* III / *Bam*H I restriction fragment and renamed pBI121CODE. Col-0 plants transformed with pBI121CODE were selected by spraying with 100 mg/L kanamycin for the first few days following germination.

Floral dip transformation

This *Agrobacterium tumefaciens* floral dip transformation method is based on that by Clough and Bent (1998). Plants were grown under long days until flowering when first bolts were clipped to encourage proliferation of many secondary bolts.

Four to six days after clipping healthy fecund plants that had many immature flower clusters were selected for dipping.

For the dipping suspension, a single colony of *Agrobacterium* carrying the gene of interest on a binary vector (pGreen or pBI121), was grown at 28°C in 10 ml of LB containing 100 µg/ml rifampicin, 50 µg/ml gentamycin and 30 µg/ml kanamycin, until saturation. The 10 ml culture was then subcultured into 500 ml of LB with the same antibiotics and grown at 28°C overnight. *Agrobacterium* was recovered by centrifugation and resuspended to OD600 = 0.8 in 5% (w/v) sucrose solution with 0.05% Silwet L-77 as a surfactant.

Approximately 500 ml of *Agrobacterium* suspension was required for every two or three plants dipped. Above-ground parts of each plant were dipped for 2-3 seconds with gentle agitation. Dipping the rosette of the plants ensured that shorter axillary inflorescences would be submerged. Dipped plants were covered under Saran wrap for 24 hours to maintain high humidity and grown until seed (putative transformants) could be harvested.

GUS staining

Plants were grown under long day conditions in the greenhouse. Plant tissue was vacuum infiltrated in 1-3 ml of solution containing 25 mM phosphate buffer, pH 7.0, 0.25% Triton X-100, 1.25 mM potassium ferricyanide, 1.25 mM potassium ferrocyanide, 0.25 mM EDTA, 1 mg/ml X-Gluc (5-bromo-4-chloro-3indolyl-β-D-glucuronide), and incubated overnight at 37°C. Tissue was then cleared and photographed in 70% ethanol.

2.5 Image analysis

Plant images

Digital images of plants were captured with a ScanJet 6100C/T (Hewlett Packard).

in situ hybridisation images

Sections were viewed and photographed using a Polyvar microscope (Riechert-Jung) under a mixture of UV and brightfield illumination.

GUS staining images

Images were captured using a Nikon Coolpix 950 digital camera mounted on an Olympus B061 microscope.

Image manipulation

Images were enhanced using Adobe Photoshop v5.5.

3 Results

3.1 The *Arabidopsis PHAN* homologue is *ASYMMETRIC LEAVES1*

3.11 *AtPHAN* encodes a 367 amino-acid MYB-like transcription factor

3.12 Reverse genetic screens

3.13 Complementation of *asymmetric leaves1* with *AtPHAN*

3.14 Phenotypic characterisation of *as1* mutants

3.15 *AS1* is expressed in lateral organ initials

3.16 Analysis of an *AS1* promoter-GUS construct in transgenic *Arabidopsis*

3.2 Genetic interactions of *AS1*

3.21 Interactions of *AS1* with characterised developmental mutants

3.22 *AS1* function is independent of the *CLVIWUS* interaction

3.23 A novel phenotype is displayed by *as1 stm* double mutants

3.24 *AS1* is misexpressed in *stm-1* embryos

3.25 *STM* expression is unaffected in *as1* mutants

3.3 *knox* genes are negatively regulated by *AS1*

3.31 *KNAT1* is ectopically expressed in *as1* lateral organs

3.32 Ectopic *knox* reporter gene expression in *as1* seedlings

3.33 Constitutive expression of *KNAT1* in an *as1* background

3.34 Constitutive expression of *KNAT1* rescues meristem function in an *stm* background

3 Results

3.1 The *Arabidopsis PHAN* homologue is *ASYMMETRIC LEAVES1*

3.11 *AtPHAN* encodes a 367 amino-acid MYB-like transcription factor

The *Arabidopsis* orthologue of the MYB transcription factor *PHANTASTICA* (*PHAN*), *AtPHAN* had been isolated following a low stringency screening of *Arabidopsis* cDNA and genomic libraries with an *Antirrhinum PHAN* DNA probe (Andrew Hudson). A genomic clone pATGB, that contained approximately 6 kb of a *BamHI* fragment in pBluescript, was sequenced and found to contain the entire open reading frame of *AtPHAN* and several kilobases of upstream promoter sequence. Comparison of this sequence with that of cDNA clones revealed that *AtPHAN* contained a single 329 bp intron in the 5' UTR. The intron, located 50 nucleotides upstream of the translation start site, is conserved in the related *PHAN* gene of *Antirrhinum* (Waites *et al.*, 1998) and the *RS2* gene of maize (Timmermans *et al.*, Tsiantis *et al.*; 1999a) indicating structural as well as sequence similarities between *PHAN*-like genes.

Figure 3.1 shows the sequence of *AtPHAN* and the predicted protein it encodes (Genbank database accession numbers: AC004684; GI:3236245). The open reading frame of *AtPHAN* showed the potential to encode a MYB transcription factor 367 amino acids in length. Translation of *AtPHAN* was assumed to start with an ATG codon and terminate on a TGA codon, the last amino acid residue being proline. The molecular weight of the protein product was predicted to be 42243 Daltons. The *AtPHAN* gene has also been named *AtMYB91* in line with the proposed nomenclature for transcription factors and is one of a total of 125 R2R3 MYB family members in *Arabidopsis* (Kranz *et al.*, 1998; Stracke *et al.*, 2001). MYB proteins of the R2R3 class consequently make up the single largest transcription factor family in *Arabidopsis* and are themselves specific to plants

(Meissner *et al.*, 1999). Each repeat of the DNA-binding domain, R2 and R3, is predicted to fold into a helix-turn-helix motif featuring three helices per repeat (Kranz *et al.*, 1998). AtPHAN contains a conserved N-terminal MYB domain consisting of two imperfect repeats, an R2 consisting of 55 amino acids and an R3 of 51 amino acids. The R2 repeat begins at amino acid position 2 and there are no residues that separate the R3 repeat, which begins at amino acid position 57. Most R2R3 MYB transcription factors in *Arabidopsis* contain repeats that are 53 amino acids in length (Stracke *et al.*, 2001), although the length of the R2 and R3 repeats in AtPHAN is in line with other PHAN-like proteins (Timmermans *et al.*,1999). Both the MYB domain and COOH-terminus of AtPHAN share a high degree of amino acid identity with PHAN proteins from *Antirrhinum*, maize, tobacco and tomato (Figure 3.2). The C-terminal region of AtPHAN contains no other recognisable domains although presumably could be involved in protein-protein interactions that facilitate DNA binding.

The isolation of multiple clones of a single *PHAN*-like gene from the original screening with an *Antirrhinum PHAN* DNA probe strongly suggested that *AtPHAN* was the only *PHAN*-like gene in the *Arabidopsis* genome, this was confirmed following completion of the *Arabidopsis* genome sequence (Arabidopsis Genome Initiative, 2000). *Arabidopsis* therefore differs from the dicotyledonous *Antirrhinum*, which encodes at least two *PHAN*-like family members (Waites *et al.*, 1998), and the monocotyledonous maize, which contains at least one other *RS2*-like gene (M. Timmermans, pers. communication).

A

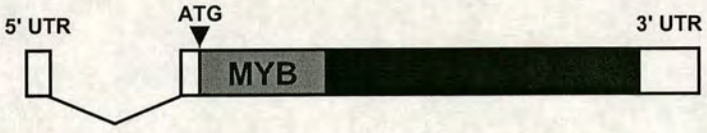

B

```
GCAAATCTGTGTGATGGAAGTTGCTCTTGAGTTTGGGATTATTTATCTTTTCAATATCAT
TTGATGAAGAAGGATGGTGAGATGGGAAGAAGTGATGTCAGGAGGAGTAGGAGATGAAAG
^                                                   M  K  E    3

AGAGACAACGTTGGAGTGGTGAAGAAGATGCATTGTTACGTGCTTACGTTAGACAGTTCG
  R  Q  R  W  S  G  E  E  D  A  L  L  R  A  Y  V  R  Q  F  G   23

GTCCGAGAGAATGGCATCTTGTGTCTGAGCGTATGAACAAACCTTTGAACCGTGACGCCA
  P  R  E  W  H  L  V  S  E  R  M  N  K  P  L  N  R  D  A  K   43

AGTCTTGTTTAGAGAGATGGAAGAATTATCTTAAGCCAGGGATCAAGAAAGGGTCTTTGA
  S  C  L  E  R  W  K  N  Y  L  K  P  G  I  K  K  G  S  L  T   63

CAGAGGAAGAGCAGAGGCTTGTGATCCGTCTTCAGGAGAAACACGGCAACAAGTGGAAGA
  E  E  E  Q  R  L  V  I  R  L  Q  E  K  H  G  N  K  W  K  K   83

AGATTGCTGCTGAGGTTCCCGGGAGGACGGCAAAGCGGTTAGGGAAGTGGTGGGAAGTGT
  I  A  A  E  V  P  G  R  T  A  K  R  L  G  K  W  W  E  V  F  103

TTAAGGAGAAGCAACAGAGAGAAGAGAAAGAGAGTAACAAGAGAGTTGAGCCTATTGACG
  K  E  K  Q  Q  R  E  E  K  E  S  N  K  R  V  E  P  I  D  E  123

AGAGTAAGTACGATCGGATTCTCGAGAGTTTCGCTGAGAAGCTTGTCAAAGAGCGGTCTA
  S  K  Y  D  R  I  L  E  S  F  A  E  K  L  V  K  E  R  S  N  143

ACGTTGTCCCTGCTGCTGCCGCTGCTGCAACGGTTGTGATGGCTAATTCGAATGGAGGGT
  V  V  P  A  A  A  A  A  A  T  V  V  M  A  N  S  N  G  G  F  163

TTTTACATTCTGAACAACAAGTTCAGCCTCCTAACCCAGTGATCCCGCCTTGGTTAGCTA
  L  H  S  E  Q  Q  V  Q  P  P  N  P  V  I  P  P  W  L  A  T  183

CTTCTAACAATGGGAACAATGTTGTTGCAAGGCCTCCCTCGGTAACTTTGACATTATCGC
  S  N  N  G  N  N  V  V  A  R  P  P  S  V  T  L  T  L  S  P  203

CTTCCACAGTGGCTGCAGCTGCGCCTCAACCGCCAATCCCGTGGCTGCAGCAGCAACAGC
  S  T  V  A  A  A  A  P  Q  P  P  I  P  W  L  Q  Q  Q  Q  P  223

CTGAGAGAGCACATAACGGTCCAGGGGGACTTGTGTTAGGGAGTATGATGCCGTCTTGTA
  E  R  A  E  N  G  P  G  G  L  V  L  G  S  M  M  P  S  C  S  243

GTGGGAGTAGCGAGAGTGTGTTCTTGTCAGAGCTTGTGGAGTGTTGTAGAGAGTTGGAGG
  G  S  S  E  S  V  F  L  S  E  L  V  E  C  C  R  E  L  E  E  263

AAGGGCACCGAGCTTGGGCAGACCATAAGAAAGAGGCTGCATGGAGGCTAAGAAGGCTGG
  G  H  R  A  W  A  D  H  K  K  E  A  A  W  R  L  R  R  L  E  283

AGCTGCAGCTAGAGTCAGAGAAGACGTGTAGACAAAGGGAGAAGATGGAGGAGATTGAGG
  L  Q  L  E  S  E  K  T  C  R  Q  R  E  K  M  E  E  I  E  A  303

CAAAGATGAAAGCTCTTAGGGAAGAGCAGAAGAACGCAATGGAGAAGATCGAAGGAGAGT
  K  M  K  A  L  R  E  E  Q  K  N  A  M  E  K  I  E  G  E  Y  323

ACAGAGAACAGCTCGTTGGTTTGAGGCGAGACGCAGAGGCCAAAGACCAGAAACTGGCTG
  R  E  Q  L  V  G  L  R  R  D  A  E  A  K  D  Q  K  L  A  D  343

ATCAATGGACCTCTAGGCATATCAGACTCACCAAGTTTCTTGAACAACAAATGGGTTGCA
  Q  W  T  S  R  H  I  R  L  T  K  F  L  E  Q  Q  M  G  C  R  363

GATTAGACCGCCCCTGAACCGTCTCCTAAACTCTTTGTTGTAACTTGTAATGTAATGTAA
  L  D  R  P  *                                               367

GGTTTTTTTTTTGTTTTTTTTTGTTTTTTTTTGTCTTTGATCATTTGGGTGTCTCCAATG
TTTACTTAGACTTTTGGGTTCCTTACCTCAGCTTTGTATTTGTTTCTTTTACCTTTGTGT
TCCATTTATCACTTCAGTTTATCCATGGCTTTGTTTTCTCAAGCTTGATGTTGATTTAGT
CAGCTGCAACACTTTGGTTTATAAATAAAATCGATTTATATC
```

Figure 3.1 Structure of the *AtPHAN* locus

(**A**) Map of the *AtPHAN* genomic region. Boxes represent exons, pointed line represents an intron. White boxes denote untranslated regions (UTR's), the grey region denotes the conserved MYB domain. (**B**) The amino acid sequence of AtPHAN is shown below its cDNA nucleotide sequence. Splicing of an intron in the 5' UTR occurs at the position denoted by an arrow. The two MYB repeats of the AtPHAN protein are underlined.

Figure 3.2 Pile-up of *AtPHAN* and other *PHAN*-like amino acid sequences isolated from monocotyledonous and dicotyledonous plant species

Different colours are used to highlight different amino acids and dots indicate gaps in the alignment. Key: **as1**, *AtPHAN/AS1* (*Arabidopsis*); **tobphan**, *NtPHAN* (Tobacco); **tomphan**, *LePHAN* (Tomato); **phan**, *PHAN* (*Antirrhinum*); **rs2**, *RS2* (Maize); **rob**, '*PHAN*-like gene' (*Antirrhinum*).

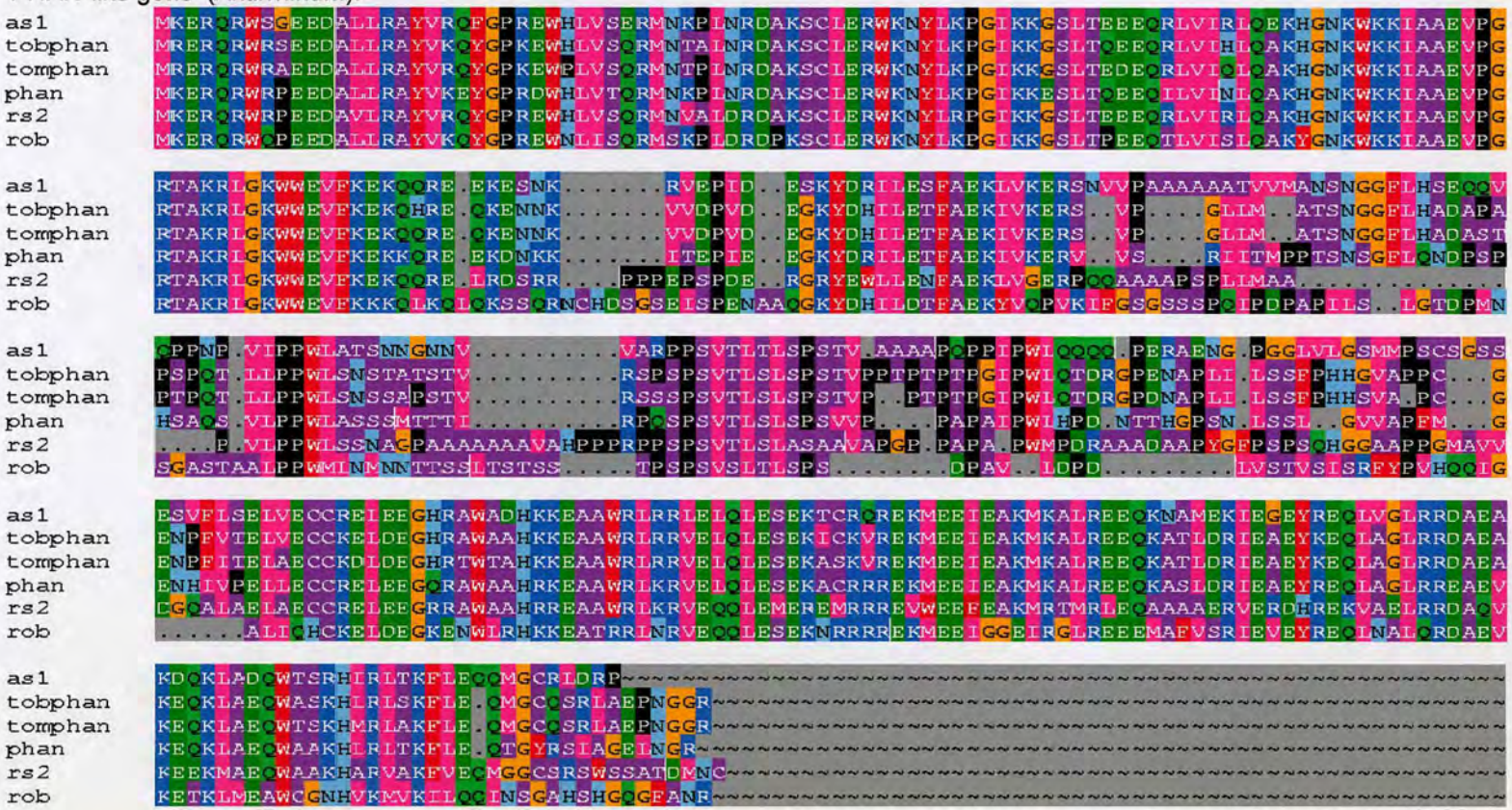

3.12 Reverse genetic screens

To identify the function of *AtPHAN*, a reverse genetic approach was instigated to attempt to isolate an *Arabidopsis* line that carried a transposon or T-DNA insertion in the gene.

The SLAT collection

The Sainsbury Laboratory *Arabidopsis* (dSpm) Transposants (SLAT) collection was generated in the laboratory of Jonathan Jones in Norwich (Tissier *et al.*, 1999). The lines based on the maize Enhancer/Suppressor-mutator (En/Spm) element were generated in a Columbia (Col-0) background. A single T-DNA construct carried a nonautonomous defective Spm (dSpm) element containing a phosphinothricin herbicide resistance (BAR) gene, flanked by a transposase expression cassette and a counterselectable marker gene. Progeny were selected for presence of dSpm and absence of the original T-DNA locus. Therefore each transposant was likely to carry a single copy of dSpm elsewhere in the genome.

Genomic DNA was available to screen in superpools representing 48 pools of 50 transposant lines each. Therefore each DNA superpool represented approximately 2400 plants. Initially, 11 superpools were available to screen. DNA extracted from these pools was used in reverse genetic screens, by polymerase chain reaction (PCR) using primers from the dSpm transposon and from the *AtPHAN* gene (*see Materials and Methods*). Four *AtPHAN* primers were designed; two flanked the *AtPHAN* gene and two were nested within these for a secondary round of PCR. Also four dSpm primers were designed; one towards each end of the transposon with another two nested outside these. In the primary round of PCR, two dSpm primers were used with two *AtPHAN* primers in all four combinations, on each of the 11 superpool DNA templates. In a secondary round of PCR the appropriate nested primers were used on the product of the primary PCR.

Primary and nested PCR products for each superpool were electrophoresed on agarose gels and Southern blotted onto nylon filters. A genomic *AtPHAN* PCR probe was amplified and radiolabelled, then hybridised to the filters in order to detect specific products of the screen (see *Materials and Methods*). Although many PCR products were visualised on agarose gels, Southern hybridisation failed to identify an *AtPHAN* specific product from a primary screen which gave a smaller specific band in a subsequent nested round of PCR. An *AtPHAN* PCR fragment was run on each gel to ensure that the probe was able to detect specific products. It was concluded that there was not a dSpm insertion at the *AtPHAN* locus in the collection of lines used to generate the superpool DNA.

A second strategy to screen for insertions in the SLAT collection was made possible with a filter (SLAT filter) on which inverse PCR (*i*PCR) products from insertions in DNA pools had been spotted. The *i*PCR method uses PCR, but it has the primers oriented in the reverse direction of the usual orientation. The template for the reverse primers is a restriction fragment that has been ligated upon itself to form a circle. The SLAT filter was hybridised with the *AtPHAN* probe and subsequently analysed for positives. The first screen of the SLAT filter with an *AtPHAN* probe identified a potential hit corresponding to the pool 01.10 (superpool 01, subpool 10) representing 50 transposant lines. To check the validity of this hybridisation the filter was stripped and reprobed which gave the same result. Seed of pool 01.10 was ordered and grown. Genomic DNA extraction was carried out on leaf tissue bulked from all plants that were grown. Overall, approximately 150 seedlings were grown to ensure a high probability of coverage assuming that similar amounts of seed from each transposant line had been pooled. None of the seedlings observed in the pool were identified to have a mutant leaf phenotype. The screen for a dSpm insertion was carried out using the same PCR method as before. Once again however, no specific bands were detected when probed with *AtPHAN*. Since *i*PCR had been used to produce the SLAT filter, this technique was repeated on this pool alone. Although a large number of *i*PCR products were generated, as visualised on agarose gels, none proved to be *AtPHAN* specific when probed. One explanation for these results is

that the *i*PCR products detected on the SLAT filter were not derived from pool 01.10 and that this pool may have been contaminated at some stage. The initial hybridisation of the SLAT filter may not have been specific.

A large-scale screen for insertions in R2R3 MYB genes was attempted by Meissner *et al.* (1999). These authors were also unable to successfully identify a knockout in *AtPHAN* either in the SLAT collection, further transposant populations or T-DNA-insertion populations.

3.13 Complementation of *asymmetric leaves1* with *AtPHAN*

AtPHAN was previously mapped by RFLP to 64 cM on chromosome 2 of *Arabidopsis* (Andrew Hudson). Since reverse screens were unsuccessful in isolating an insertion in the *AtPHAN* gene, existing mutants that mapped close on the *Arabidopsis* classical map were considered as candidate *AtPHAN* mutants. A recessive leaf mutant with an unknown product, *asymmetric leaves1*, was considered for its map proximity (Linkage group 2; Rédei, [1965]) and vegetative phenotype. *asymmetric leaves1-1* is a classical mutation in *Arabidopsis* that disrupts development of cotyledons, leaves and floral organs and was first described by Rédei and Hirono in 1964. The *as1* mutation segregates as a single, recessive Mendelian trait. The mutant leaf phenotype is noticeable for its short petioles and lobed, rumpled leaves and is readily distinguishable from wild type. The *magnifica* mutation first described by Reinholz (1947) is allelic to *as1-1* and therefore termed *as1-magnifica* here. The two alleles share similar phenotypic characteristics although *as1-magnifica* has a larger rosette and a greater degree of leaf-curling.

To test whether *AtPHAN* might correspond to the *AS1* gene, genomic DNA was extracted from wild type Columbia plants and from two *as1* mutants, *as1-1* (Figure 3.3A) and *as1-magnifica* (Figure 3.3B). Amplification of a 1892 bp *AtPHAN* PCR fragment was attempted using the purified genomic DNA as a template. The two oligonucleotides used to prime the reaction were selected on the basis that they would amplify the transcribed region of *AtPHAN* from the upstream 5' UTR through to the 3' UTR allowing it to be sequenced in both mutants. As a control, primers that amplified part of the *CURLY LEAF* gene (Goodrich *et al.*, 1997) were used in identical reactions with the same cycling conditions on all types of genomic template.

The results of the PCR showed that the expected ~1.9 kb *AtPHAN* fragment could be amplified from genomic DNA template of wild type plants, and also that a fragment of the same size was amplified from template isolated from *as1-1* mutant

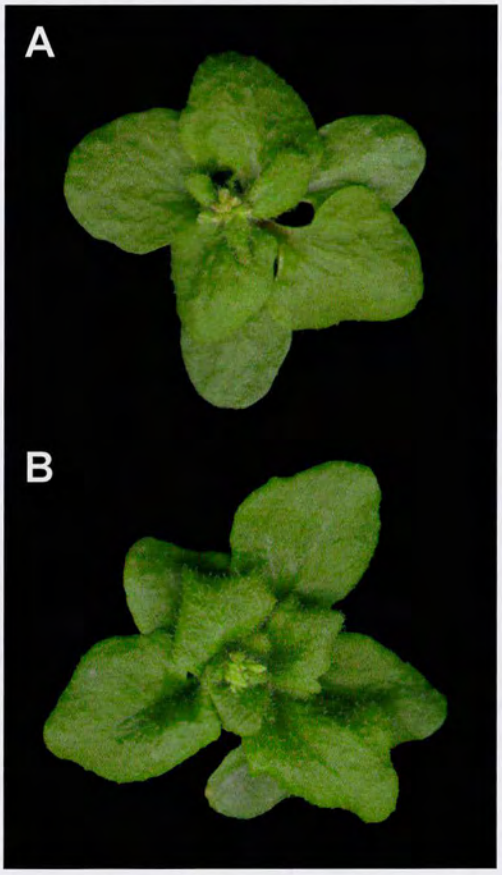

Figure 3.3 The *as1-1* and *as1-magnifica* alleles of *Arabidopsis thaliana*
Homozygous mutants carrying the recessive *as1-1* (**A**) or *as1-magnifica* (**B**) alleles.

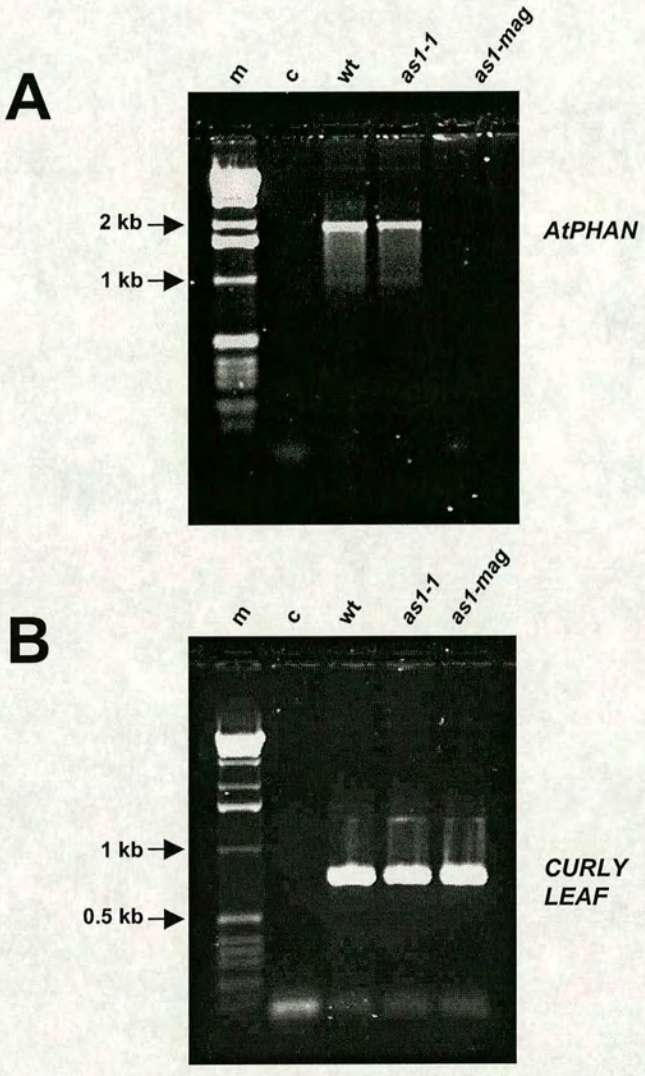

Figure 3.4 PCR amplification of *AtPHAN* from different genetic backgrounds

(**A**) Amplification of the *AtPHAN* coding region, (**B**) amplification of part of the *CURLY LEAF* locus as a positive control. **c**, control with no added DNA template to test for contamination; **wt**, wild type; ***as1-1***, *asymmetric leaves1-1* mutant; ***as1-mag***, *as1-magnifica* mutant; **m**, 1 kb marker.

plants (Figure 3.4A). However no fragment of this size was observed from the reaction performed with *as1-magnifica* DNA as a template. However, control amplification of a predicted 706 bp *CURLY LEAF* DNA fragment was similar in all reactions regardless of template (Figure 3.4B). This suggested that the template for amplification of an *AtPHAN* transcription product appeared to be disrupted in alleles of *as1-magnifica* consistent with *as1* mutants being defective at the *AtPHAN* locus. Lack of amplification from *as1-magnifica* was consistent with a large reorganisation (e.g. a deletion) while amplification of the *AtPHAN* band from *as1-1* genomic DNA suggested that this allele might carry a base deletion or substitution that would not greatly affect the size of the PCR product.

To investigate these initial PCR results further, complementation of the *as1* mutation was attempted by insertion of a transgene carrying the wild type *AtPHAN* gene. The ~6 kb genomic *Bam*H I fragment in pATGB, containing the *AtPHAN* promoter and coding region, was subcloned into the binary vector pGreen carrying the *Bar-R* resistance gene. The resulting pGreen-*AtPHAN* vector was introduced into *Agrobacterium* and used to transform the two mutants, *as1-1* and *as1-magnifica*. The floral dip method was used for *Agrobacterium*-mediated *Arabidopsis* transformation. Progeny was collected from dipped plants that were allowed to self and seedlings in the progeny were subjected to BASTA selection. Transformation was observed at a low frequency, only one resistant T1 plant from ~1000 seedlings was obtained from transformation of each allele. Each T1 plant was selfed for analysis in the next generation. Growth of both T1s was as for wild type *Arabidopsis* during all stages of development.

A family of T2 plants from transformation of the *as1-1* mutant were sown and scored for phenotype. Of 212 plants in the family, 150 had a wild type phenotype and the remaining 62 plants yielded an *as1-1* phenotype. This 3:1 ratio was expected if *AtPHAN* complemented the *asymmetric leaves1* mutation and the T1 parent was hemizygous for a single transgene locus. Additionally, T2 plants with an *as1-1* phenotype were predicted not to carry the complementing transgene and therefore not be resistant to BASTA. All T2 plants were sprayed with BASTA

following phenotype recognition and all of the 62 *as1-1* plants died. All of the remaining 150 wild type plants were resistant and therefore were assumed to carry the transgene, which was able to complement the mutant *as1-1* product and allow proper development.

Analysis of T2 plants from transformation of *as1-magnifica* mutants yielded similar results. From one family of 135 siblings, 101 resembled wild type seedlings and 34 had an *as1-magnifica* phenotype. This also was an approximate 3:1 ratio. As before, plants with the *asymmetric leaves1* phenotype were not resistant to BASTA treatment unlike the wild type phenotype siblings that carried at least one copy of the transgene.

These results showed that *AtPHAN* encoded a fully functional product that was either defective or absent in both *as1-1* and *as1-magnifica* mutants and that all sequences required for expression were present within the ~6 kb *Bam*H I fragment. Since *AtPHAN* was deduced to be *ASYMMETRIC LEAVES1* (*AS1*), the latter name was taken to be the name of this gene and is referred to as this in the remainder of this text.

To identify the *as1-1* mutation, sequence was obtained of the PCR product amplified from genomic *as1-1* DNA. Comparison of this sequence and wild type sequences from Col-0 and L*er* revealed that *as1-1* had been derived from the Col-0 allele and had a single base deletion within the *AS1* coding region. As a result of the base deletion, the translational reading frame is altered such that 3 nonsense amino acids are encoded before a termination codon that truncates the mutant product (Figure 3.5).

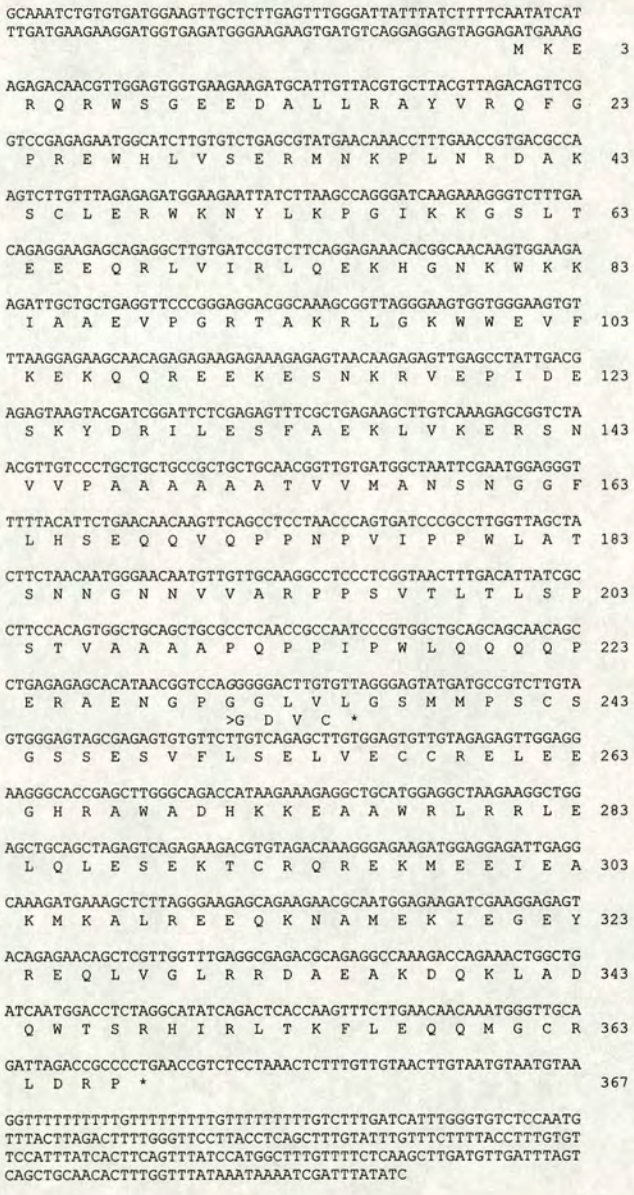

Figure 3.5 Structure of the *as1-1* mutant allele
The amino acid sequence of AS1 is shown below its cDNA nucleotide sequence. The deletion of a guanine base (G) in the sequence of the *as1-1* allele is shown italicised. As a result of this single base deletion a truncated mutant protein is potentially encoded. The altered amino acid sequence is shown below that of the wild type allele.

3.14 Phenotypic characterisation of *as1* mutants

Rédei and Hirono first described a class of *Arabidopsis* mutants with similar rosette leaf morphology in 1964 assigning to them the name, *asymmetric leaves* (*as*) mutants. The *as* mutants and other leaf shape/colour mutants were utilised as genetic markers for linkage map construction. Allelism tests have since shown that existing stock centre *asymmetric leaves* mutants fall into just two complementation groups; *as1* and *as2* (Serrano-Cartagena *et al.*, 1999). *magnifica* an X-ray-induced mutant, (Reinholz, 1947), was first reported to be allelic to *as1* by Barabas and Redei (1971). Berna *et al.* (1999) performed complementation analyses with EMS-induced mutations from a large-scale leaf mutant screen, however, new mutants identified with the *asymmetric leaves* phenotype fell into the existing two complementation groups corresponding to *as1* and *as2*. The recessive *as2* mutation, which conditions longer petioles than *as1*, is epistatic to the *as1* mutation suggesting that both genes are involved in the same process (Serrano-Cartagena *et al.*, 1999; Ori *et al.*, 2000). This text however is concerned with the description of the *asymmetric leaves1* mutation.

Shown in Figure 3.6, the rosette of *as1* (B) appears denser than a wild type rosette (A) due to the shorter length of *as1* petioles. The spoon-shaped appearance of a wild type rosette leaf (Figures 3.7A) contrasts strongly with the heart-shaped rosette leaf produced by an *as1* mutant (Figure 3.7B) during the vegetative phase of plant growth. The leaves of *as1* take on a characteristic uneven rumpled appearance as a result of slight wrinkling of the lamina which itself is broader than in wild type rosette leaves. Leaf blades exhibit a varying degree of bilateral asymmetry and often show prominent outgrowths or lobes which subdivide the mutant leaf lamina. Formation of lobes was restricted to the base of leaves as previously observed (Tsukaya and Uchimiya, 1997). The appearance of the leaves also differs from wild type due to the margins unevenly curling downwards. Both features of *as1* leaves modify the bilateral symmetry, assuming its proximodistal axis to be the prominent midvein. All leaves exhibit altered morphology although the lobing of leaves occurs to a lesser extent in

Figure 3.6 Vegetative development
Wild type *Arabidopsis* - Columbia ecotype (**A**) and *as1-1* mutant (**B**) showing compact rosette morphology and aberrant leaf phenotype. *Bar = 10 mm*

Figure 3.7 Rosette leaf development
Wild type *Arabidopsis* (**A**) showing spoon-shaped leaf morphology and (**B**) *as1-1* mutant with heart-shaped phenotype, margins that curl downward, a rumpled lamina and reduced petiole length. *Bar = 5 mm*

Figure 3.8 *as1* floral development
A wild type inflorescence (**A**) and an *as1-1* mutant inflorescence (**B**). Flowers of an *as1-1* mutant have a distinct protruding pistil due to shortened sepals and petals which would normally enclose it (compare flowers at similar stage of development indicated by white arrows). The inflorescence stem is also wider than wild type.

early leaves and increases in later leaves (Tsukaya and Uchimiya, 1997). Lobing of leaves is not well understood but each lobe may represent a new proximodistal axis of growth within the leaf. The asymmetric phenotype suggests disruption of the mediolateral axis also, however, no evidence was found from SEM analysis of leaf surfaces that suggested disruption of the dorsoventral axis.

In the reproductive phase of plant development, the *as1* mutation (Figure 3.8A) results in inflorescences and flowers that do not appear to differ greatly from wild type (Figure 3.8B) in terms of morphology. Organ number in flowers is normal although length of floral organs such as petals was reduced (Tsukaya and Uchimiya, 1997). As a result of this, flowers display a prominent pistil, which facilitates genetic crosses of these mutants as pollen acceptors (Barabas and Redei, 1971). Tsukaya and Uchimiya (1997) have previously determined that there is no significant difference in the lengths of *as1* hypocotyls or roots with respect to the Columbia wild type.

The phenotype of *as1* and *as2* mutants is similar, however, *as1* mutants display a far more compact rosette of heart-shaped leaves due to shorter petiole length. Cotyledons are slightly shorter and more rounded than wild type although difficult to distinguish from wild type plants until later in development, when rosette leaves with short petioles emerge from the meristem. In the first recorded mutant allele of *as1*, named *magnifica*, occasional ectopic shoots are observed on the adaxial side of rosette leaf petioles (Byrne *et al.*, 2000).

The observation of ectopic meristems on *as1* mutant leaf petioles is similar to what is observed in *35S::KNAT1* transgenic plants which also exhibit severely lobed leaves (Chuck *et al.*, 1996; Tsukaya and Uchimiya, 1997). The *as1* mutation gives a lobing phenotype that is similar to that of *35S::KNAT1* plants, although *as1* conditions a weaker severity of lobing. More lobing is evident on *35S::KNAT1* leaves and lobes are present along all the length of the margins and not restricted to basal regions. The rumpled leaf effect of the *as1* mutation was also noted to be reminiscent of transgenic tobacco plants that either overexpress *KNAT1*,

overexpress the maize *knottted1* gene, or that overproduce cytokinins (Sinha *et al.*, 1993; Hewelt *et al.*, 1994; Chuck *et al.*, 1996).

Since the *AS1* gene was found to be highly homologous to *PHAN* in *Antirrhinum* and *RS2* in maize (Timmermans *et al.*, 1999), the mutant phenotypes of these genes were expected to share similar developmental deficiencies in their respective species. The most obvious functional respect in which *PHAN*-like genes are similar is that they are all perturbed in leaf development as a result of loss-of-function mutations. The heart-shaped leaf phenotype seen in *as1* mutants is also observed in *phan* mutants (Waites and Hudson, 1995) and may reflect perturbation of placement of identities along the organ proximodistal axis. One view of this is that the distal region of the leaf, the blade, is transformed to a proximal organ identity, such as the stem or petiole, in the case of *phan* needle-like leaves which display a lack of dorsoventrality (Tsiantis *et al.*, 1999a). In heart-shaped leaves this could be interpreted that a proximalising effect disrupts normal positional identities within the leaf, such that stem or petiole identity encroaches on blade identity. In *Arabidopsis*, a conversion to stem rather than petiole identity would seem more feasible since *as1* petioles are actually shorter than wild type. Also, if petiolisation occurs in *Antirrhinum phan* needle-like leaves, this does not explain why *phan* leaves are radially symmetrical whereas petioles exhibit dorsoventral symmetry in cell types of the vasculature and surrounding tissue (Waites and Hudson, 1995).

Neither *as1* or *rs2* mutant leaves display dorsoventral defects suggesting that the *PHAN* gene in *Antirrhinum* may have an additional role in specifying the dorsoventral axis of lateral organs. In maize and *Arabidopsis* such a function may be obscured by redundant partners of the *PHAN*-like genes, although this is harder to explain in *Arabidopsis* where the only *PHAN*-like gene is *AS1*. Another possibility is that the *phan* mutant background might be null for another factor. Alternatively, the *as1-1* and *as1-magnifica* mutations might not be null, and retain sufficient activity to specify dorsoventral asymmetry. Otherwise, it appears *PHAN*-

like genes are unlikely to have a generalised dorsoventral specifying role across the angiosperms.

PHAN also appears to have an additional role in maintaining activity of SAMs non-cell autonomously since *phan* mutant SAMs are quiescent (Waites and Hudson, 1995). Neither *AS1* or *RS2* activity is required for maintenance of functional meristems in *Arabidopsis* or maize respectively. This appears to support evidence that dorsalising factors or tissues in leaves, such as *PHAN*, are associated with SAM maintenance whereas *AS1* and *RS2* are not specifiers of dorsality and are not directly required for SAM maintenance.

3.15 *AS1* is expressed in lateral organ initials

The expression of *PHAN* in *Antirrhinum* occurs in initials of lateral organs throughout postembryonic development (Waites *et al.*, 1998) suggesting that a similar expression pattern might be found for *AS1* mRNA. This would also be consistent with the perturbed development of lateral organs in *as1* mutants. To characterise the role of *AS1* in wild type *Arabidopsis* development, the mRNA expression pattern was investigated using *in situ* hybridisation, a technique that has contributed towards the dissection of function of many *Arabidopsis* developmental genes. A 516 bp region, which included the region encoding the 124 C-terminal amino acids and the 3' UTR (downstream of the conserved MYB domain), was transcribed to give an antisense RNA probe. The RNA was labelled using digoxygenin-11-UTP (see *Materials and Methods*).

The *AS1* expression pattern was investigated throughout *Arabidopsis* development including the stage of embryogenesis. Embryonic expression had not previously been characterised for the *PHAN* gene of *Antirrhinum* or other known *PHAN*-like genes and is considered following discussion of expression in vegetative and reproductive phases.

When the digoxygenin-labelled antisense *AS1* probe was hybridised to serial sections of wild type (Columbia) vegetative apices, *AS1* mRNA was detected in emerging leaf primordia as early as P0 such that signal marked leaf initials on the flanks of the meristem that were not yet visible as bulges. Levels of *AS1* mRNA were maintained in leaf primordia through P1 and P2, but gradually decreased until P4 stage and signal was not seen in primordia of stages later than this (Figure 3.9A). The petioles of the cotyledons were seen to have signal that was weak and correlated with cells of the vasculature. This was continuous with a domain passing below the vegetative meristem and into the hypocotyl of the seedling. However, *AS1* expression was not detected in the meristem itself except at its periphery where organ formation is initiated. Therefore, as predicted, *AS1* is expressed at an early stage of leaf initiation appearing to very closely match the

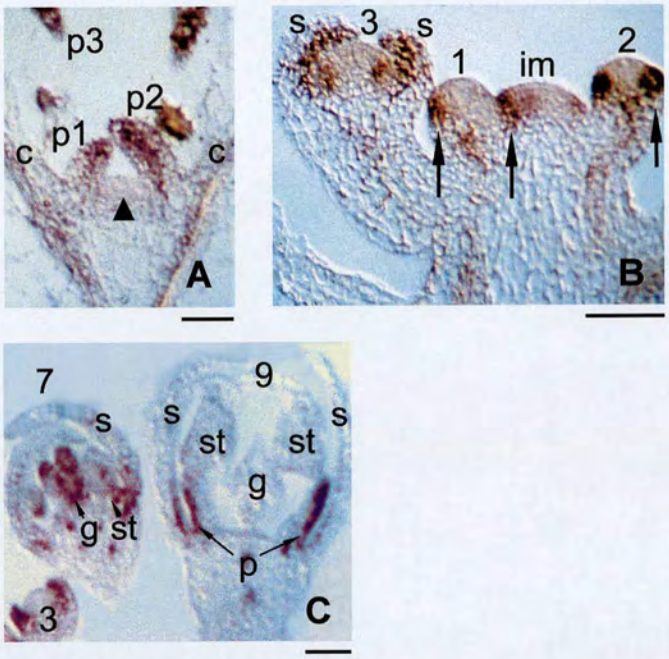

Figure 3.9 Expression of *AS1*

In situ hybridisation showing expression of *AS1* in a wild type vegetative apex (**A**), a wild type inflorescence apex (**B**) and wild type floral stages (**C**). *AS1* expression is confined to organ primordia and is absent from the SAM. An arrowhead indicates SAM initials and arrows in **B** indicate the cryptic bract and initials of the lowermost sepal. Numbers in (**B**) and (**C**) indicate floral stages. **c**, cotyledon; **im**, inflorescence meristem; **s**, sepal; **p**, petal; **st**, stamen; **g**, gynoecium; **p1**-**p3**, leaves of increasing developmental age. *Bars = 25µm.*

expression pattern of *PHAN* in *Antirrhinum*. The *AS1* expression pattern is also in accordance with the phenotypic differences between wild type and *as1* mutants where it is seen that development is perturbed by the stage that leaves have visibly emerged.

The vegetative phase of development is followed by the reproductive phase, whereupon the vegetative SAM becomes an inflorescence SAM capable of initiating floral meristems, which in turn each produce a flower. The inflorescence apex initially generates cauline leaves (bracts) at each node, with a floral meristem being produced in the axil of each bract. Floral meristems produce the four types of floral organs - sepals, petals, stamens and carpels in concentric whorls. Each longitudinal section through the inflorescence captured different stages of floral meristems and floral organ development. In sections of apices, early floral meristems could be seen initiating on the flanks of the inflorescence meristem and later floral meristems, initiating sepal, petal, stamen and carpel primordia in order, were also observed.

Wild type inflorescence apices showed *AS1* transcript localised in a pattern similar to that observed for vegetative apices. *AS1* mRNA was associated with the early development of floral buds on the flanks of the inflorescence meristem but absent from the remainder of the floral meristem (Figure 3.9B). This domain of early expression appeared to correlate with the lowermost sepal initials at a stage before the sepal primordia had become morphologically distinct. Interestingly, *AS1* RNA was detected on the flanks of inflorescence meristems in cells that would give rise to this domain in floral meristems. This corresponded to the 'cryptic bract', a region where expression of *AINTEGUMENTA*, and downregulation of *SHOOTMERISTEMLESS* RNA appear to suggest the existence of a bract primordium, which although initially specified does not grow (Long and Barton, 2000). The detection of *AS1* transcript in the domain subtending floral meristem initiation provides further evidence of this phenomenon and suggests that the lowermost sepal (which develops before the others) might be partly equivalent to a

bract. Expression of *AS1* was also observed on the flanks of the inflorescence stem and centrally in pedicels, which appeared to be continuous (Figure 3.9B).

By the floritypic stage, signal was detected in sepal, petal and to a lesser extent stamen and carpel primordia. At later stages of floral development, *AS1* expression became restricted in all floral organs and by stage 9, expression was observed only at the base of sepals and petals (Figure 3.9C). As had previously been observed in leaves, signal was seen to weaken as the organs matured. These findings were also similar to the observed expression of *PHAN* in *Antirrhinum* inflorescences. However, *as1* mutants are not as severely affected in their floral development in comparison to leaves. Floral organs appear reduced in length but their overall development is not severely disrupted.

During embryogenesis, cells are specified to become cotyledons, meristem, hypocotyl or root. Expression of *AS1* was therefore examined during embryogenesis. *AS1* transcript was first detected as weak signal in several subepidermal cells in wild type late-globular stage embryos. The emergence of cotyledons occurs at the transition/early-heart stage of embryogenesis as two bulges on the flanks of the apex. *AS1* mRNA is seen before this stage, at late-globular stage in two domains of expression that correlate with both initiating cotyledon primordia, whilst downregulation of *AS1* occurs in the centre of the apex, between the cotyledons, in the presumptive SAM initial cells (data not shown). *AS1* continues to be expressed at high levels, as interpreted by the very strong staining, in the cotyledon primordia throughout the heart stage (Figure 3.10A). Serial sections through a heart stage embryo reveal *AS1* transcript in cells of the saddle (Figure 3.10B), either side of the presumptive cells of the SAM which do not express *AS1*. *AS1* expression is persistent in cotyledon primordia throughout late heart-stage (Figure 3.10C).

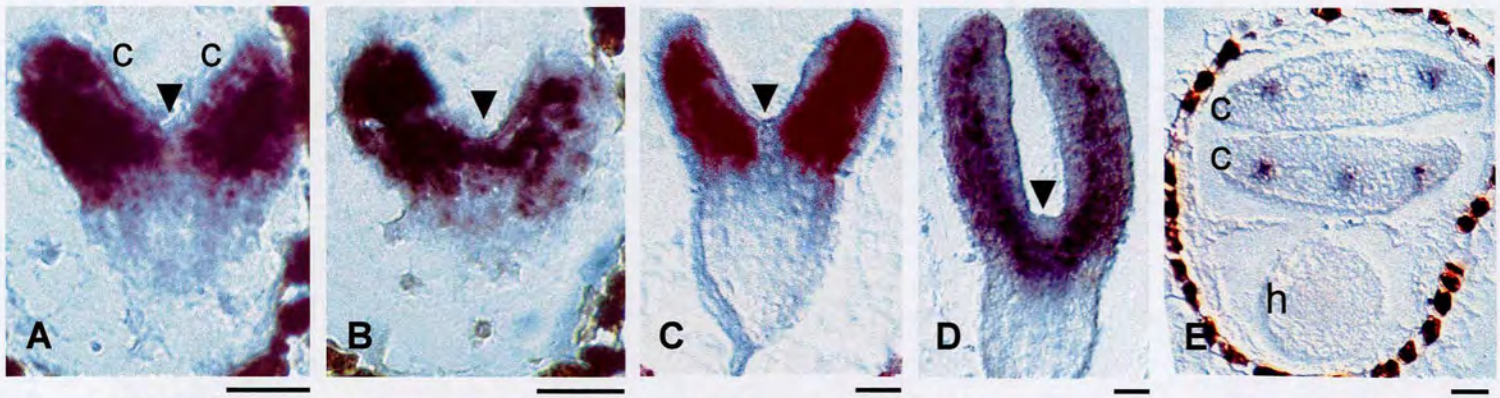

Figure 3.10 *AS1* expression in wild type *Arabidopsis* embryos
Figures (**A**)-(**E**) show localisation of *AS1* transcript (blue/purple colour) in sections of embryos at successive stages of development. *AS1* is expressed throughout cotyledon primordia and absent from SAM initial cells (arrowheads) at early-heart stage (**A**). An adjacent section of the same embryo 7 µm apart (**B**) shows *AS1 is* expressed in cells of the saddle (arrowhead). At late-heart stage (**C**) *AS1* is clearly missing from the presumptive SAM, and also at torpedo stage (**D**) where the SAM becomes morphologically distinct. The domain of expression is seen to expand to below the SAM at this stage. In embryos at walking-stick stage (**E**), transcript is restricted to cells associated with the vasculature within cotyledon primordia. **c**, cotyledon; **h**, hypocotyl. *Bars = 25µm.*

By the torpedo stage the SAM is morphologically distinct as a mound of cells between the emerging cotyledon primordia. Whilst *AS1* mRNA is not present in cells of the SAM, expression is observed throughout cotyledon primordia and in the developing vasculature that runs from the presumptive hypocotyl below the SAM, into each of the two cotyledon primordia (Figure 3.10D). At the upturned-U stage of embryogenesis the expanding cotyledons are bent double over the hypocotyl. Levels of *AS1* expression become reduced throughout the cotyledons and transcript is localised to several veins in each cotyledon (Figure 3.10E) and was also detected in the vasculature of the presumptive hypocotyl.

The expression pattern of *AS1* throughout embryogenesis is in accordance with its role as a marker of lateral organs, which in embryogenesis are the cotyledons, and with the phenotype of *as1* mutants, which have more heart-shaped cotyledons compared to wild type. Interestingly, *AS1* expression is first initiated at approximately the same time as the meristem expresses the *knox* gene, *STM*, at the late-globular stage of embryogenesis (Long *et al.*, 1996). *AS1* largely remains in a complementary pattern of expression throughout embryogenesis and in successive stages of development, *AS1* on in organ primordia and *STM* on in the meristem, raising the possibility of negative interaction between these two loci. *AS1* expression in the vasculature suggests that it may have a role in vascular tissue differentiation or patterning. It would be interesting to observe whether vascular organisation or pattern differs from that in wild type organs.

The expression of *AS1* in *as1-1* mutant apices was examined by *in situ* hybridisation. Weak signal was observed in mutant embryo, vegetative and inflorescence apices in a pattern that did not differ from that observed in wild type apices (data not shown). This suggests that C-terminal sequences may be required for autoregulation or that mRNA stability is reduced.

3.16 Analysis of an *AS1* promoter-GUS construct in transgenic *Arabidopsis*

A genomic fragment containing ~2.7kb of DNA 5' to the *AS1* start codon had been shown to be sufficient for normal *AS1* function (*see Results 3.13*). In order to determine whether this region of the *AS1* promoter was sufficient itself to spatially regulate expression of *AS1* in organ primordia, as observed with *in situ* hybridisation of *AS1* transcripts, an *AS1* promoter-GUS fusion construct was introduced into wild type *Arabidopsis* plants. A construct pBI121CODE was generated with approximately 2.7 kb of the *AS1* promoter, 5' UTR, and intron, fused upstream of a GUS reporter gene, *uidA* in the vector pBI121 (Clontech). This was used to transform wild type (Col-0) plants and two independent transformants, pBI121CODE2 and pBI121CODE3, were recovered in the T1 following selection for the transgene with kanamycin. GUS activity was detected in each.

Progeny from each self-fertilised transformant were selected to study expression of *AS1* during the vegetative phase of development. T2 seedlings were assayed at 9 days postgermination since 2-4 leaf primordia were visible. GUS activity was detected in approximately three-quarters of seedlings, as predicted for progeny segregating a single transgene locus. All of the seedlings assayed for GUS activity showed little variability in staining.

Figure 3.11 shows stained plant tissue from only the pBI121CODE3 line, which was termed an *AS1::GUS* reporter for convenience. The strongest staining observed in transformants was in the earliest leaf primordia emerging on the flanks of the apical meristem (Figure 3.11A). In the seedling shown, a pair of densely stained leaf primordia (l3 and l4) can be clearly detected at opposite sides of a non-staining meristem (not visible). Fully expanded cotyledons showed little or no *AS1*::GUS expression except for light staining associated with vasculature at the base of petioles. In older leaf primordia that had taken on the characteristic

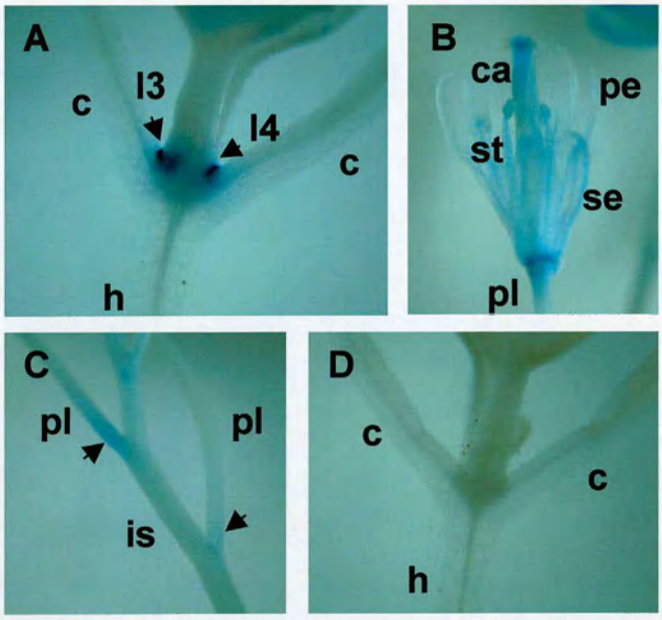

Figure 3.11 *AS1::GUS* expression in *Arabidopsis* transformants

Vegetative development of an *AS1::GUS* seedling (**A**). Strong GUS expression in the initiating 3rd and 4th true leaf primordia (black arrows) is depicted by blue staining either side of the first pair of rosette leaves. (**B**) shows GUS expression in a mature flower and it is also observed at the base of pedicels (**C**) as indicated by black arrows. A seedling (**D**) from a family segregating the transgene does not show GUS expression. **c**, cotyledon; **l**, leaf primordium; **h**, hypocotyl; **se**, sepal; **pe**, petal; **st**, stamen; **ca**, carpel; **pl**, pedicel; **is**, inflorescence stem.

dorsoventral flattened shape of a leaf blade and petiole, patchy light staining was observed in some seedlings though generally stain was absent. Staining also appeared absent from the apical hypocotyl.

In stained inflorescences, flowers of both lines displayed identical levels and patterns of staining. Both transgenics had GUS activity visible in floral organs at a low level of staining, a result in agreement with the disappearance of transcript from later floral organ primordia as shown by *in situ* hybridisation. In fully developed flowers weak staining was observed in prominent veins of sepals and petals (Figure 3.11B). GUS activity appeared more prominent throughout stamens. In the female gynoecium staining was strongly observed at the tips of the carpels. Further low levels of staining were observed at the base of the flower at the most distal end of each pedicel. In contrast to the *in situ* hybridisation experiments, GUS stain was observed at the base of each pedicel where it connected to the inflorescence stem (Figure 3.11C).

The *AS1* promoter also drove GUS expression strongly throughout the roots of seedlings and strongly within root meristems. This observation was surprising since *in situ* hybridisation at various stages of embryogenesis with an *AS1* probe did not detect expression in the embryonic root. If the GUS activity in roots reflected *AS1* activity it would be reasonable to expect detection of transcript in this region at a period when tissue identities are conferred. For this reason GUS staining in roots under control of this promoter region is likely to be unrepresentative of *AS1* expression and function. Perhaps other regulatory sequences are necessary for correctly limiting *AS1* expression to organ primordia. Otherwise RNA turnover might account for the conflicting observations. Except for this domain of expression, expression of the *AS1::GUS* reporter coincided with aerial lateral organ development, in agreement with the observations of *AS1* mRNA localisation shown by *in situ* hybridisation experiments. Therefore it can be assumed that the *AS1* promoter is sufficient to direct expression in *Arabidopsis* organ primordia.

3.2 Genetic interactions of *AS1*

3.21 Interactions of *AS1* with characterised developmental mutants

The *as1-1* and *as1-magnifica* mutants were used in the following crosses to determine possible genetic interactions. These were not assumed to be null *as1* mutants although they represented the severest alleles available for genetic studies. The following crosses did not take into account phenotypic differences that could occur as a result of crossing into a background that may contain other modifiers. The distinctive *as1* mutant rosette leaf and floral defects were used as phenotypic criteria for selecting for *as1* mutations in segregating populations.

The *CUP-SHAPED COTYLEDON* genes

The expression pattern of *AS1* suggests that it may have an early role during embryogenesis in specification of organ identity. Expression of the redundantly acting *CUC1* and *CUC2* genes mark the incipient shoot apical meristem as well as the boundaries of cotyledon primordia, consistent with a proposed role in SAM formation and cotyledon separation (Aida *et al.*,1999; Takada *et al*, 2001). Since these genes have a domain of expression adjacent to the expression domain of *AS1*, they potentially interact with *AS1* in wild type embryo development. Double mutations in *CUC1* and *CUC2* result in the lack of an embryonic SAM and a nearly complete fusion of the cotyledons, however each single mutant is basically normal, less than 1% of single mutants show cotyledon fusion along one side of the margins (Aida *et al.*, 1997). A triple *as1 cuc1 cuc2* mutant was constructed to determine the relationship between *AS1*, *CUC1* and *CUC2*.

For construction of the triple mutants, plants homozygous for *as1-1* were crossed with plants homozygous for *cuc1* and heterozygous for *cuc2*. A single F2 family that segregated both *cuc1 cuc2* (seedlings with fused cotyledons lacking postembryonic tissues) and *as1-1* mutants was selected. In this family, approximately 1/16 of seedlings (18 of 273) with the *cuc1 cuc2* double mutant phenotype were observed. Approximately 1/4 (70 of 273) of the other F2

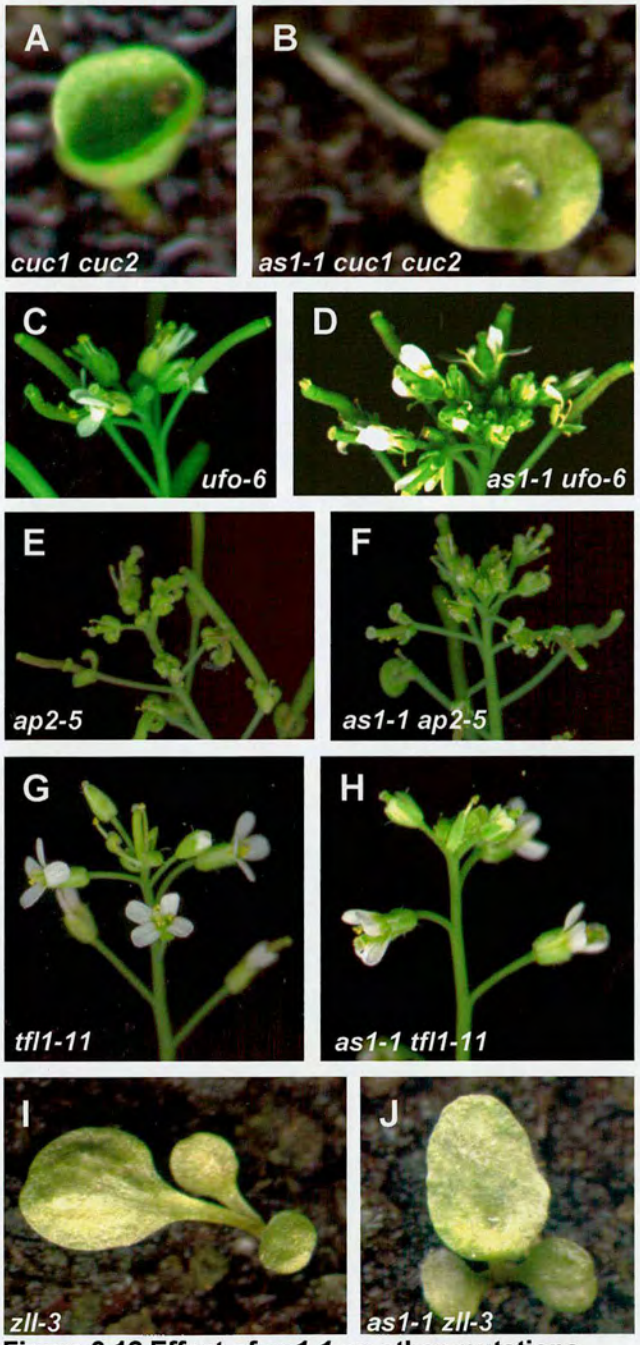

Figure 3.12 Effect of *as1-1* on other mutations
Single or double mutants (**A**) *cuc1 cuc2*, (**C**) *ufo-6*, (**E**) *ap2-5*, (**G**) *tfl1-11*, (**I**) *zll-3* that were crossed to *as1-1* mutants. Combined mutant phenotypes are shown of (**B**) *as1-1 cuc1 cuc2*, (**D**) *as1-1 ufo-6*, (**F**) *as1-1 ap2-5*, (**H**) *as1-1 tfl1-11*, and (**J**) *as1-1 zll-3*.

seedlings conditioned *as1-1* phenotypes and the remaining seedlings appeared wild type. Since no novel phenotype was observed, F3 progeny were grown from several *as1-1* F2 individuals. One F3 family was selected that segregated the *cuc1 cuc2* phenotype. Exactly 1/16 of segregants with the *cuc1 cuc2* phenotype (3 of 48) were observed. Since the F2 parent was predicted to be homozygous for the recessive *as1-1* mutation and heterozygous for both *cuc1* and *cuc2* mutations, these individuals were assumed to represent *as1 cuc1 cuc2* triple mutants. All remaining seedlings in the F3 displayed *as1-1* phenotypes, and therefore were assumed not to be homozygous for both *cuc* mutations.

The results of the genetic cross indicated that the *as1 cuc1 cuc2* triple mutant (Figure 3.12B) displays the same phenotype as the *cuc1 cuc2* (Figure 3.12A) double mutant, showing fused cup-shaped cotyledons and complete lack of an embryonic SAM. This epistasis of *cuc1 cuc2* to *as1* is consistent with *AS1* not being functional in the *cuc1 cuc2* double mutant. This suggests that *CUC1* and *CUC2* act before *AS1* in wild type development. *CUC1* and *CUC2* are needed for the formation of normal cotyledons and leaves. The *as1* mutant phenotype suggests that development of cotyledons and leaves is affected at a later stage of development. Therefore the failure to produce these in *cuc1 cuc2* double mutants might obscure the *as1* mutant phenotype.

The *UNUSUAL FLORAL ORGANS* gene

UNUSUAL FLORAL ORGANS (*UFO*) is weakly expressed in the SAM centre and strongly at the SAM periphery throughout *Arabidopsis* development. Since organs are derived from cells at the SAM periphery it was decided to test for interaction between the *AS1* and *UFO* genes using the respective mutants. The *ufo* mutant has flowers with variable homeotic organ transformations. A weak allele, *ufo-6* was used for crossing to an *as1-1* mutant since it was fertile. *ufo-6* mutants in the F2 were identified by variable organ number or homeotic transformations. In the F2 from the cross, a total of 74 plants were observed to segregate 47 wild type

plants: 11 *ufo-6* mutants: 12 *as1-1* mutants: 4 *ufo-6 as1-1* double mutants. This was approximate to a Mendelian 9:3:3:1 ratio.

The phenotype of the double mutants observed appeared additive of both single mutations. The double mutants entirely resembled *as1-1* single mutants until the reproductive phase of growth. However, flowers consisted of highly variable organ numbers and homeotic transformations (Figure 3.12D) as for *ufo-6* single mutant flowers (Figure 3.12C). Since the phenotype of the *as1-1 ufo-6* double mutant appeared to combine the vegetative and floral defects of both respective single mutations it was concluded that *UFO* and *AS1* have separate roles in *Arabidopsis* development.

The *APETALA2* gene

APETALA2 (AP2) is expressed in organ primordia throughout *Arabidopsis* development although it only conveys a homeotic floral phenotype. To assess if *AP2* and *AS1* have a role in development that is masked by redundancy double mutants were made. Sixty-two F2 plants were observed for segregation of the *as1-1* and the *ap2-5* mutations (plants with a reduced petal number). These segregated a 9:3:3:1 Mendelian ratio as 38 wild type plants: 12 *as1-1* mutants: 9 *ap2-5* mutants: 3 *as1-1 ap2-5* double mutants. The three individuals that were assumed to be double mutants resembled the *as1-1* single mutant until the stage of flowering. Upon flowering the double mutants displayed the *ap2-5* phenotype (Figures 3.12E and F) and suggested an entirely additive effect results in plants carrying both single mutations. If *AP2* does have an additional redundant role in vegetative development this is unlikely to be a result of interaction with the *AS1* gene product.

The *TERMINAL FLOWER1* gene

TERMINAL FLOWER1 (*TFL1*) is an inflorescence meristem identity gene, and *tfl1* mutants develop a terminal flower at the apex of the inflorescence. Since *AS1* is

also expressed in the inflorescence apex at the sites of organ initiation double mutants of *as1-1* and *tfl1-11* were made. F2 plants were scored following the production of several inflorescences each; those with perturbed determinacy were identified as *tfl1-11* mutants. The 58 F2 plants observed segregated 27 wild type plants: 12 *as1-1* mutants: 15 *tfl1-11* mutants: 4 *as1-1 tfl1-11* double mutants. The frequency of double mutants was ~1/16 as expected. The *as1-1 tfl1-11* double mutants resembled *as1-1* plants however inflorescences eventually terminated with a characteristic terminal flower as observed in *tfl1-11* single mutants (Figure 3.12G and H). This phenotype was additive and suggests that the *AS1* and *TFL1* genes do not interact in wild type *Arabidopsis* inflorescence development.

The *PINHEAD/ZWILLE* gene

Mutations at the *PNH/ZLL* locus result in plants that have a defective embryonic SAM and that often terminate at the apex with a pin or leaf-like structure. Normally *PNH/ZLL* is expressed in the SAM and adaxially in cotyledon primordia overlapping with the expression domain of *AS1* in the embryo. A plant heterozygous for the recessive strong *zll-3* mutant allele was crossed to a homozygous *as1-1* mutant. Several F1 plants were selfed and the F2 families observed for segregation of the *zll-3* shootless phenotype. In an F2 of 121 seedlings there were counted 73 wild type plants, 33 *as1-1* mutants and 11 *zll-3* mutants. However no novel phenotype was observed that could be identified as an *as1-1 zll-3* double mutant. Since a higher frequency of *as1-1* phenotypes were observed over *zll-3* phenotypes, F3 plants were scored to deduce whether the *as1-1* mutation was epistatic to the *zll-3* mutation.

Six F2 siblings displaying the *as1-1* mutant phenotype, and therefore assumed to be homozygous for the *as1-1* mutation, were selfed and segregation of F3 seedlings was observed. Three F3 families segregated a *zll-3* mutant phenotype that was likely to represent the *as1-1 zll-3* double mutant at near the expected frequency of 1/4 (combined F3 segregation of 24 double mutants in a total of 81 plants) for a predicted parental genotype of *as1-1/as1-1 zll-3/+*. All other seedlings

in the F3 displayed an *as1-1* mutant phenotype. In three other F3 families, only the *as1-1* phenotype was observed and therefore the F2 parents were predicted to lack the *zll-3* mutation. The *as1-1 zll-3* double mutants were therefore identical to *zll-3* single mutants (Figure 3.12I and J) showing that the *zll-3* mutation is actually epistatic to the *as1-1* mutation and proving the original F2 phenotype frequencies to be misleading. Therefore *PNH/ZLL* is likely to act upstream of *AS1* in wild type development. Since *PNH/ZLL* is required for producing a normal embryonic SAM and subsequent leaf production, the *as1* mutant phenotype might be obscured by the *pnh/zll* mutant phenotype.

3.22 *AS1* function is independent of the *CLV/WUS* interaction

In *Arabidopsis* shoot and floral meristems, the *WUSCHEL* (*WUS*) gene is required for stem cell identity (Laux *et al.*, 1996; Mayer *et al.*, 1998). In contrast the *CLAVATA1*, *2*, and *3* (*CLV*) genes are thought to restrict stem cell identity and therefore to promote organ initiation. A self regulatory system in the shoot meristem has been proposed to involve interaction of these genes to control the size of the stem cell population from embryogenesis onwards. Since organ initiation involves recruitment of the daughter cells of the stem cell population, interaction of these regulators with regulators of organ initiation seemed feasible. To study genetic interactions between *AS1*, involved in organ initiation, and the *CLV/WUS* genes, involved in stem cell regulation, double mutant combinations were analysed throughout development.

Mutations in any of the *CLV* genes result in delayed organ initiation, leading to an accumulation of meristem cells and therefore an increase in the size of the shoot meristem (Clark *et al.*, 1993, Clark *et al.*, 1995; Kayes and Clark, 1998; Laufs *et al.*, 1998). The probable null allele *clv3-2* (Clark *et al.*, 1995) was tested for interaction with *as1*. The dome shaped *clv3* shoot meristems are enlarged relative to wild type, and the inflorescence meristems initiate many flowers around their periphery as a result (Figure 3.13A). Stems of *clv* mutants are also thicker relative to wild type. The inflorescence meristems of *as1-1* mutants are the same size as those of the wild type.

Pollen of *clv3-2* was crossed onto an *as1-1* mutant individual and segregation of mutant phenotypes observed in the F2 generation. Of 60 individuals of the *as1-1/clv3-2* cross, 25 wild type plants were observed, 18 *as1-1* single mutants, 15 *clv3-2* single mutants and 2 plants with a novel phenotype. This ratio approximated to 9:3:3:1, suggesting that the novel phenotype represented *as1-1 clv3-2* double mutants. The 2 presumptive double mutants had the rosette leaf phenotype of *as1-1* single mutants (Figure 3.13C). Emergence of the

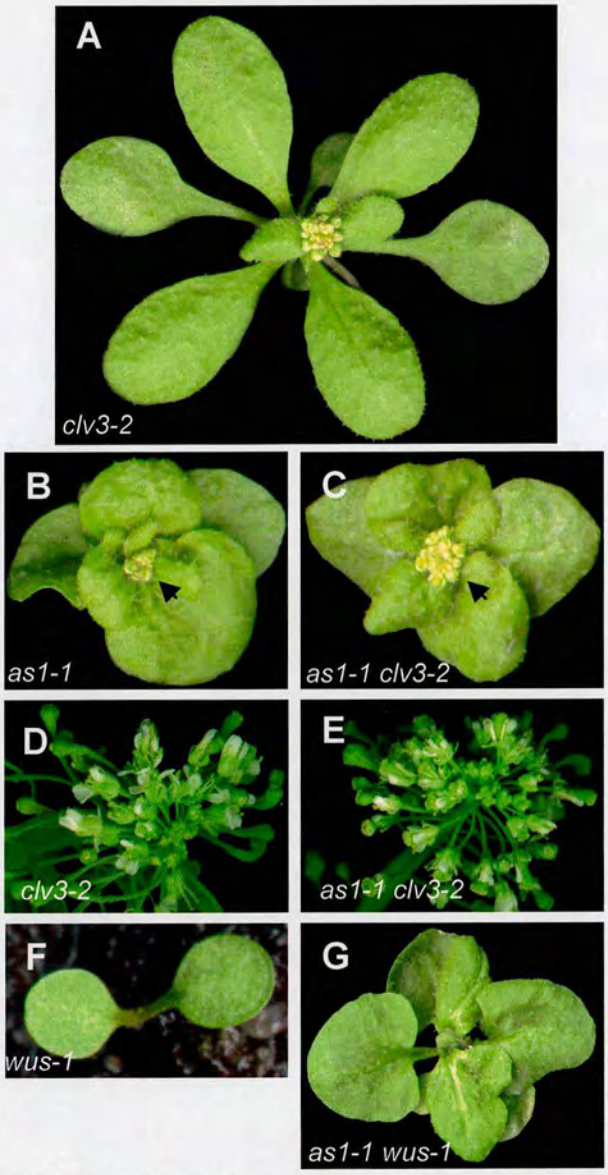

Figure 3.13 Effect of *as1-1* on *clv3-2 and wus-1* mutations
A *clv3-2* mutant (**A**) has an enlarged meristem and produces more flowers than wild type. Comparison of an *as1-1* (**B**) and an *as1-1 clv3-2* double mutant (**C**) reveals an additive phenotype. In (**C**) the leaves resemble those of an *as1* mutant whilst the large apex (compare apices indicated by black arrows) is typical of a *clv3-2* mutant. Further, *clv3-2* mutants (**D**) produce bent club-shaped siliques which are also observed in the *as1-1 clv3-2* double mutant (**E**), suggesting that *as1* and the *clavata* genes function in independent pathways. (**F**) a *wus-1* mutant and (**G**) an *as1-1 wus-1* double mutant of the same age have defective meristems and have terminated primordia initiation. The *as1-1 wus-1* double mutant has the vegetative phenotype of an *as1-1* mutant.

inflorescence meristem however revealed significantly more flowers than in an *as1-1* mutant (compare Figures 3.13B and C) and wider inflorescence stems, both attributes of *clv* mutants. Florally, *clv* mutants produce short, wide, club-shaped siliques that often take on a bent appearance (Figure 3.13D). Siliques of the *as1-1 clv3-2* double mutant (Figure 3.13E) were identical to the single *clv3-2* mutant. These observations suggest that the *as1-1* and *clv3-2* mutations have an additive effect and therefore the *AS1* and *CLV* genes are likely to regulate different targets.

Plants heterozygous for *wus*-1 were crossed to *as1-1* mutants. Plants were selfed in the F1 and F2 progeny were observed for segregation of the *wus-1* phenotype. A total of 70 plants were observed in an F3 family that segregated the *wus-1* phenotype. The frequency of seedling phenotypes were as follows; 30 wild type: 16 wus-1: 23 as1-1: 4 novel seedling phenotypes. The frequency of novel phenotypes indicated that they were likely to be *as1-1 wus-1* double mutant seedlings.

as1-1 wus-1 double mutants were similar in overall plant architecture to *wus-1* mutants, each seedling terminated growth in the vegetative phase of development after production of several pairs of leaves. However rosette leaves of *as1-1 wus-1* doubles were heart-shaped, rumpled and margins were curled as observed for vegetative development of *as1-1* mutants. The combination of both mutant phenotypes in the *as1-1 wus-1* double mutant indicated that the effect of both mutations upon *Arabidopsis* development is additive. Therefore this is consistent with the functional product of the *AS1* gene acting in a separate developmental pathway to *WUS* in the meristem. The results of the *clv* and *wus* crosses indicate that the role of *AS1* is independent of the signalling network that regulates maintenance of the stem cell population in the *Arabidopsis* SAM.

3.23 A novel phenotype is displayed by *as1 stm* double mutants

AS1 was found to be expressed in lateral organ initials in a complementary domain to *STM* expression. Loss-of-function alleles of both *AS1* and *STM* were available to analyse the effect of both mutations in the same genetic background. *STM* was chosen for crossing as it is the only *knox* gene with a known loss-of-function allele. Since *stm-1* mutants are known to be infertile, plants heterozygous for the strong *stm-1* allele (Figure 3.14A; Barton and Poethig 1993) were crossed as males to *as1-1* (Figure 3.14B) and *as1-magnifica* mutants.

In the cross with the *as1-1* mutant, plants resembling wild type were selected from the F1 and selfed. In F2 progeny that segregated the *stm-1* mutation the following percentages for each phenotypic class were observed - wild type (54 %): *as1-1* (24 %): *stm-1* (16 %): novel phenotype (6%). The frequency at which the novel phenotype occurred in the F2, ~1/16, suggested that it represented the *as1-1 stm-1* double mutant.

In the vegetative phase of development *as1-1 stm-1* mutants were indistinguishable from *as1-1* single mutants, cotyledons and rosette leaves of the double mutant resembled those of the *as1-1* mutant (Figure 3.14C). The *as1-1 stm-1* double mutants were therefore able to form an embryonic SAM and maintain it post-embryonically. This differs from the rare 'escape' phenotype of *stm-1* single mutants in which an ectopic SAM is formed from the hypocotyl (Barton and Poethig, 1993). In reproductive development, *as1-1 stm-1* double mutants differed from *as1-1* single mutants and wild type. Although overall shoot architecture of *as1-1 stm-1* was similar to wild type plants, lateral shoots generally formed subtended by cauline leaves in place of flowers. Double mutants could first be identified prior to expansion of the inflorescence stem. In *as1* single mutants cauline leaves subtending the first flower were observed following production of a rosette, however at the same developmental stage in double mutants, only cauline leaves were visible and flowers appeared absent (compare Figures 3.14B and C). Cauline leaves were also asymmetric and lobed like the *as1-1* single

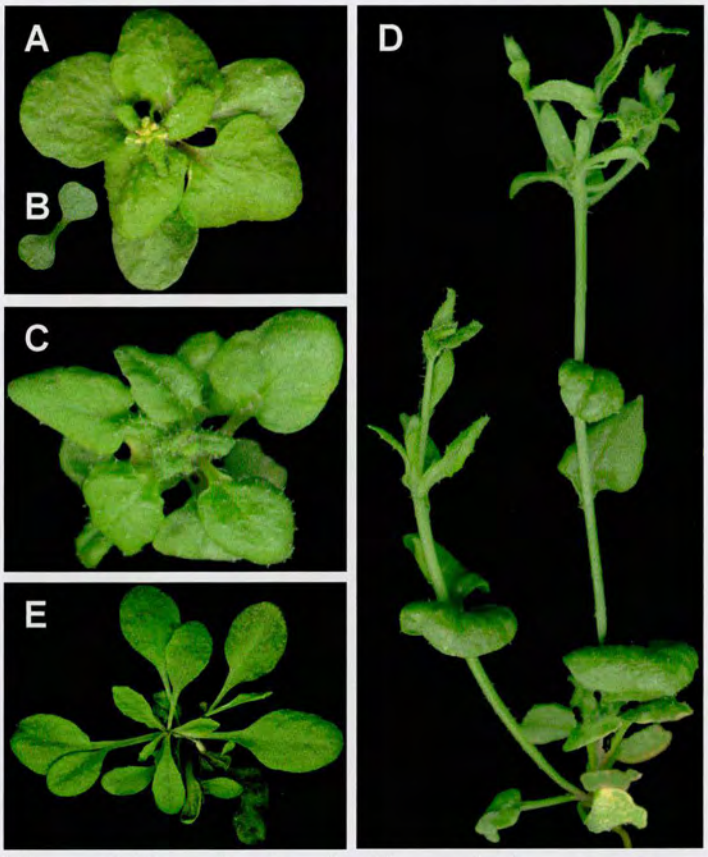

Figure 3.14 *as1 stm* double mutants possess a functional meristem

Vegetative phenotype of *as1-1* (**A**) and *stm-1* (**B**) which arrests growth postembryonically due to loss of meristematic activity. In *as1-1 stm-1* double mutants, vegetative development (**C**) mimics that of *as1* mutants in terms of perturbed leaf development. In the reproductive phase (**D**) the inflorescence is similar to weak *stm* mutants producing incomplete infertile flowers and a greater number of axillary stems. A plant predicticted to be heterozygous for *as1-magnifica* and homozygous for *stm-1* is shown in (**E**).

mutant phenotype. Close spacing of cauline leaves on inflorescence stems gave plants a bushy appearance and occasional flowers that formed were incomplete. Flowers typically had reduced petal and stamen numbers and always lacked a central carpel. A weak allele, *stm-2* probably lacks an embryonic SAM although usually forms a bushy plant with aerial rosettes, a reduced number of flowers and a reduced number of petals, stamens and carpels (Clark *et al.*, 1996; Endrizzi *et al.*, 1996). The *as1-1 stm-1* double mutant phenotype therefore resembled that conditioned by a weak *stm* allele. Since the proposed *as1-1 stm-1* double mutant was infertile, genotyping was not possible by analysis of its progeny.

Instead F2 individuals with an *as1-1* phenotype, assumed to be homozygous for the recessive *as1-1* allele, were selfed and the F3 generation scored. One of the three F2 parents segregated only *as1-1* phenotype F3 individuals and therefore had the predicted genotype *as1-1/as1-1 STM+/STM+*. In progeny of the remaining two F2 parents, three quarters of F3 individuals (92/123) conditioned *as1-1* single mutant phenotypes and one quarter for the weak *stm* phenotype (31/123), observed following transition into the reproductive phase of development. Parents of F3 progeny which segregated in this way were assumed to have the genotype *as1-1/as1-1 stm-1/+*. This data verified that the novel phenotype observed was the *as1-1 stm-1* double mutant. Possible modifiers in the *as1-1* background therefore seemed unlikely to be responsible for rescuing the *stm-1* mutants. Byrne and others (2000) genotyped the presumptive *as1-1 stm-1* double mutant and confirmed it to be homozygous for the *stm-1* mutation.

The *as1-1 stm-1* phenotype showed that *as1-1* suppresses the *stm-1* mutation in embryonic and vegetative growth and restores a functional SAM capable of postembryonic growth. However, in reproductive development *as1-1* only partially suppresses the *stm-1* phenotype. In terms of leaf development, the *stm-1* mutation had no effect on the phenotype of the *as1-1* single mutant phenotype at any stage of development since all leaves appeared asymmetric and lobed. This also suggested that misexpression of *STM* in leaves of *as1-1* mutants was unlikely to be responsible for the asymmetric leaf phenotype.

The analysis of F2 progeny from the cross with *as1-magnifica* and *stm-1*/+ plants was similar although a further new phenotype was seen. Of 121 F2 plants scored the following frequencies were observed - wild type (62.8 %): *as1-magnifica* (19.0 %): *stm-1* (10.7 %): novel phenotypes (7.4 %). Of nine plants with a novel phenotype, 6 plants resembled the phenotype described before, possessing rosette leaf morphology typical of *as1-magnifica* mutants and development in the reproductive phase as for a weak *stm* mutant. The three other plants differed only in leaf appearance, leaves were wild type instead of asymmetric. It was predicted that the dose of *AS1* in a homozygous *stm-1* background was likely to be responsible for the 2 different phenotypes. The latter phenotype was assumed to represent plants with the genotype *as1-mag*/+ *stm-1*/*stm-1* (Figure 3.14E). Despite observing a low frequency for this genotype it was not possible to verify this prediction in progeny due to infertility associated with homozygous *stm-1* mutants. Also unfortunately of five phenotypically wild type F2 parents that were selfed, only wild type and *as1-1* mutants segregated in the progeny suggesting that none of the parents selected carried the *stm-1* mutation initially. However if the prediction is correct it suggests that while the asymmetric leaf phenotype is only observed if plants are homozygous for *as1*, a functional meristem just requires the loss of one functional *AS1* copy.

Similar results from the cross with either *as1-1* or *as1-magnifica* indicated that both of the *as1* alleles are of similar severity although partial *AS1* activity may remain. These data suggest that if *STM* activity is lost, a functional meristem is not formed and if both *STM* and *AS1* activity is lost, a functional meristem is restored. The data also suggest that the leaf phenotype associated with *as1* single mutants was not dependent on *STM* activity.

The weak female sterile *stm-2* allele was also crossed to an *as1-1* mutant as a heterozygote. An F2 was found that segregated the *stm-2* mutation and the following phenotype frequencies were found. In a total of 175 siblings the observed ratio was 128 wild type plants: 34 *as1-1* mutants: 5 *stm-2* mutants: 8

as1-1 stm-2 double mutants. The phenotype conditioned by the double mutants was very similar to the *as1-1* single mutant phenotype, although flowers still resembled those of the *stm-2* mutant and no seed could be harvested. However the double mutants did not have other characteristic features of the *stm-2* mutant such as a bushy vegetative phenotype and aerial rosettes. The *as1-1 stm-2* double mutants segregated at a near expected frequency although the number of *stm-2* single mutants appeared low suggesting that perhaps different doses of the *as1-1* mutation may give different phenotypes. To verify that the novel phenotype observed was homozygous for both mutations, F2 parents with an *as1-1* homozygous phenotype were selfed and the F3 progeny observed. In a total of 57 plants that were observed in an *stm-2* segregating F3, 49 conditioned an *as1-1* phenotype and 8 plants were the proposed *as1-1 stm-2* double mutant. Since no other phenotypes were seen these were most probably double mutants. It was concluded that the *as1-1* mutation could therefore also suppress a weak *stm* allele at least embryonically and vegetatively, although only partial suppression was observed in the reproductive phase of development as with the strong *stm-1* allele.

3.24 *AS1* is misexpressed in *stm-1* embryos

Since at the embryonic stage at least, loss of *AS1* activity was able to suppress the effects of the *stm-1* mutation on the meristem, *in situ* hybridisation experiments were performed to investigate whether *AS1* was expressed ectopically in *stm-1* mutant embryos. Since homozygous *stm-1* mutants are infertile and do not produce siliques, analysis of *AS1* expression was examined in embryos from the siliques of individuals that were heterozygous for the strong *stm-1* allele. Therefore 25% of embryos are expected to be *stm-1* homozygotes. Siliques of a heterozygous *stm-1/+* parent were harvested taking the 15 most apical siliques to capture all stages of embryo development. Expression of *AS1* in these embryos was investigated using the same antisense riboprobe that had previously been used for localising *AS1* transcript in wild type tissues.

By the heart-stage of development, wild type embryos express *STM* in cells of the presumptive SAM, between the emerging cotyledon primordia (Long *et al.*, 1996; Long and Barton, 1998; Aida *et al.*, 1999). By this stage the *stm-1* mutant phenotype is not yet apparent (Barton and Poethig, 1993) so phenotypic identification of homozygous *stm-1* mutant embryos was not possible. Previously it was demonstrated that *AS1* expression at the heart-stage of embryogenesis is localised to the subepidermal cells of emerging cotyledon primordia but absent from cells of the presumptive SAM (Figure 3.15A). Following *in situ* hybridisation of the *AS1* probe with sections of siliques, expected to segregate approximately 1/4 embryos homozygous for *stm-1*, 13 of 60 embryos observed at heart-stage showed *AS1* expression throughout the apical part of the embryo (Figure 3.15B). The *AS1* expression domain in these embryos encompassed cells of the presumptive SAM as well as cells of the cotyledon primordia. Furthermore, a series of sections through a heart-stage *stm-1* mutant embryo were probed to eliminate the possibility that it might just be cells flanking the presumptive SAM that were expressing *AS1*. *AS1* was seen to be expressed in the apex of all the serial sections (Figure 3.16A-E). The genetic and molecular interaction between *AS1* and the *knox* gene *STM* suggests a mechanism whereby *STM* represses *AS1*

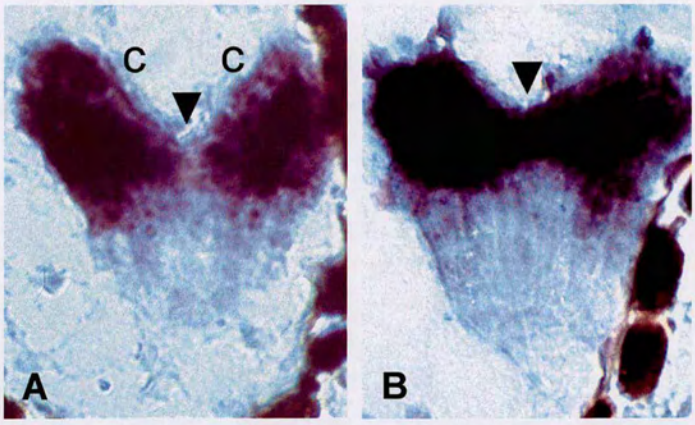

Figure 3.15 *AS1* is misexpressed in *stm-1* embryos
In a wild type heart-stage embryo (**A**) *AS1* is expressed in the cotyledons and absent from the presumptive SAM (arrowheads). In an *stm-1* mutant heart-stage embryo (**B**) *AS1* is expressed in the cotyledons and the presumptive SAM. **c**, cotyledon. *Bars =25μm.*

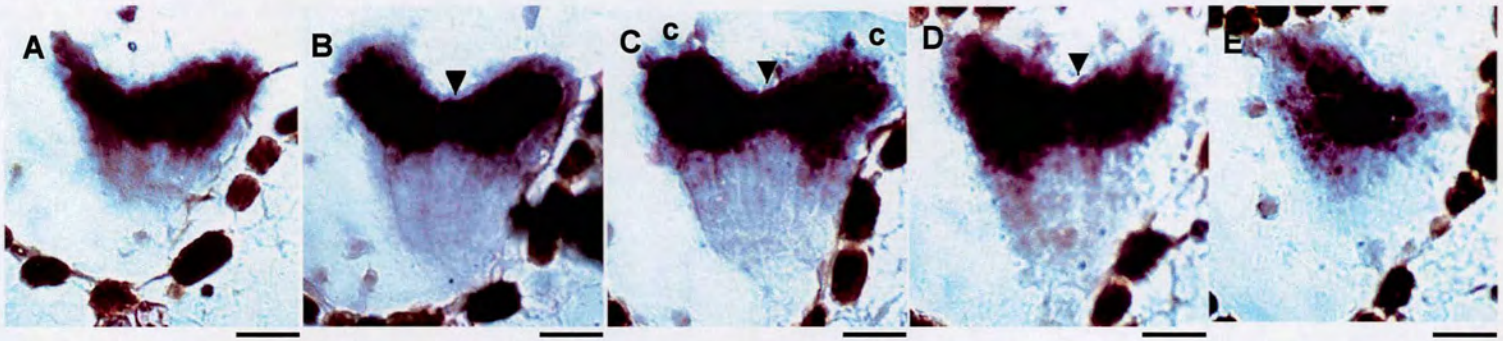

Figure 3.16 *AS1* expression in serial sections of an *stm-1* mutant embryo
(**A**)-(**E**) are serial sections 7μm thick, through an *stm-1* mutant heart-stage embryo. *AS1* transcript is detected in the two cotyledon primordia and also at the embryo apex inbetween the cotyledons in all cells of the presumptive SAM indicated by arrowheads. **c**, cotyledon. *Bars = 25μm.*

in cells of the meristem. In the meristem, *STM* expressing cells appear to occupy a separate domain to organ founder cells on the flank of the meristem that express *AS1*. Hybridisation of *AS1* and *STM* antisense RNA probes to serial sections of an *Arabidopsis* embryo would be a good test of this assumption. However, these results suggest that loss of *STM* activity in cells of the meristem allows the ectopic expression of *AS1* in the presumptive SAM. In wild type development, the SAM becomes apparent by the torpedo stage of embryogenesis, but *STM* which is required for SAM development, is expressed earlier in the SAM initials of globular stage embryos. Since ectopic *AS1* expression was observed at the heart stage of *stm-1* embryogenesis this is consistent with *STM* repression of *AS1* rather than attributed to the loss of SAM cells in *stm-1* embryos.

The phenotype of *stm-1* mutants suggests that the embryonic meristem is never formed and that instead organ fate is conferred to the cells of the apical region that would normally form a functional and active SAM. These molecular epistasis results suggest that the subsequent derepression or misexpression of *AS1* could itself be responsible for causing the *stm-1* terminal meristem phenotype. Continuous *AS1* expression across the base of the cotyledon primordia and apex may also explain the partial fusion of the cotyledons that is observed in *stm-1* mutants. *AS1* expression in apical cells of *stm-1* embryos could either be directly responsible for the *stm-1* phenotype, or result from indirect effects on other genetic pathways that affect expression of *AS1*. Because *AS1* expression coincides with the timing of a cell's commitment to organ fate its role could be to confer organ fate to cells. The role of *STM* in wild type plants may therefore be to confer meristematic establishment and maintenance as a result of downregulating *AS1* and repressing organ fate. Conversely, *AS1* expression could be indicative of a loss of meristem fate rather than conferring organ fate. However, it cannot be ruled out that *AS1* expression occurs as a result of a cell's determination to organ fate rather than being sufficient for this. It would be interesting to see if overexpression of *AS1* results in *Arabidopsis* plants that lack functional meristems.

3.25 *STM* expression is unaffected in *as1* mutants

STM expression was examined in *as1* mutant apices for the following reasons:

1) The reciprocal expression patterns of *STM* and *AS1* in *Arabidopsis* suggests that mutual repression may exist in the shoot apical meristem to separate their functional domains. *STM* represses *AS1* in cells of the shoot apical meristem and as such may maintain the undifferentiated state of these cells. *STM* expression disappears from organ initials at about the time they begin to express *AS1* (Long and Barton, 1996). Therefore, *AS1* might be required to repress *STM* in organs.

2) *PHAN*-like genes have been shown to act as negative regulators of *knox* gene expression in maize and *Antirrhinum* (Timmermans *et al.*, Tsiantis *et al.*; 1999).

3) Misexpression of *knox* genes in leaves is associated with the conditioning of aberrant morphologies. *STM* misexpression may be a determinant of the *as1* mutant phenotype.

in situ hybridisation experiments were performed on both wild type and *as1* mutant apices to ensure that the *STM* probe detected a pattern of RNA expression consistent with previously reported results by Long and Barton (1996).

In inflorescence apices, *AS1* expressing floral organ primordia, such as sepals and petals, initiate on the flanks of floral meristems. Neither wild type (Figure 3.17A) nor *as1* mutant (Figure 3.17B) floral organ primordia were seen to express *STM* transcript at any floral stage. STM expression was detected only in the meristem and hypocotyl only in each inflorescence. Therefore *STM* expression appears unchanged in *as1* mutants.

The expression pattern of *STM* in wild type embryogenesis has been well characterised (Long *et al.*, 1996; Long and Barton; 1998). It is found in presumptive SAM initials and cells of the SAM throughout late stages of embryogenesis. *STM* expression was also observed during embryogenesis in *as1* mutant embryos. *STM* was detected in the same pattern as wild type in cells of the SAM, and not in cells of the cotyledon primordia (Figure 3.17C). Similarly, in

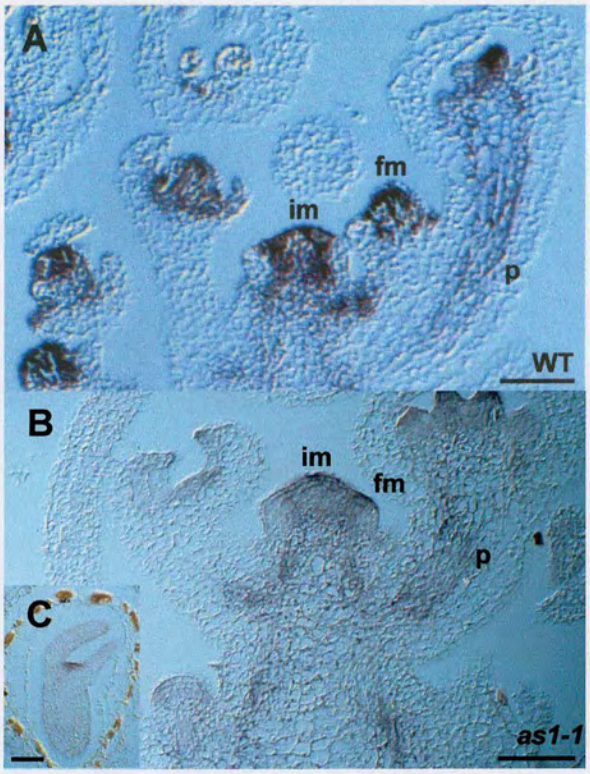

Figure 3.17 *STM* expression in *as1-1* mutants
In (**A**) a wild type inflorescence and (**B**) an *as1-1* inflorecence, *STM* expression is detected in meristems, stem and pedicels in a similar pattern and not detected in lateral organs. In an *as1-1* bending-cotyledon stage embryo (**C**) inset, *STM* transcript is detected as normal in cells of the SAM and absent from cotyledon primordia. **im**, inflorescence meristem; **fm**; floral meristem; **p**, pedicel. *Bars = 25μm*

rosette and cauline leaves of *as1* mutants it was not possible to detect ectopic *STM* transcript outside its normal domain of expression in cells of the meristem (data not shown).

Reporter gene expression

A further test to examine whether *STM* was misexpressed in *as1* organs was to assay *STM* reporter gene expression in *as1* mutants. A transgenic *Arabidopsis* line carrying the *STM* promoter upstream of the *uidA* gene, which encodes the β-glucuronidase (GUS) protein, was crossed to *as1* mutants. In stained *AS1+* seedlings of the transgenic line (Figure 3.18A), GUS activity could be detected strongly in the meristem and to a lesser degree in the surrounding apical region of the hypocotyl. Stain was not seen in the emerging leaf primordia, leaves or cotyledons. All F1 plants were predicted to be heterozygous for the *as1* mutation and to carry a single copy of the reporter transgene. A dosage-dependent effect of the *as1* mutation upon *STM* expression was not observed for any of the F1 seedlings. GUS staining was observed in the same pattern as the original parent line.

In a selected F2 family, approximately a quarter of all seedlings displayed an *as1* phenotype. GUS activity was detected in 21 of 27 seedlings with the *as1* phenotype as predicted for inheritance of a single, unlinked copy of the transgene. In all *as1* seedlings that carried the transgene, GUS activity was detected in a dense staining pattern in the meristem, and lighter staining throughout the surrounding apical region of the hypocotyl, as observed in the original line (Figure 3.18B). Staining was not apparent in cotyledons, emerging leaf primordia or later leaves. GUS stain was not detected in seedlings predicted to lack the transgene (Figure 3.18C). These results provide further evidence that *STM* is not regulated by *AS1*.

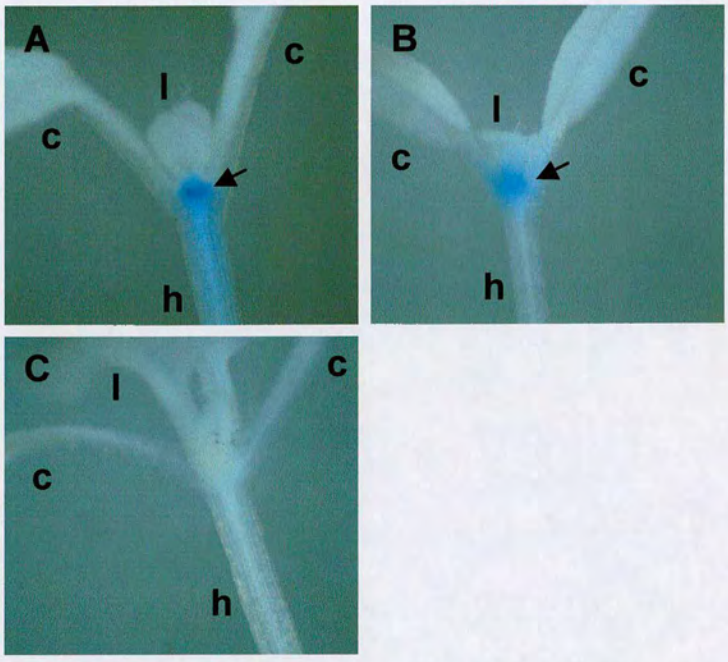

Figure 3.18 Expression of *STM::GUS* in *as1* seedlings
The wild type seedling (**A**) shows strong GUS expression in the meristem (black arrow) and also weaker staining below the meristem in the hypocotyl. The *as1-1* mutant seedling (**B**) as recognised by its shorter petiole length and down-curled cotyledons displays the same pattern of GUS staining in the meristem (black arrows). A seedling (**C**) of the same family, predicted not to carry the transgene shows no staining. **c**, cotyledon; **l**, leaf; **h**, hypocotyl.

Despite evidence that *PHAN*-like genes repress *knox* genes in other species, *AS1* is not a negative regulator of *STM*. The complementary domains of *AS1* and *STM* expression in the developing *Arabidopsis* meristem could be explained by the meristem specific repression of *AS1* by *STM*. The *as1* phenotype however cannot be explained by ectopic *STM* expression in developing organs. Furthermore, RT-PCR evidence agrees with the findings of *in situ* hybridisation demonstrating that *STM* is not found in *as1* mutant organs (data not shown and Byrne *et al.*, 2000). The downregulation of *STM* from sites of organ initiation in wild type *Arabidopsis* must therefore be controlled by other factors yet to be identified. *AS1* may still function as a repressor of other *Arabidopsis knox* genes.

3.3 *knox* genes are negatively regulated by *as1*

3.31 *KNAT1* is ectopically expressed in *as1* lateral organs

The expression of the *knox* gene *KNAT1* was compared in wild type and *as1* mutants for two reasons.

1) Other genes that encode *PHAN*-like proteins are negative regulators of *knox* genes in that they prevent *knox* expression in organs (Waites *et al.*, 1998; Tsiantis *et al.*, Timmermans *et al.*; 1999). 2) Ectopic expression of *KNAT1* under the control of a constitutive promoter results in *Arabidopsis* results in a leaf-lobing phenotype similar to aspects of the *as1* lobed leaf phenotype (Lincoln *et al.*, 1994; Chuck *et al.*, 1996).

A *KNAT1* probe was hybridised to tissue sections of wild type and *as1* mutant apices at various stages of development. *KNAT1* wild type expression patterns have been reported by Lincoln *et al.* (1994) and were repeated here to ensure that the probe recognised *KNAT1* transcript faithfully and to show comparative results.

Expression was first examined in wild type embryo development. Contrary to Lincoln *et al.* (1994), *KNAT1* expression was detectable in embryogenesis. Initially *KNAT1* expression was seen in lateral regions of the presumptive hypocotyl of the heart stage embryo (Figure 3.19A and B). By the torpedo stage of development, *KNAT1* was observed in a cylindrical domain in lateral areas of the hypocotyl (Figure 3.19C and D). Longitudinal sections through this cylinder reveal two apical-basal stripes of *KNAT1* expression. Transcript was not observed in either the apical region of the embryo or the region that gives rise to the roots. In bending cotyledon stage embryos, *KNAT1* expression expands in correlation with the expanding hypocotyl region (Figure 3.19E) and this pattern remains unchanged through maturation of the embryo at the upturned-U stage (Figure 3.19F). In all stages of embryo development, *KNAT1* is apparently absent from cells that form

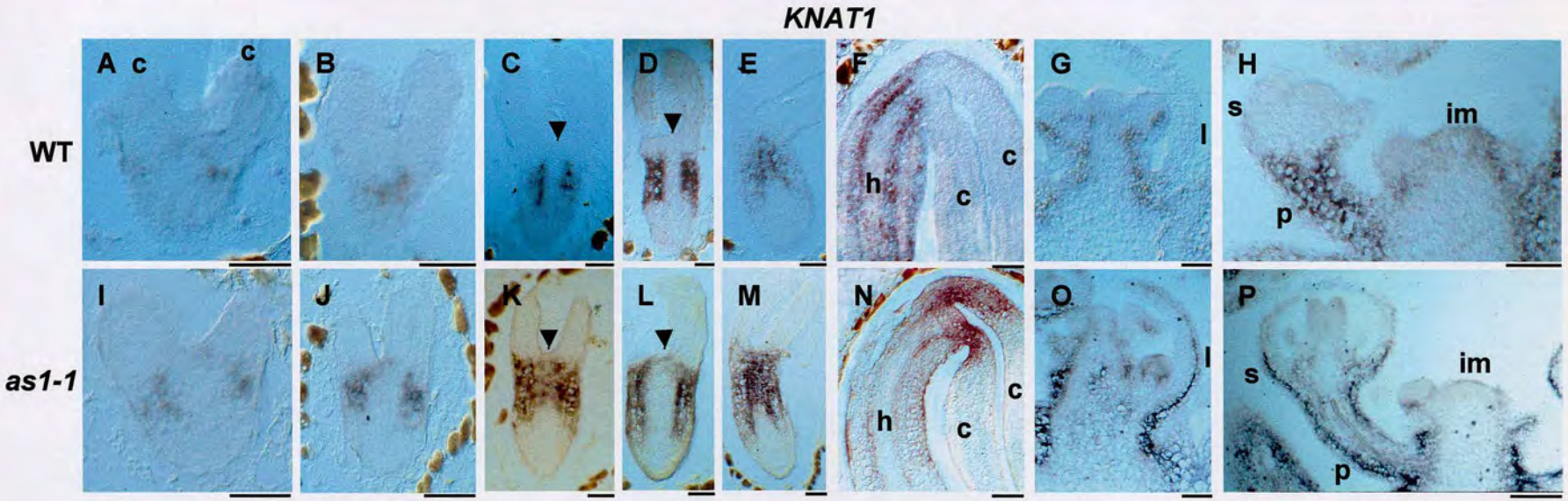

Figure 3.19 *KNAT1* expression in wild type and *as1-1* mutant *Arabidopsis* development
(**A**)-(**H**) show *KNAT1* expression, determined by *in situ* hybridisation, in sections of wild type plants, (**I**)-(**P**) show *KNAT1* expression in sections of *as1-1* mutants. Transcript is seen as purple to dark brown clolour. Stages of development are; (**A**) and (**I**) heart-stage embryo, (**B**) and (**J**) late-heart/torpedo stage embryo, (**C**) and (**K**) torpedo stage embryo (frontal longitudinal), (**D**) and (**L**) torpedo stage embryo (sagittal longitudinal), (**E**) and (**M**) bending-cotyledon embryo, (**F**) and (**N**) upturned-U embryo, (**G**) and (**O**) vegetative/reproductive transition, (**H**) and (**P**) inflorescence apex. *Note* not all sections are median [e.g. (**E**), (**K**) and (**M**)]. Arrowheads indicate SAM position. **c**, cotyledon; **h**, hypocotyl; **l**, leaf; **im**, inflorescence meristem; **s**, sepal; **p**, pedicel. *Bars* = 25μm.

the SAM and the cotyledons. In early *as1* mutant embryos *KNAT1* transcript was localised in a similar pattern to wild type. However, in later stages of embryogenesis the cylinder of expression extended ectopically to a more apical position to below the presumptive SAM and cotyledon cells. Heart-stage *as1* embryos appeared to show normal *KNAT1* expression in lateral presumptive hypocotyl regions (Figure 3.19I and J). Ectopic apical expression was detected in torpedo, and bending cotyledon stage *as1* embryos (Figure 3.19K-M). At the cotyledon bending stage, ectopic *KNAT1* expression was visible in *as1* embryos at the base of the expanding cotyledons although not detected more distally in the cotyledons (Figure 3.19M). Walking-stick stage embryos were seen to have a larger domain of *KNAT1* expression at the base of the cotyledons, either side of the morphologically distinct embryonic SAM (Figure 3.19N). *KNAT1* transcript distribution was strong in the proximal third of the cotyledon primordia length, but not detected distally.

Longitudinal sections of seedlings that had undergone transition to flowering showed both rosette and cauline leaves at several stages of development and were ideal to observe whether *KNAT1* was ectopically expressed in *as1* mutant leaves. In wild type apices, *KNAT1* was confined to the outer cell layers or cortex of the primary inflorescence stem and a low level of expression at the base of the inflorescence meristem. *KNAT1* transcript was also distributed at the base of leaf primordia, however transcript was not observed in leaves (Figure 3.19G). Florally, depending on the plane of the section, *KNAT1* transcript was observed in cells encircling the base of floral primordia. Expression extended into the cortex of developing pedicels but stopped abruptly at the base of lateral inflorescence meristems and flowers.

This was compared to the *KNAT1* expression pattern in *as1* mutants. Patchy *KNAT1* expression was seen in proximal regions of *as1* rosette leaves, stronger levels of *KNAT1* were found in newly initiated *as1* cauline leaves (Figure 3.19O). The pattern of expression in proximal parts of the leaf primordia appeared

continuous, not patchy, and largely in abaxial tissues. More distally, the expression appeared patchy but generally localised to abaxial cell types.

In later wild type inflorescences (Figure 3.19H), *KNAT1* transcript was detected along the length of the inflorescence stem, in layers of the cortex. Pedicels also strongly expressed *KNAT1*, however transcript was absent from the three outer whorls of flowers; sepals, petals and stamens. No expression was detected in the inflorescence meristem or floral meristems.

The expression of *KNAT1* in *as1* mutant inflorescences (Figure 3.19P) was similarly strong in lateral areas of the inflorescence stem and in pedicels, and not detected in inflorescence or floral meristems. Florally however, it was noticeable that in sepals and petals, the leaf-like lateral organs of flowers, *KNAT1* transcript was present. Levels of expression were stronger in proximal regions of these organs, and lower levels of message were observed distally.

The most dramatic phenotypic effects of *KNAT1* overexpressed are on leaf development (Lincoln *et al.*, 1994). This suggests that misexpression of *KNAT1* in *as1* mutant leaves may be responsible for the altered development in these organs. Rosette and cauline leaves of *35S::KNAT1* transformants exhibit deep lobing, curling and wrinkling. These defects are also features of *as1* leaves, although lobing is not as pronounced and the final leaf shapes differ considerably. Sepal, petal and stamen length is reduced in both *35S::KNAT1* transformants and *as1* mutants compared to wild type flowers. In *as1* floral development, ectopic *KNAT1* expression was observed in floral organs. Ectopic *KNAT1* expression in *as1* mutant organs was generally observed in a gradient. Higher levels of *KNAT1* expression were detected proximally in organs and lower levels were detected distally.

The results described here indicate that *KNAT1* misexpression may result in the aberrant lateral organs seen in *as1* mutants. This hypothesis is supported by the severe organ phenotypes observed in *35S::KNAT1* transformants. Since wild type

plants do not express *KNAT1* normally in organs that express a functional *AS1* product, it can be postulated that *AS1* is a repressor of *KNAT1* in these organs. Therefore in *as1* mutants, *KNAT1* is able to be expressed due to a lack of repression by *AS1* in organ primordia.

3.32 Ectopic *knox* reporter gene expression in *as1* seedlings

To further test whether *knox* genes are ectopically expressed in *as1* mutant organs, transgenic plants were utilised that express the reporter β-glucuronisidase (GUS) from the *KNAT1* or *KNAT2* promoter. The *KNAT1::GUS* line crossed into an *as1-1* mutant did not give results, later this was found to be due to linkage of the *KNAT1::GUS* transgene to *AS1*. *KNAT2::GUS* was crossed into an *as1-1* mutant and results were obtained. An F2 family was selected on the basis that it segregated around one quarter of *as1-1* seedlings to three-quarters wild type seedlings. Of the *as1-1* seedlings around three-quarters stained positive for GUS indicating the presence of the *KNAT2::GUS* transgene.

In F2 seedlings with a wild type phenotype, strong staining was observed at the apex and much of the hypocotyl but not in leaves or leaf primordia except in the proximal regions of petioles (Figure 3.20A). *KNAT2::GUS* expression in *as1-1* seedlings was similar although leaf primordia were generally observed to have light staining (Figure 3.20B). In petioles staining was observed proximally extending distally to the base of the blade. Occasional light patches of staining were also observed on margins of several seedlings.

This ectopic expression of *KNAT2* in *as1-1* mutants demonstrates that *AS1* is also likely to negatively regulate *KNAT2* as well as *KNAT1* in lateral organs. Since *KNAT2* normally functions in the meristem and hypocotyl, and not in lateral organs it is possible that ectopic expression of *KNAT2* in *as1-1* mutant lateral organs may contribute to the observed mutant phenotype. A combination of *knox* gene misexpression in primordia may disrupt axes of organ development in *as1* mutants.

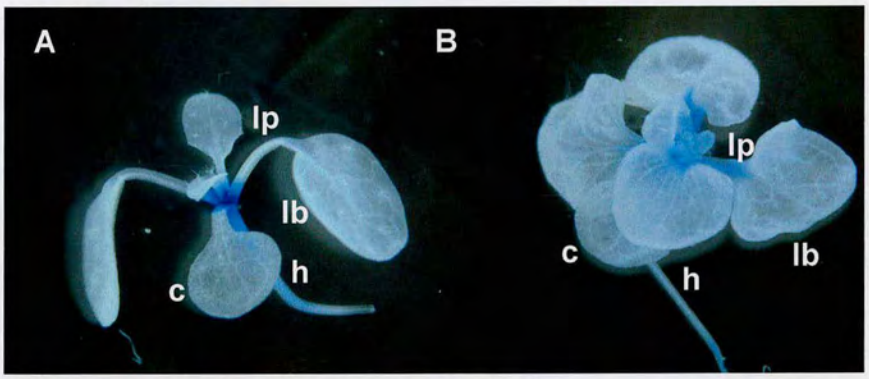

Figure 3.20 *KNAT2::GUS* in *as1* mutants
KNAT2::GUS expression in wild type (**A**). *KNAT2::GUS* expression in an *as1-1* mutant (**B**). In both (**A**) and (**B**) stain is seen to mark the meristem, hypocotyl, and proximal regions of the petiole. Furthermore in (**B**) staining is detected weakly in early leaf primordia, throughout petioles and in proximal regions of older leaves. **c**, cotyledon; **h**, hypocotyl; **lp**, leaf petiole; **lb**, leaf blade.

3.33 Constitutive expression of *KNAT1* in an *as1* background

The *knox* gene *KNAT1* was observed to be misexpressed in *as1* mutant organ primordia. *as1* mutations have broadly similar phenotypic effects to *KNAT1* misexpression. This raises two possibilities.

1) The effects of the *as1* mutation may result from ectopic expression of *KNAT1*. In this case it might be expected that the *35S::KNAT1* phenotype is epistatic to the *as1* mutation since it has a more severe phenotype. 2) That ectopic *KNAT1* expression represses *AS1* activity accounting for the similarity in phenotype between *35S::KNAT1* and *as1* mutants. In this case, the phenotype conditioned by *35S::KNAT1* might be expected to be independent of *AS1* activity.

A *35S::KNAT1* transgenic plant was crossed to an *as1-1* mutant and an F1 selected that had the original transgenic phenotype. A total of 236 F2 siblings were grown and phenotypes that segregated in this family were 74 wild-type: 16 *as1-1*: 120 *35S::KNAT1*: and 26 seedlings with a new phenotype. All resulting phenotypes are shown in Figure 3.21A-D. The new phenotype greatly resembled the *as1-1* mutant phenotype although lobing was much more apparent during the stage of rosette leaf development. The ratios were difficult to interpret given segregation for the *as1-1* mutation and the *35S::KNAT1* transgene. If the novel phenotype represented *35S::KNAT1* in a homozygous *as1-1* background ~3/16 or ~44 of these would have been expected. Therefore F2 plants were selected for selfing and analysis was undertaken of the F3 generation.

Initially, three F2 parents that exhibited the phenotype of the original *KNAT1* transgenic line were selected, these were selfed and phenotypes of F3 progeny were observed. For the first individual, 37/51 seedlings exhibited a phenotype identical to the *KNAT1* transgenic line and 14/51 seedlings resembled the enhanced *as1-1* phenotype with increased severity of lobing. Similarly in progeny of the second F2 parent, 47/64 seedlings resembled *KNAT1* transgenics whereas 17/64 seedlings gave the enhanced *as1-1* phenotype. The frequencies in the F3 approximated to a 3:1 ratio of *35S::KNAT1* seedlings to seedlings with an

Figure 3.21 Effect of overexpressing *KNAT1* in an *as1* mutant background

(**A**), (**B**), (**C**) and (**D**) show the four F2 phenotypes that segregate out of a cross between *35S::KNAT1* and an *as1-1* homozygous mutant. The presumed genotypes are (**A**) wild type, (**B**) *as1-1* mutant, (**C**) *35S::KNAT1*, and (**D**) *35S::KNAT1 as1-1* mutant.

enhanced *as1-1* phenotype. In the other F3 population, all 80 siblings showed a *35S::KNAT1* phenotype and no other phenotypes were observed. Therefore, two of the three F2 parents were assumed to represent plants heterozygous for the *as1-1* mutation and with two copies of the *KNAT1* transgene since only one quarter of plants gave rise to an asymmetric leaf phenotype but all plants displayed severe lobing. Since the other F2 parent gave rise to progeny without an asymmetric leaf phenotype it was assumed to represent a plant that did not carry the *as1-1* allele but carried two copies of the *KNAT1* transgene.

The frequencies observed in the F3 populations suggested that plants with an enhanced *as1-1* phenotype were homozygous for the *as1-1* mutation and carried at least a single copy of the *KNAT1* transgene. To test this assumption, five F3 populations that derived from selfed F2 parents selected for an enhanced *as1-1* phenotype were analysed. In all five F3 families, all seedlings exhibited morphology of the enhanced *as1-1* phenotype. Since the severe phenotype correlated with the *KNAT1* transgene, the five selected F2 parents were assumed to carry two copies of the transgene and be homozygous for the *as1-1* mutation. Presumably if an F2 parent had carried only a single transgene then the unenhanced *as1-1* phenotype would have segregated in the F3 along with the observed enhanced phenotype, however such an F3 population was not observed.

From these data it was concluded that constitutive *KNAT1* expression in a homozygous *as1-1* mutant enhances the lobed phenotype in leaves. Early *as1-1* mutant leaves have few lobes located proximally whereas later leaves have more lobes extending distally toward the leaf tip. Early leaves of seedlings with an enhanced *as1-1* phenotype however displayed prominent proximal lobing. The first pair of leaves never displayed signs of lobing - consistent with the appearance of the first pair of leaves observed in *KNAT1* transgenic seedlings. Therefore *KNAT1* misexpression in leaves appeared likely to be responsible for lobing. In *as1-1* mutants, which misexpress *KNAT1*, lobing of leaves was observed. The severity of lobing increased in *as1-1* mutants that also

constitutively express a *KNAT1* transgene. Therefore high levels of *KNAT1* expression in developing leaf primordia might be associated directly with increased severity of lobing. Another interpretation of these results is that development of asymmetry in the *as1-1* leaf shape is not a result of *KNAT1* misexpression in primordia since *KNAT1* transgenic seedlings in a wild type background do not acquire this characteristic. Whether the timing of *KNAT1* misexpression in leaf primordia is a factor in the acquisition of asymmetric leaf development cannot be deduced from this data. However previous work showed that *KNAT1* is misexpressed in both young and old leaf primordia in *as1-1* mutants (Byrne *et al.*, 2000). This suggests that the asymmetric leaf phenotype is not the result of *KNAT1* misexpression.

3.34 Constitutive expression of *KNAT1* rescues meristem function in an *stm* background

In the meristem, *STM* expression overlaps with the related *knox* genes *KNAT1* and *KNAT2*. *STM* has been found to repress *AS1*, which in turn, represses *KNAT1* and *KNAT2*. Therefore in *as1 stm* double mutants, other *knox* genes might substitute for loss of *STM* activity in the absence of *AS1*. However, *AS1* activity may prevent this from occurring in *stm* mutants. If this is the case, then in strong *stm* alleles which terminate after formation of cotyledons, a functional meristem may be restored by activating *KNAT1* expression. Since in strong *stm* alleles during embryogenesis, ectopic *AS1* expression in the SAM is potentially acting to confer organ fate and repress *knox* activity, constitutive expression of *KNAT1* product in the apex would be predicted to override *AS1* activity and restore a functional meristem. Experiments with a *KNAT1::GUS* reporter line (Ori *et al.*, 2000) suggest that repression by *AS1* requires sequences 5' to the *KNAT1* coding region. Therefore *AS1*-independent *KNAT1* expression could be achieved from a different promoter, e.g. the constitutively active CaMV 35S promoter.

To test whether constitutive expression of *KNAT1* could complement the loss of *STM* activity, a *35S::KNAT1* transgenic plant was crossed to a plant heterozygous for the *stm-1* mutation. As described earlier, plants homozygous for the *stm-1* mutation lack a functional meristem which results in a lack of postembryonic growth. The *35S::KNAT1* transgene results in plants with a deeply lobed leaf phenotype. An F1 individual with the lobed leaf phenotype was selected and selfed. In the F2 population, 291 individuals were examined to identify potential homozygous *stm-1* mutants that also constitutively expressed *KNAT1*.

Wild type phenotypes were found amongst the F2 population at an expected ratio of 3/16 (57 plants out of a total 291). Plants were identified in the F2 that had the phenotype of terminated growth following production of only a pair of cotyledons. The phenotype of these plants was considered to be identical to that of homozygous *stm-1* mutant individuals. This confirmed that the F1 individual

originally selected was heterozygous for the *stm-1* mutation. However, the number of *stm-1* mutants was just 22, a ratio of approximately 1/16 of all F2 plants. If the constitutive expression of *KNAT1* was to have no effect on plants homozygous for *stm-1,* then a ratio of 4/16 was expected. As a result of identifying only around a quarter of the expected amount of 'meristemless' individuals it seemed likely that the overexpression of *KNAT1* was having an ameliorating effect on the terminal phenotype of some *stm-1* mutant individuals. This result could not be attributed to a small sample number of plants observed since 291 siblings were observed. Probability suggests that this high sample number should give a realistic frequency outcome.

Although genotyping would be needed to confirm the validity of this data, it at least indicates that there may be a degree of functional redundancy between *knox* gene members in *Arabidopsis*. *stm-1* mutants harbouring the *35S::KNAT1* transgene would be expected to express *KNAT1* in the SAM during embryogenesis. Therefore, *KNAT1* expression in the shoot apex may be sufficient to overcome the lack of *STM* activity and rescue a functional meristem. It would be interesting if *STM* expression, examined by RT-PCR or *in situ* hybridisation, could not be observed in F2 individuals with functional meristems. Functional redundancy of *knox* genes is also hinted by the ability of *as1 stm* double mutants to initiate and maintain functional meristems. It appears that the negative regulation of *KNAT* genes by *AS1* may have a role in how this occurs.

4 Discussion

AS1 is an *Arabidopsis PHAN*-like MYB gene expressed in initiating lateral organs

The *PHAN* gene of *Antirrhinum majus* and the *RS2* gene of *Zea Mays* encode members of a MYB transcription factor family specific to plants with a function in repressing class I *knox* genes during leaf development (Schneeberger *et al.*, 1998; Waites *et al.*, 1998; Timmermans *et al.*, 1999; Tsiantis *et al.*, 1999a). Here, the only member of this family to be found in *Arabidopsis* was shown to correspond to *ASYMMETRIC LEAVES1 (AS1)* by complementation of the corresponding mutant and by fine mapping (Byrne *et al.*, 2000). In *as1* mutants, as in *phan* and *rs2* mutants, normal leaf development is disrupted giving rise to plants with asymmetric, lobed leaves implicating that the wild type *AS1* gene may regulate growth along one or more axes during leaf initiation. *AS1* has a role in the regulation of *Arabidopsis* development in the embryogenic, vegetative and reproductive phases. To understand how it functions at the molecular level, the expression pattern of *AS1* was fully characterised using mRNA *in situ* hybridisation and reporter gene expression. This revealed that *AS1* expression coincides with the determination of lateral organ identity, analogous to other known *PHAN*-like genes. Similarly, *AS1* transcript is absent from cells of the SAM throughout development and it therefore has an expression pattern that is complementary to class I *knox* genes that have overlapping expression patterns within the meristem and unexpanded stem. The *knox* genes are downregulated at sites of organ initiation and in *Arabidopsis* the *knox* protein STM at least is essential for meristem function (Barton and Poethig, 1993; Long *et al.*, 1996).

Exclusion of *knox* proteins from leaf founder cells is believed to be important in the acquisition of leaf fate (Smith *et al.*, 1992; Jackson *et al.*, 1994). Ectopic expression of *knox* genes in leaves of different plants results in dramatic tissue transformations, including ectopic meristematic activity (Sinha *et al.*, 1993; Lincoln *et al.*, 1994; Schneeberger *et al.*, 1995; Chuck *et al.*, 1996; Sentoku *et al.*, 2000).

Although the role of *knox* genes is not properly understood, recent evidence suggests they might regulate plant development by modifying the levels of specific phytohormones, including gibberellins and cytokinins (Tsiantis, 2001).

Control of Cell Fate in the Shoot Apical Meristem

Using two independently derived *as1* mutants it was shown that *AS1* negatively regulates the *knox* genes *KNAT1* and *KNAT2* during organ initiation in *Arabidopsis*. Significantly, however, ectopic expression of *STM* was not observed in *as1* mutants. Furthermore *AS1* transcripts accumulated in a wider expression domain in *stm* mutants than in wild type embryos suggesting that *STM* negatively regulates *AS1* in the stem cell population of the meristem. Evidence for this interaction is seen in *as1 stm* double mutants since *as1* mutations can suppress the meristem maintenance defects of *stm*. Presumably this could occur because *KNAT1* and *KNAT2* are derepressed. Thereby this allows us to propose a new model for the interactions that control shoot patterning (Figure 4.1).

In the model for wild type gene action, *STM* is on in the wild type meristem and stops *AS1* (a marker of organ fate) from being expressed thereby allowing maintenance of the undifferentiated state in SAM cells. At sites of new organ initiation in the peripheral zone of the meristem, *STM* is downregulated, allowing expression of *AS1* and the commitment of these cells to an organ fate. In a strong *stm* mutant however, *AS1* is ectopically expressed in central cells of the meristem and consequently repression of the meristem genes *KNAT1* and *KNAT2* is achieved. This results in an *stm* mutant that lacks a functional meristem. It is proposed that in an *as1 stm* double mutant, the *knox* genes *KNAT1* and *KNAT2* are no longer repressed and a functional meristem is restored. Isolation of loss-of-function mutants of *KNAT1* and *KNAT2* should test whether this derepression occurs in meristems. Another test of this model would be to study *KNAT1* and *KNAT2* expression in *as1 stm* mutants to determine whether they are expressed in wider domains relating to recovery of a functional meristem. If this is the case, it would suggest that *KNAT1*, *KNAT2* and *STM* are redundant.

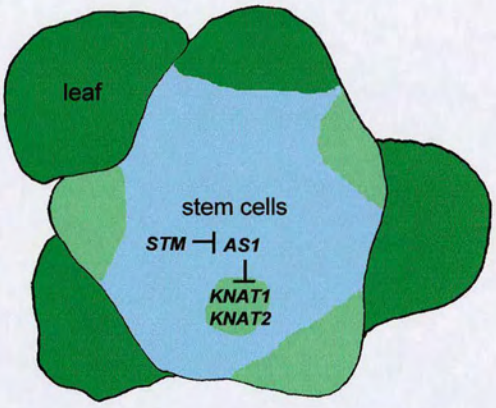

Figure 4.1 Model of organ initiation in the *Arabidopsis* SAM

A graphical representation of a shoot meristem initiating leaf primordia is shown. In this model *STM* is expressed throughout the meristem (light blue) but is downregulated in organ founder cells allowing expression of *AS1* (light green). In organs, *AS1* acts to repress the *knox* genes *KNAT1* and *KNAT2*. Older leaf primordia that no longer express *AS1* are dark green. SAM redrawn from Clark (2001).

However, the different, yet overlapping, expression patterns of these *knox* genes in wild type development infer that they may have additional roles in the tissues where they are expressed. *KNAT1* and *KNAT2* may have developmental roles where they are expressed in regions of the expanding stem and in pedicels. Therefore, loss-of-function mutants may reveal stem and pedicel phenotypes. Promoter swap studies between *KNAT1*, *KNAT2*, and *STM* may determine whether differences in *knox* gene expression patterns reflect different developmental roles. Another *Arabidopsis knox* gene, *KNAT6* that is also misexpressed in *as1* mutant organs, may also act redundantly (Semiarti *et al.*, 2001).

These findings also enable us to propose that the only function of *AS1* is to repress other *knox* genes that redundantly with *STM* promote SAM fate. Unlike other *Arabidopsis knox* genes, the expression pattern of *STM* appeared to be unchanged in *as1* mutants. This result was also demonstrated in a similar *in situ* hybridisation experiment by Ori and others (2000). However, it cannot be discounted that *STM* may be expressed below the level of detection, or in occasional patches of *as1* mutant leaves. Indeed, Semiarti and others (2001) suggest that *STM* expression can be detected in *as1* mutant leaves. A comparison of overexpression phenotypes however appears to support evidence for separate roles of STM and the other *Arabidopsis* knox proteins. Whilst *35S::KNAT1* plants display dramatic leaf phenotypes and normal shoot architecture, *35S::STM* plants are severely stunted and possess a highly disorganised shoot that produces leaf-like bulges that do not develop into mature leaves (Williams, 1998).

Although *AS1* promotes organ fate, the phenotype of the *as1* mutant suggests that *AS1* is not required for organ outgrowth. Similarly, in *stm-1* mutants, organ outgrowth is not observed in the meristem where misexpression of *AS1* occurs. What is not currently understood is how *STM* is downregulated in organ founder cells within the meristem. In future, it will be interesting to discover the underlying mechanisms responsible for this downregulation. In embryogenesis and

vegetative development, it also remains to be determined if *STM* has additional roles other than acting as a repressor of *AS1* and whether loss of repression is sufficient for the *stm-1* phenotype. Since in reproductive development, the *as1* mutation only partially suppresses the meristem defects of *stm-1*, *STM* is likely to have an additional role independent of *AS1* function. In summary, it can be said that the *AS1/knox* genetic pathway defines a mechanism for differentiating between meristem cells and organ founder cells within the SAM and demonstrates that genes expressed in organ primordia interact with meristematic genes to regulate shoot morphogenesis. However, it also remains to be tested whether this represents a conserved mechanism within angiosperms.

Genetic epistasis experiments demonstrated that the *as1* mutation has no effect on either the *cuc1 cuc2* or *pnh/zll* mutant phenotypes. Characterisation of *STM* expression in these mutants suggests that a wild type function of these genes is to maintain *STM* expression in *Arabidopsis* embryogenesis. Loss of *AS1* activity in *as1 stm-1* mutants is proposed to be sufficient to suppress the meristem defects resulting from loss of *STM* activity. However, loss of *AS1* activity is not able to suppress the meristem defects of either *cuc1 cuc2* or *pnh/zll* mutants. This suggests that both the *cuc1 cuc2* and *pnh/zll* mutant phenotypes do not solely result from their inability to maintain *STM* expression in embryogenesis. It is proposed that redundantly acting *knox* genes, such as *KNAT1* and *KNAT2*, are able to restore meristem function in the absence of *AS1* and *STM* activity. Therefore, it is possible that these genes are not able to perform the same function in *cuc1 cuc2* and *pnh/zll* mutants. It is intriguing to speculate that *CUC1* and *CUC2*, and *PNH/ZLL* may be required for the maintenance of *knox* gene expression. This could be investigated by observing whether *KNAT1* and *KNAT2* expression is detected in *cuc1 cuc2* and *pnh/zll* mutants.

If *AS1* interacts with *knox* genes to maintain a functional meristem and distinguish central stem cells and their derivatives from flanking cells that are incorporated into organs, it might be expected that this mechanism is linked to the *CLV/WUS* interactions that function to maintain the stem cell population within the central

zone of the SAM. Both *stm* mutants and *wus* mutants lack stem cells, however, *wus* alleles are epistatic to *clv* mutations and *clv stm* double mutants display an additive phenotype that suggests that these genes function competitively. Double mutants of *as1 clv* and *as1 wus* were constructed and these also displayed additive phenotypes. This suggests there is independence between the interactions of *AS1* and *knox* genes in the peripheral zone, and *CLV* and *WUS* in the central zone of the shoot apex.

Control of Leaf Development

It is likely that misexpression of *KNAT1* and *KNAT2* causes the lobed phenotype seen in *as1* mutants. The *as1* leaf phenotype is similar, but slightly less severe, than lobing observed by overexpression of either *KNAT1* or *KNAT2*. In a recent study, Ori and others (2000) described the characterisation of *as1* and *as2* mutants and similarly found that *KNAT1* and *KNAT2* are ectopically expressed in both mutants. Furthermore, it was shown that a mutation in *SERRATE* (*SE*), which encodes a chromatin remodelling factor (Prigge and Wagner, 2001), conditions an enhancement of the *as1* and *as2* phenotypes. In the corresponding double mutants, leaf lobing was more severe and ectopic meristematic activity was observed. This phenotype was interpreted to be more accurately phenocopying transgenic *Arabidopsis* that overexpress *knox* genes. However, *knox* genes do not appear to be misexpressed in an *se* single mutant, or indeed further misexpressed in an *as1 se* double mutant suggesting that chromatin regulation may be a control point of *knox* target gene expression by negatively regulating such targets. No direct evidence exists for the regulation of *knox* genes by chromatin regulation, although during animal embryo development Polycomb-group proteins act to repress homeobox genes and in *Arabidopsis*, the Polycomb-like *CURLY LEAF* gene is required to repress floral homeotic genes in leaves (Goodrich *et al.*, 1997).

Leaf lobing could be explained if *knox* gene misexpression disrupts normal axes of growth in early leaf formation. The effect of *KNAT1* overexpression in *as1*

mutants causes an increase in leaf lobing. However, asymmetry of the leaf phenotype, a perturbation of the mediolateral axis, is not a direct result of *KNAT1* misexpression in leaves. It will be important to determine the exact contribution that misexpression of each *knox* gene has on the development of *as1* leaves and other lateral organs. This might be deduced by comparing combinations of *knox* (*knat1*, *knat2*, and *knat6*) loss-of-function mutations in an *as1* mutant background. Interestingly, the formation of ectopic SAMs on leaf surfaces in ectopic *knox* expression studies suggests that at least some *knox* genes are sufficient to implement SAM-specific developmental programs rather than just restricting the differentiation of cells. These findings also correlate with the proposed model whereby *KNAT1* and/or *KNAT2* are required to be active in the meristem for it to be functional.

Axis Formation

AS1, PHAN and RS2 appear to have similar roles in excluding *knox* proteins in developing leaves of their respective species. However, mutations in these genes do not result in equivalent phenotypic outcomes, which has led to various interpretations of the role of this class of genes. The *as1* mutant of *Arabidopsis* and the *rs2* mutant of maize appear to lack any dorsoventral defects associated with *phan* mutants of *Antirrhinum* that exhibit radialised leaves. It could be interpreted that PHAN has an additional role to AS1 and RS2, in specification of the dorsoventral axis. Perhaps AS1 and RS2 also have a role in specifying the dorsoventral axis of leaves but it is masked because they perform this role in conjunction with other factors and therefore cannot be seen with single mutant analysis. The different phenotypes of *phan*-like mutants might also be accounted for if there has been divergence of common downstream targets of these genes in their respective species.

It could also be possible that *PHAN*-like genes have only a *knox*-repressing role across angiosperms and not a generalised role in specifying the dorsoventral axis. One interpretation is that the effect of ectopic *knox* expression in different species

is sufficient to condition the range of different phenotypes that are observed. Proximal to distal transformations seen in *rs2* mutant leaves, blade (distal) becoming sheath (proximal), could have occurred in *phan* mutant radial leaves such that stem or petiole tissue identity has replaced distal blade identity. Molecular markers for proximal and distal leaf identities would be useful for determining whether this could explain the *phan* mutant phenotype. Perhaps in the meristem, the boundary between cells expressing *knox* genes and cells not expressing *knox* genes is important for the specification of the dorsoventral axis. If this boundary is shifted in *phan* mutants, it could affect the correct dorsoventral development of leaves. In *Antirrhinum*, *knox* expression may be related to expression of genes that are involved in specifying polarity.

The *Mouse ear* mutant of tomato which displays almost bladeless leaves conditions ectopic expression of the *knox TKN2*, a similar phenotype can also be obtained by overexpression of *TKN2* (Chen *et al.*, 1997; Parnis *et al.*, 1997). This evidence suggests that ectopic *knox* expression may be sufficient to interfere with dorsoventral axis specification. Compound leaf development may also be able to shed more light on *PHAN*-like gene function. Koltai and Bird (2000) have shown that tomato *PHAN* and *knox* transcripts are localised to overlapping domains of expression in the shoot apex. The expression of *knox* genes in wild type primordia development may give rise to the dissected leaflets of compound leaves (Hareven *et al.*, 1996; Janssen *et al.*, 1998). However, expression of the *knox* gene *PSKN1* is down-regulated in pea compound leaf primordia (Hofer *et al.*, 2001). *PSKN1* transcripts were detected in the shoot apical meristem, but not detected in newly initiated and developing compound leaf primordia. These findings suggest that tomato and pea may use different developmental processes in the generation of their compound leaves.

Phytohormones

Since organs initiate in response to a phyllotactic prepattern it is interesting to speculate on a possible link between *AS1* and phytohormones. Ectopic

expression of *knox* genes in dicotyledonous plants can give phenotypes that include decreased apical dominance, shoot vivipary, and leaf lobing as observed in *as1* mutants. Similar phenotypes are observed in transgenic plants that overexpess a cytokinin biosynthetic gene, or that underproduce auxin and therefore have a relatively high cytokinin to auxin ratio (Estruch *et al.*, 1991; Li *et al.*, 1992). This observation suggests that auxin may directly regulate *AS1* function, or more specifically that cytokinins might act through the activation of homeobox genes. In a study by Rupp and others (1999) transgenic *Arabidopsis* were produced that could overexpress the cytokinin-synthesising *ipt* gene of the T-DNA of *Agrobacterium tumefaciens*. Cytokinin overproduction in these plants gave rise to a lobed rosette leaf phenotype typical of the effects of *knox* overexpression. The transgenic plants were observed to have increased steady state levels of both *KNAT1* and *STM* transcripts in young leaves and stem tissue. This evidence suggests that cytokinins may act upstream of *KNAT1* and *STM* in a common pathway regulating shoot meristem establishment and/or maintenance. Therefore this hypothesis links the biological activities of plant hormones to the role of *AS1* since it is upregulated in the shoot periphery concurrent with downregulation of *KNAT1* and *STM*. It would be interesting to discover whether there are high levels of cytokinins in the central zone of the meristem that maintain *knox* gene activation, and lower levels of cytokinins on the flank of the meristem allowing organ initiation through the inactivation of *knox* genes.

It is known that auxin acts as an inductive signal for the development of vascular elements in the shoot (Sachs, 1991). Maize *rs2* mutant leaves show aberrant vascular development (Schneeberger *et al.*, 1998) suggesting auxin homeostasis may be perturbed in *rs2* mutants. Indeed a reduction in polar auxin transport has been observed in *rs2* mutants (Tsiantis *et al.*, 1999b). It was deduced that aberrant polar auxin transport in *rs2* mutants was likely to result from, rather than cause ectopic *knox* gene expression, since levels of *knox* gene expression in wild type plants treated with a polar auxin transport inhibitor did not differ from those that were untreated. Therefore, plant growth regulators could be targets of *knox* genes however an indirect link also cannot be discounted. It remains to be seen

whether any aspects of the *as1* mutant phenotype are associated with aberrant control of plant growth regulators.

References

Aida M., Ishida T., Fukaki H., Fujisawa H., and Tasaka M. (1997). Genes involved in organ separation in *Arabidopsis*: an analysis of the *cup-shaped cotyledon* mutant. Plant Cell **9**, 841-857.

Aida M., Ishida T., and Tasaka M. (1999). Shoot apical meristem and cotyledon formation during *Arabidopsis* embryogenesis: interaction among the *CUP-SHAPED COTYLEDON* and *SHOOT MERISTEMLESS* genes. Development **126**, 1563-1570.

Arabidopsis Genome Initiative. (2000). Analysis of the genome sequence of the flowering plant *Arabidopsis thaliana*. Nature **408**, 796-815.

Barabas Z., and Rédei G.P. (1971). Facilitation of crossing by the use of appropriate parental stocks. Arabidopsis Information Service **8**, 7-8.

Barton M. K., and Poethig R. S. (1993). Formation of the shoot apical meristem in *Arabidopsis thaliana*: an analysis of development in the wild type and in the *shoot meristemless* mutant. Development **119**, 823-831.

Becraft P.W., Stinard P.S., and McCarty D.R. (1996) CRINKLY4: A TNFR-like receptor kinase involved in maize epidermal differentiation. Science **273**, 1406-1409.

Berna G., Robles P., and Micol J.L. (1999). A mutational analysis of leaf morphogenesis in *Arabidopsis thaliana*. Genetics **152**, 729-742.

Bohmert K., Camus I., Bellini C., Bouchez D., Caboche M., and Benning C. (1998). *AGO1* defines a novel locus of *Arabidopsis* controlling leaf development. EMBO Journal **17**, 170-180.

Bowman, J. (1994). *Arabidopsis*: An Atlas of Morphology and Development., Ed., Springer-Verlag, New York:

Bowman J.L., and Smyth D.R. (1999). *CRABS CLAW*, a gene that regulates carpel and nectary development in *Arabidopsis*, encodes a novel protein with zinc finger and helix-loop-helix domains. Development **126**, 2387-2396.

Bowman J.L., and Eshed Y. (2000). Formation and maintenance of the shoot apical meristem. Trends in Plant Science **5**, 110-115.

Brand U., Fletcher J.C., Hobe M., Meyerowitz E.M., and Simon R. (2000). Dependence of stem cell fate in *Arabidopsis* on a feedback loop regulated by *CLV3* activity. Science **289**, 617-619.

Byrne M.E., Barley R., Curtis M., Arroyo J.M., Dunham M., Hudson A., and Martienssen R.A. (2000). *Asymmetric leaves1* mediates leaf patterning and stem cell function in *Arabidopsis*. Nature **408**, 967-971.

Chen J.J., Janssen B.J., Williams A., and Sinha N. (1997). A gene fusion at a homeobox locus: alterations in leaf shape and implications for morphological evolution. Plant Cell **9**, 1289-1304.

Chuck G., Lincoln C., and Hake S. (1996). *KNAT1* induces lobed leaves with ectopic meristems when overexpressed in *Arabidopsis*. Plant Cell **8**, 1277-1289.

Clark S.E., Running M.P., and Meyerowitz E.M. (1993). *CLAVATA1*, a regulator of meristem and flower development in *Arabidopsis*. Development **119**, 397-418.

Clark S.E., Running M.P. and Meyerowitz E.M. (1995). *CLAVATA3* is a specific regulator of shoot and floral meristem development affecting the same processes as *CLAVATA1*. Development **121**, 2057-2067.

Clark S.E., Jacobsen S.E., Levin J.Z., and Meyerowitz E.M. (1996). The *CLAVATA* and *SHOOT MERISTEMLESS* loci competitively regulate meristem activity in *Arabidopsis*. Development **122**, 1567-1575.

Clark S.E., Williams R.W., and Meyerowitz E.M. (1997). The *CLAVATA1* gene encodes a putative receptor kinase that controls shoot and floral meristem size in *Arabidopsis*. Cell **89**, 575-585.

Clark S.E. (2001). Cell signalling at the shoot meristem. Nature Reviews Molecular Cell Biology **2**, 276-284.

Clough S.J., and Bent A.F. (1998). Floral dip: a simplified method for *Agrobacterium*-mediated transformation of *Arabidopsis thaliana.* Plant Journal **16**, 735-743.

Dermen H. (1953). Periclinal cytochimeras and origin of tissues in stem and leaf of peach. American Journal of Botany **40**, 154-168.

Dockx J., Quaedvlieg N., Keultjes G., Kock P., Weisbeek P., and Smeekens S. (1995). The homeobox gene *ATK1* of *Arabidopsis thaliana* is expressed in the shoot apex of the seedling and in flowers and inflorescence stems of mature plants. Plant Molecular Biology **28**, 723-737.

Elliott R.C., Betzner A.S., Huttner E., Oakes M.P., Tucker W.Q.J., Gerentes D., Perez P., and Smyth D.R. (1996). *AINTEGUMENTA*, an *APETALA2*-like gene of *Arabidopsis* with pleiotropic roles in ovule development and floral organ growth. Plant Cell **8**, 155-168.

Endrizzi K., Moussian B., Haecker A., Levin J.Z., and Laux T. (1996). The *SHOOT MERISTEMLESS* gene is required for maintenance of undifferentiated cells in *Arabidopsis* shoot and floral meristems and acts at a different regulatory

level than the meristem genes *WUSCHEL* and *ZWILLE*. Plant Journal **10**, 967-979.

Estruch J.J., Prinsen E., van Onckelen H., Schell J., and Spena A. (1991). *Viviparous* leaves produced by somatic activation of an inactive cytokinin-synthesizing gene. Science **254**, 1364-1367.

Fleming A.J., McQueenMason S., Mandel T., and Kuhlemeier C. (1997). Induction of leaf primordia by the cell wall protein expansin. Science **276**, 1415-1418.

Fletcher J.C., Brand U., Running M.P., Simon R., and Meyerowitz E.M. (1999). Signaling of cell fate decisions by *CLAVATA3* in *Arabidopsis* shoot meristems. Science **283**, 1911-1914.

Gälweiler L., Guan C., Müller A., Wisman E., Mendgen K., Yephremov A., and Palme K. (1998) Regulation of polar auxin transport by AtPIN1 in *Arabidopsis* vascular tissue. Science **282**, 2201-2202.

Gisel A., Barella S., Hempel F.D., and Zambryski P.C. (1999). Temporal and spatial regulation of symplastic trafficking during development in *Arabidopsis thaliana* apices. Development **126**, 1879-1889.

Goodrich J., Puangsomlee P., Martin M., Long D., Meyerowitz E.M., and Coupland G. (1997). A polycomb-group gene regulates homeotic gene expression in *Arabidopsis*. Nature **386**, 44-51.

Granger C.L., Callos J.D., and Medford J.I. (1996). Isolation of an *Arabidopsis* homologue of the maize homeobox *Knotted-1* gene. Plant Molecular Biology **31**, 373-378.

Haber A.H. (1962). Nonessentiality of concurrent cell divisions for degree of polarization of leaf growth. I. Studies with radiation induced mitotic inhibition. American Journal of Botany **49**, 583–89.

Hareven D., Gutfinger T., Parnis A., Eshed Y., and Lifschitz E. (1996). The making of a compound leaf: genetic manipulation of leaf architecture in tomato. Cell **84**, 735-744.

Harper L., and Freeling M. (1996). Studies on early leaf development. Current Opinions in Biotechnology **7**, 139-144.

Hewelt A., Prinsen E., Schell J., Van Onckelen H., and Schmulling T. (1994). Promoter tagging with a promoterless *ipt* gene leads to cytokinin-induced phenotypic variability in transgenic tobacco plants: implications of gene dosage effects. Plant Journal **6**, 879-891.

Hofer J., Gourlay C., Michael A., and Ellis T.H. (2001). Expression of a class 1 *knotted1*-like homeobox gene is down-regulated in pea compound leaf primordia. Plant Molecular Biology **45**, 387-398.

Hudson A. (2000). Development of symmetry in plants. Annual Reviews in Plant Physiology and Molecular Biology **51**, 349-370.

Ishida T., Aida M., Takada S., and Tasaka M. (2000). Involvement of *CUP-SHAPED COTYLEDON* genes in gynoecium and ovule development in *Arabidopsis thaliana*. Plant and Cell Physiology **41**, 60-67.

Jackson D., Veit B., and Hake S. (1994). Expression of maize *knotted1* related homeobox genes in the shoot apical meristem predicts patterns of morphogenesis in the vegetative shoot. Development **120**, 405-413.

Janssen B.J., Lund L., and Sinha N. (1998). Overexpression of a homeobox gene, *LeT6*, reveals indeterminate features in the tomato compound leaf. Plant Physiology **117**, 771-786.

Jeong S., Trotochaud A.E., and Clark S.E. (1999). The *Arabidopsis CLAVATA2* gene encodes a receptor-like protein required for the stability of the *CLAVATA1* receptor-like kinase. Plant Cell **11**, 1925-1934.

Jofuku K.D., den Boer B.G., Van Montagu M., Okamuro J.K. (1994). Control of *Arabidopsis* flower and seed development by the homeotic gene *APETALA2*. Plant Cell **6**, 1211-25.

Jürgens G., Mayer U., Torres-Ruiz R.A., Berleth T., and Miséra S. (1991). Genetic-analysis of pattern-formation in the *Arabidopsis* embryo. Development **Supplement1**, 27-38.

Kayes J.M., and Clark S.E. (1998). *CLAVATA2*, a regulator of meristem and organ development in *Arabidopsis*. Development **125**, 3843-3851.

Kerstetter R.A., Laudencia-Chingcuanco D., Smith L.G., and Hake S. (1997). Loss-of-function mutations in the maize homeobox gene, *knotted1*, are defective in shoot meristem maintenance. Development **124**, 3045-3054.

Kim G.T., Tsukaya H., and Uchimiya H. (1998). The *ROTUNDIFOLIA3* gene of *Arabidopsis thaliana* encodes a new member of the cytochrome P-450 family that is required for the regulated polar elongation of leaf cells. Genes and Development **12**, 2381-2391.

Koltai H., and Bird D.M. (2000). Epistatic repression of *PHANTASTICA* and class 1 *KNOTTED* genes is uncoupled in tomato. Plant Journal **22**, 455-459.

Kranz H.D., Denekamp M., Greco R., Jin H., Leyva A., Meissner R.C., Petroni K., Urzainqui A., Bevan M., Martin C., Smeekens S., Tonelli C., Paz-Ares J., and Weisshaar B. (1998). Towards functional characterisation of the members of the R2R3-MYB gene family from *Arabidopsis thaliana*. Plant Journal **16**, 263-276.

Krizek B.A. (1999). Ectopic expression of *AINTEGUMENTA* in *Arabidopsis* plants results in increased growth of floral organs. Developmental Genetics **25**, 224-236.

Laufs P., Grandjean O., Jonak C., Kiéu K., and Traas J. (1998a). Cellular parameters of the shoot apical meristem in *Arabidopsis*. Plant Cell **10**, 1375-1389.

Laufs P., Dockx J., Kronenberger J., and Traas J. (1998b). *MGOUN1* and *MGOUN2*: two genes required for primordium initiation at the shoot apical and floral meristems in *Arabidopsis thaliana*. Development **125**, 1253-1260.

Laux T., Mayer K.F., Berger J., and Jürgens G. (1996). The *WUSCHEL* gene is required for shoot and floral meristem integrity in *Arabidopsis* Development **122**, 87-96.

Lee I., Wolfe D.S., Nilsson O., and Weigel D. (1997). A *LEAFY* co-regulator encoded by *UNUSUAL FLORAL ORGANS*. Current Biology **7**, 95-104.

Levin J.Z., and Meyerowitz E.M. (1995). *UFO*: An *Arabidopsis* gene involved in both floral meristem and floral organ development. Plant Cell **7**, 529-548.

Leyser H.M.O., and Furner I.J. (1992). Characterization of three shoot apical meristem mutants of *Arabidopsis-thaliana.* Development **116**, 397-403.

Li Y., Hagen G., and Guilfoyle T.J. (1992). Altered morphology in transgenic tobacco plants that overproduce cytokinins in specific tissues and organs. Developmental Biology **153**, 386-395.

Lin X.Y., Kaul S.S., Rounsley S., Shea T.P., Benito M.I., Town C.D., Fujii C.Y., Mason T., Bowman C.L., Barnstead M., Feldblyum T.V., Buell C.R., Ketchum K.A., Lee J., Ronning C.M., Koo H.L., Moffat K.S., Cronin L.A., Shen M., Pai G., Van Aken S., Umayam L., Tallon L.J., Gill J.E., Adams M.D., Carrera A.J., Creasy T.H., Goodman H.M., Somerville C.R., Copenhaver G.P., Preuss D., Nierman W.C., White O., Eisen J.A., Salzberg S.L., Fraser C.M., and Venter J.C. (1999). Sequence and analysis of chromosome 2 of the plant *Arabidopsis thaliana*. Nature **402**, 761-769.

Lincoln C., Long J., Yamaguchi J., Serikawa K., and Hake S. (1994). A *knotted1*-like homeobox gene in *Arabidopsis* is expressed in the vegetative meristem and dramatically alters leaf morphology when overexpressed in transgenic plants. Plant Cell **6**, 1859-1876.

Long J.A., Moan E.I., Medford J.I., and Barton M.K. (1996). A member of the *KNOTTED* class of homeodomain proteins encoded by the *STM* gene of *Arabidopsis*. Nature **379**, 66-69.

Long J.A., and Barton M.K. (1998). The development of apical embryonic pattern in *Arabidopsis*. Development **125**, 3027-3035.

Long J., and Barton M.K. (2000). Initiation of axillary and floral meristems in *Arabidopsis*. Developmental Biology **218**, 341-353.

Lyndon R.F. (1982). Changes in polarity of growth during leaf initiation in the pea, *Pisum-sativum*-L. Annals of Botany **49**, 281-290.

Lynn K., Fernandez A., Aida M., Sedbrook J., Tasaka M., Masson P., and Barton M.K. (1999). The *PINHEAD/ZWILLE* gene acts pleiotropically in *Arabidopsis* development and has overlapping functions with the *ARGONAUTE1* gene. Development **126**, 469-481.

Mansfield S.G., and Briarty L.G. (1992). Cotyledon cell-development in *Arabidopsis-thaliana* during reserve deposition. Canadian Journal of Botany **70**, 151-164.

Martienssen R., and Dolan L. in Patterns in vegetative development, *Arabidopsis*. Annual Plant Reviews (eds Anderson, M. & Roberts, J.) 262-297 (Sheffield Academic Press, Sheffield, 1998).

Martienssen R., and McCombie W.R. (2001). The first plant genome. Cell **105**, 571-574.

Mayer U., Torres-Ruiz R.A., Berleth T., Miséra S., and Jürgens G. (1991). Mutations affecting body organization in the *Arabidopsis* embryo. Nature **353**, 402-407.

Mayer K.F., Schoof H., Haecker A., Lenhard M., Jürgens G., and Laux T. (1998). Role of *WUSCHEL* in regulating stem cell fate in the *Arabidopsis* shoot meristem. Cell **95**, 805-815.

McConnell J.R., and Barton M.K. (1998). Leaf polarity and meristem formation in *Arabidopsis*. Development **125**, 2935-2942.

McConnell J.R., Emery J., Eshed Y., Bao N., Bowman J., and Barton M.K. (2001). Role of *PHABULOSA* and *PHAVOLUTA* in determining radial patterning in shoots. Nature **411**, 709-713.

McHale N.A., and Marcotrigiano M. (1998). *LAM1* is required for dorsoventrality and lateral growth of the leaf blade in *Nicotiana*. Development **125**, 4235-4243.

Meissner R.C., Jin H., Cominelli E., Denekamp M., Fuertes A., Greco R., Kranz H.D., Penfield S., Petroni K., Urzainqui A., Martin C., Paz-Ares J., Smeekens S., Tonelli C., Weisshaar B., Baumann E., Klimyuk V., Marillonnet S., Patel K.,

Speulman E., Tissier A.F., Bouchez D., Jones J.D.G., Pereira A., Wisman E., and Bevan M. (1999). Function Search in a Large Transcription Factor Gene Family in *Arabidopsis*: Assessing the Potential of Reverse Genetics to Identify Insertional Mutations in R2R3 *MYB* Genes. Plant Cell **11**, 1827-1840.

Mizukami Y., and Fischer R.L. (2000). Plant organ size control: *AINTEGUMENTA* regulates growth and cell numbers during organogenesis. Proceedings of the National Academy of Sciences of the United States of America **97**, 942-947.

Moussian B., Schoof H., Haecker A., Jürgens G., and Laux T. (1998). Role of the *ZWILLE* gene in the regulation of central shoot meristem cell fate during *Arabidopsis* embryogenesis. EMBO Journal **17**, 1799-1809.

Ori N., Eshed Y., Chuck G., Bowman J.L., and Hake S. (2000). Mechanisms that control *knox* gene expression in the *Arabidopsis* shoot. Development **127**, 5523-5532.

Parnis A., Cohen O., Gutfinger T., Hareven D., Zamir D., and Lifschitz E. (1997). The dominant developmental mutants of tomato, *Mouse-ear* and *Curl*, are associated with distinct modes of abnormal transcriptional regulation of a *Knotted* gene. Plant Cell **9**, 2143-2158.

Poethig R.S., and Sussex I.M. (1985) The cellular parameters of leaf development in tobacco: a clonal analysis. Planta **165**, 170-189.

Prigge M.J., and Wagner D.R. (2001). The *Arabidopsis SERRATE* gene encodes a zinc-finger protein required for normal shoot development. Plant Cell **13**, 1263-1279.

Redei G.P., and Hirono Y. (1964). Linkage studies. Arabidopsis Information Service **1**, 9-10.

Redéi G.P. (1965). Non-mendelian megagametogenesis in *Arabidopsis*. Genetics **51**, 857-872.

Reinhardt D., Wittwer F., Mandel T., and Kuhlemeier C. (1998). Localized upregulation of a new expansin gene predicts the site of leaf formation in the tomato meristem. Plant Cell **10**, 1427-1437.

Reinhardt D., Mandel T., and Kuhlemeier C. (2000). Auxin regulates the initiation and radial position of plant lateral organs. Plant Cell **12**, 507-518.

Reinholz E. (1947). Auslosung von rontgen-mutationen bei *Arabidopsis thaliana* (L.) HEYNH. und ihre bedeutung fur die pflanzenzuchtung und evolutionstheorie. Fiat Report **1006**, 1-70.

Reinholz E. (1965). *Arabidopsis thaliana* (L.) HEYNH. als Objekt fur genetische und entwicklungsphysiologische Untersuchungen. Arabidopsis Information Service **1Supplement**, 24.

Reiser L., Sanchez-Baracaldo P., and Hake S. (2000). Knots in the family tree: evolutionary relationships and functions of *knox* homeobox genes. Plant Molecular Biology **42**, 151-166.

Rupp H.M., Frank M., Werner T., Strnad M., and Schmulling T. (1999). Increased steady state mRNA levels of the *STM* and *KNAT1* homeobox genes in cytokinin overproducing *Arabidopsis thaliana* indicate a role for cytokinins in the shoot apical meristem. Plant Journal **18**, 557-563.

Sachs T. (1991). Pattern Formation in Plant Tissues. Cambridge University Press, Cambridge,UK. pp25-34.

Sawa S., Watanabe K., Goto K., Liu Y.G., Shibata D., Kanaya E., Morita E.H., and Okada K. (1999). *FILAMENTOUS FLOWER*, a meristem and organ identity

gene of *Arabidopsis*, encodes a protein with a zinc finger and HMG-related domains. Genes and Development **13**, 1079-1088.

Scanlon M.J., Schneeberger R.G., and Freeling M. (1996). The maize mutant *narrow sheath* fails to establish leaf margin identity in a meristematic domain. Development **122**, 1683-1691.

Scanlon M.J., and Freeling M. (1997). Clonal sectors reveal that a specific meristematic domain is not utilized in the maize mutant *narrow sheath*. Developmental Biology **182**, 52-66.

Scanlon M.J. (2000). *NARROW SHEATH1* functions from two meristematic foci during founder-cell recruitment in maize leaf development. Development **127**, 4573-4585.

Schneeberger R.G., Becraft P.W., Hake S., and Freeling M. (1995). Ectopic expression of the *knox* homeo box gene *rough sheath1* alters cell fate in the maize leaf. Genes and Development **9**, 2292-2304.

Schneeberger R., Tsiantis M., Freeling M., and Langdale J.A. (1998). The *rough sheath2* gene negatively regulates homeobox gene expression during maize leaf development. Development **125**, 2857-2865.

Schoof H., Lenhard M., Haecker A., Mayer K.F., Jürgens G., and Laux T. (2000). The stem cell population of *Arabidopsis* shoot meristems is maintained by a regulatory loop between the *CLAVATA* and *WUSCHEL* genes. Cell **100**, 635-644.

Semiarti E., Ueno Y., Tsukaya H., Iwakawa H., Machida C., and Machida Y. (2001). The *ASYMMETRIC LEAVES2* gene of *Arabidopsis thaliana* regulates formation of a symmetric lamina, establishment of venation and repression of meristem-related homeobox genes in leaves. Development **128**, 1771-1783.

Sentoku N., Sato Y., and Matsuoka M. (2000). Overexpression of rice *OSH* genes induces ectopic shoots on leaf sheaths of transgenic rice plants. Developmental Biology **220**, 358-364.

Serrano-Cartagena J., Robles P., Ponce M.R., and Micol J.L. (1999). Genetic analysis of leaf form mutants from the *Arabidopsis* Information Service collection. Molecular and General Genetics **261**, 725-739.

Siegfried K.R., Eshed Y., Baum S.F., Otsuga D., Drews G.N., and Bowman J.L. (1999). Members of the *YABBY* gene family specify abaxial cell fate in *Arabidopsis*. Development **126**, 4117-4128.

Sinha N.R., Williams R.E., and Hake S. (1993). Overexpression of the maize homeo box gene, *knotted-1*, causes a switch from determinate to indeterminate cell fates. Genes and Development **7**, 787-795.

Smith L.G., Greene B., Veit B., and Hake S. (1992). A dominant mutation in the maize homeobox gene, *Knotted-1*, causes its ectopic expression in leaf cells with altered fates. Development **116**, 21-30.

Smith L.G., Hake S., and Sylvester A.W. (1996). The *tangled-1* mutation alters cell division orientations throughout maize leaf development without altering leaf shape. Development **122**, 481-489.

Snow M., and Snow M. (1959). The dorsoventrality of leaf primordia. New Phytology **58**, 188-207.

Steeves T.A., and Sussex I.M. (1989). Patterns in Plant Development 2nd edition, pp. 46-61.

Stracke R., Werber M., and Weisshaar B. (2001). The *R2R3-MYB* gene family in *Arabidopsis thaliana*.Current Opinion in Plant Biology **4**, 447-456.

Sussex I.M. (1954). Experiments on the cause of dorsoventrality in leaves. Nature **174**, 351-352.

Sussex I.M. (1955). Morphogenesis in *Solanum tuberosum* L.: Experimental investigation of leaf dorsiventrality and orientation in the juvenile shoot. Phytomorphology **5**, 286-300.

Takada S., Hibara K.-i., Ishida T., and Tasaka M. (2001). The *CUP-SHAPED COTYLEDON1* gene of *Arabidopsis* regulates shoot apical meristem formation. Development **128**, 1127-1135.

Timmermans M.C., Schultes N.P., Jankovsky J.P., and Nelson T. (1998). *Leafbladeless1* is required for dorsoventrality of lateral organs in maize. Development **125**, 2813-2823.

Timmermans M.C., Hudson A., Becraft P.W., and Nelson T. (1999). ROUGH SHEATH2: a Myb protein that represses *knox* homeobox genes in maize lateral organ primordia. Science **284**, 151-153.

Tissier A.F., Marillonnet S., Klimyuk V., Patel K., Torres M.A., Murphy G., and Jones J.D.G. (1999). Multiple independent defective *Suppressor-mutator* transposon insertions in *Arabidopsis*: A tool for functional genomics. Plant Cell **11**, 1841-1852.

Trotochaud A.E., Jeong S., and Clark S.E. (2000). *CLAVATA3*, a multimeric ligand for the *CLAVATA1* receptor-kinase. Science **289**, 613-617.

Tsiantis M., Schneeberger R., Golz J.F., Freeling M., and Langdale J.A. (1999a). The maize *rough sheath2* gene and leaf development programs in monocot and dicot plants. Science **284**, 154-156.

Tsiantis M., Brown M.I., Skibinski G., and Langdale J.A. (1999b). Disruption of auxin transport is associated with aberrant leaf development in maize. Plant Physiology **121**, 1163-1168.

Tsiantis M. (2001). Control of shoot cell fate: Beyond homeoboxes. Plant Cell **13**, 733-738.

Tsuge T., and Uchimiya H. (1996). Two independent and polarized processes of cell elongation regulate leaf blade expansion in *Arabidopsis thaliana* (L) Heynh. Development **122**, 1589-1600.

Tsukaya H., and Uchimiya H. (1997). Genetic analyses of the formation of the serrated margin of leaf blades in *Arabidopsis*: combination of a mutational analysis of leaf morphogenesis with the characterization of a specific marker gene expressed in hydathodes and stipules. Molecular and General Genetics **256**, 231-238.

Vaughan J.G. (1955). The morphology and growth of the vegetative and reproductive apices of *Arabidopsis thaliana* (L.) Heynh., *Capsella bursa-pastoris* (L.) Medic. and *Anagallis arvensis* (L.). Journal of the Linnean Society of Botany **55**, 279-300.

Vernoux T., Kronenberger J., Grandjean O., Laufs P., and Traas J. (2000). *PIN-FORMED1* regulates cell fate at the periphery of the shoot apical meristem. Development **127**, 5157-5165.

Vollbrecht E., Veit B., Sinha N., and Hake S. (1991). The developmental gene *Knotted-1* is a member of a maize homeobox gene family. Nature **350**, 241-243.

Waites R., and Hudson A. (1995). *phantastica*: a gene required for dorsoventrality of leaves in *Antirrhinum majus*. Development **121**, 2143-2154.

Waites R., Selvadurai H.R., Oliver I.R., and Hudson A. (1998). The *PHANTASTICA* gene encodes a MYB transcription factor involved in growth and dorsoventrality of lateral organs in *Antirrhinum*. Cell **93**, 779-789.

West M.A.L., and Harada J.J. (1993). Embryogenesis in higher plants: An overview. Plant Cell **5**, 1361-1369.

Wilkinson M.D., and Haughn G.W. (1995). *UNUSUAL FLORAL ORGANS* controls meristem identity and organ primordia fate in *Arabidopsis*. Plant Cell **7**, 1485-1499.

Williams R.W. (1998). Plant homeobox genes: many functions stem from a common motif. Bioessays **20**, 280-282.

Asymmetric leaves1 mediates leaf patterning and stem cell function in *Arabidopsis*

Mary E. Byrne*, Ross Barley†, Mark Curtis*‡, Juana Maria Arroyo*, Maitreya Dunham*‡, Andrew Hudson† & Robert A. Martienssen*

* *Cold Spring Harbor Laboratory, 1 Bungtown Road, Cold Spring Harbor, New York 11724, USA*
† *Institute of Cell and Molecular Biology, University of Edinburgh, Edinburgh EH9 3JR, UK*

Meristem function in plants requires both the maintenance of stem cells and the specification of founder cells from which lateral organs arise. Lateral organs are patterned along proximodistal, dorsoventral and mediolateral axes[1,2]. Here we show that the *Arabidopsis* mutant *asymmetric leaves1* (*as1*) disrupts this process. *AS1* encodes a myb domain protein, closely related to *PHANTASTICA* in *Antirrhinum* and *ROUGH SHEATH2* in maize, both of which negatively regulate knotted-class homeobox genes. *AS1* negatively regulates the homeobox genes *KNAT1* and *KNAT2* and is, in turn, negatively regulated by the meristematic homeobox gene *SHOOT MERISTEMLESS*. This genetic pathway defines a mechanism for differentiating between stem cells and organ founder cells within the shoot apical meristem and demonstrates that genes expressed in organ primordia interact with meristematic genes to regulate shoot morphogenesis.

The shoot apical meristem (SAM) comprises slowly dividing stem cells at the centre and daughter cells at the periphery, from which organ founder cells are recruited. Founder cells divide rapidly, initiating the outgrowth of organ primordia while polarity is established along the proximodistal, dorsoventral and mediolateral axes[1,2]. The mechanism by which stem cell and founder cell derivatives are distinguished is obscure, but is likely to involve a highly conserved class of homeobox genes related to *KNOTTED1* in maize (*KNOX* genes). *KNOX* genes are expressed in the SAM but are downregulated in founder cells at the time of leaf initiation[3]. They are implicated in maintaining division or preventing differentiation of cells in the SAM. Loss-of-function mutations in the *Arabidopsis KNOX* gene *SHOOT MERISTEMLESS* (*STM*) result in embryos that lack a SAM[4,5]. Recessive mutations in the *kn1* gene of maize are also defective in meristem maintenance[6]. In contrast, gain-of-function mutations that result in ectopic expression of *KNOX* genes in maize disrupt normal leaf development causing distal displacement

‡ Present address: Institute of Biological Sciences, University of Wales, Aberystwyth, UK (M.C.); Genetics Department, Stanford, California 94305, USA (M.D.).

of sheath and auricle tissue into the blade[7]. In dicotyledonous plants, such as *Arabidopsis* and tobacco, misexpression of homeobox transgenes results in lobed leaves, distally displaced stipules, and occasional ectopic meristems on the adaxial leaf surface[8,9].

PHANTASTICA (*PHAN*) in *Antirrhinum* is transcribed in organ founder cells and is required to prevent expression of an *STM*-like *KNOX* gene in lateral organs[10,11]. *phan* mutants show variable defects in leaf patterning, affecting both dorsoventral and proximodistal axes[12]. *PHAN* has a myb domain found in several transcription factors and its homologue in maize is *ROUGH SHEATH2* (*RS2*)[11,13]. Mutations in *RS2* result in phenotypes comparable to dominant mutations in *KNOX* genes, and show ectopic expression of homeodomain proteins in developing leaves revealing a conserved role for *RS2* in repressing *KNOX* gene expression[11,13,14].

asymmetric leaves1 (*as1*) is a classical mutation in *Arabidopsis* that disrupts development of cotyledons, leaves and floral organs (Fig. 1)[15]. The mutant leaf lamina is subdivided into prominent outgrowths or lobes. Early leaves have few lobes located proximally, whereas later leaves have more lobes extending distally toward the leaf tip (Fig. 1c). Adult rosette leaves of *magnifica*, the first isolated mutant allele of *as1* (ref. 16), have patches of callus-like growth on the leaf lamina, and occasionally have ectopic shoots on the adaxial surface of the petiole (Fig. 1d), similar to those observed in transgenic plants misexpressing the *KNOX* gene *KNAT1* (ref. 9). In wild-type leaves the abaxial epidermis over the midvein of the leaf petiole and blade is comprised of elongated cells (Fig. 1e). In *as1* there are multiple bundles of elongated cells extending from the petiole into the blade (Fig. 1f). The enhancer trap (see Methods) ET2689 marks these elongated cells (Fig. 1g) and is expressed over a much broader region in *as1* extending in multiple directions from the petiole (Fig. 1h). This pattern reflects a change in proximodistal and mediolateral patterning of the leaf.

Loss of *AS1* activity causes defects that are similar, in many respects, to those caused by misexpression of *KNOX* transgenes[1]. We used polymerase chain reaction after reverse transcription of RNA (RT–PCR) to examine expression of the *KNOX* genes *STM*, *KNAT1* and *KNAT2* in *as1* mutants. *STM* expression in the wild type is confined to SAM cells and is absent from leaves and leaf primordia[17]. No change in the pattern of expression was detected in *as1* (Fig. 2) even at the level of *in situ* hybridization (data not shown). *KNAT1* transcripts in wild-type plants were detected in whole-shoot and inflorescence tissue but not in leaves (Fig. 2), consistent with the reported expression pattern[18]. However, *KNAT1* was ectopically expressed in *as1* leaves (Fig. 2) and, as shown by *in situ* hybridization, was ectopically expressed in the cotyledons of *as1* embryos consistent with their altered morphology (Fig. 3l and m). *KNAT2* transcripts were present at high levels in wild-type shoot and inflorescence tissue as expected[19], but also at a low level in wild-type leaves (Fig. 2). In *as1* mutant leaves, expression of *KNAT2* was upregulated (Fig. 2).

We used positional cloning to identify the *AS1* gene. *as1* had previously been mapped to chromosome 2 (ref. 15). Phenotypic and molecular markers were used to map *as1* within a 1.0-centiMorgans (cM) interval proximal to *det2*. The Arabidopsis Genome Initiative sequence in this region[20] revealed a likely candidate for

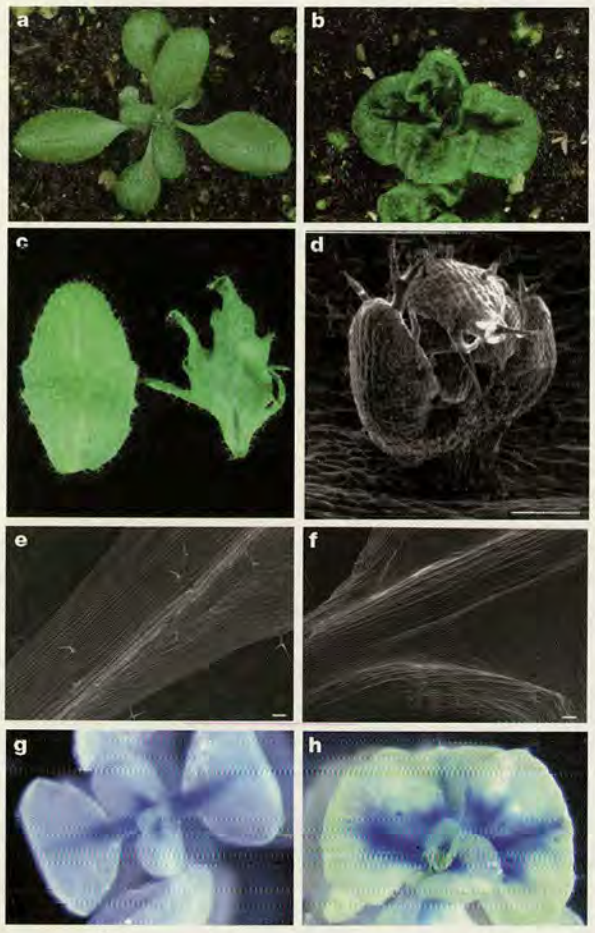

Figure 1 Comparison of *as1* mutant and wild-type *Arabidopsis*. **a**, Vegetative rosette of wild-type. Rosette leaves are elongate and spatulate in shape. **b**, Vegetative rosette of *as1*. Leaves are shorter than wild-type and have a rumpled appearance. **c**, Cauline leaf of the wild type (left), *as1* (right). The *as1* leaf has marginal lobes. **d**, Ectopic shoot in *magnifica*. **e**, Abaxial surface of wild-type leaf at the distal end of the petiole, showing elongated cells of the midvein. **f**, Abaxial surface of *as1* leaf. Elongated epidermal cells typical of the midvein occur in multiple files. **g**, ET2689 in the wild type marks cells of the midvein. **h**, In *as1* ET2689 shows much broadened GUS expression. Scale bars, 200 μm.

Figure 2 Polymerase chain reaction after reverse transcription of RNA (RT–PCR) analysis of *KNOX* gene expression in *as1* and wild type. RNA was extracted from shoots, young leaves, mature leaves and inflorescence tissues. RT–PCR reactions were performed using gene-specific primers. Products were blotted and hybridized with gene-specific probes. *STM* is detected in wild type (wt) and *as1* shoot and inflorescence, and not in leaf tissue. *KNAT1* is detected in wild type and *as1* shoot and inflorescence and is found in *as1* leaf tissue. *KNAT2* is detected in all tissues in wild type and *as1* but is upregulated in young leaves and, to a lesser extent, in mature leaves of *as1*. *RBC* transcripts were amplified as a control.

AS1 in a gene closely related to the myb transcription factor *PHAN*, which had previously been named *Atphan*[11]. Two independent *as1* alleles were sequenced and found to have mutations in *Atphan* predicted to truncate the carboxy-terminal third of the AS1 protein. *as1-magnifica* was found to result from a rearrangement at the 5′ end of the gene (likely inversion) that disrupts the promoter. A 6-kilobase (kb) genomic fragment encompassing *Atphan* complemented *as1-1* (see Methods). Together, these results confirmed that *Atphan* is *AS1*.

The expression pattern of *AS1* was examined by *in situ* hybridization. In wild-type embryos *AS1* RNA first became detectable in late globular stage, predominantly in two subepidermal domains corresponding to cotyledon initials (Fig. 3a). Expression was maintained in subepidermal cells of developing cotyledons from heart stage onwards, but was absent or reduced in cells that would subsequently form the shoot apical meristem and the cotyledon epidermis (Fig. 3b–e). After germination, *AS1* was detected in leaf founder cells from the time of primordium initiation until stage P4 and in cells associated with the cotyledon vasculature (Fig. 3f). On flowering, *AS1* RNA was detected on the flank of the inflorescence apex in a region corresponding to the "cryptic bract" (Fig. 3g)[21]. In early floral primordia *AS1* expression was first detected in the abaxial sepal primordium (Fig. 3g), and subsequently in primordia of all floral organs (Fig. 3h). This is consistent with reduced growth of these organs in *as1* flowers[15].

Our analysis of *KNOX* gene expression in *as1* showed misexpression of *KNAT1* and *KNAT2*, whereas *STM* expression was unchanged. To place *STM* in a genetic pathway relative to *AS1*, double mutants were made using a strong allele of *stm*. Embryos homozygous for *stm-1* lack a SAM and develop cotyledons that are fused at their base (Fig. 4b)[4,5]. F2 progeny from a cross between *stm-1*/+ × *as1-1*/*as1-1* segregated, at a ratio of 1/16, a novel phenotype identified as the *as1-1 stm-1* double mutant (see Methods). Double-mutant vegetative shoots and leaves were indistinguishable from *as1* single mutants (Fig. 4a and c), indicating that the embryonic and vegetative phenotype of *stm-1* was completely suppressed by loss of *AS1* activity. Epistasis of *as1* also demonstrated that the *as1* mutant phenotype was not dependent on *STM* activity, consistent with RT–PCR data showing that these plants do not misexpress *STM*.

In reproductive development, *as1-1 stm-1* double mutants differed from *as1* single mutants in continuing to generate lateral shoots, each subtended by a cauline leaf, instead of flowers (Fig. 4c). The overall shoot architecture was comparable to wild-type plants, although occasional flowers that formed resembled those conditioned by weak alleles of *stm* (Fig. 4d)[5,22]. The double-mutant phenotype showed that loss of *AS1* activity in *as1-1* was insufficient to suppress the *stm* mutant phenotype in reproductive development.

Genetic interaction between *as1* and *stm* demonstrates that *as1* can rescue the *stm* phenotype in embryonic and vegetative meristems. Given that the two genes are expressed in complementary domains, and that the expression pattern of *STM* does not change in *as1* mutants, we conclude that *STM* negatively regulates *AS1*. *In situ* hybridization of siliques (fruits) segregating 1/4 *stm* embryos revealed *AS1* expression throughout the apical half of 13 out of 60 heart stage embryos consistent with this conclusion (Fig. 3l–k).

The genetic and molecular interaction between *AS1* and *KNOX* genes allows us to propose a mechanism by which organ founder cells are distinguished from stem cells and their derivatives in the shoot apical meristem. In stem cells *STM* negatively regulates *AS1*.

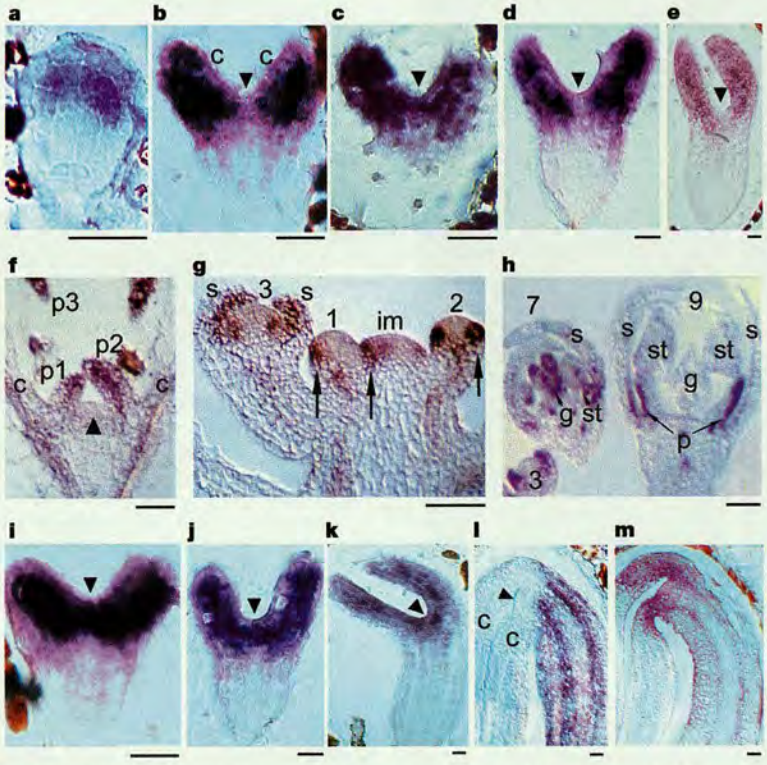

Figure 3 Expression of *AS1* and *KNAT1*. *In situ* hybridization showing expression of *AS1* (**a**–**k**) and *KNAT1* (**l**, **m**) in wild-type embryos at successive stages of development (**a**–**e**), wild-type vegetative apex (**f**) and inflorescence apices (**g**, **h**), *stm-1* mutant (**i**–**k**), wild type (**l**) and *as1* (**m**) embryos. **b** and **c** are two sections from the same embryo taken 7 μm apart. Arrowheads indicate SAM cells or their initials. Arrows in **g** indicate cryptic bract and initials of the lowermost sepal. *AS1* expression is confined to organ primordia and is absent from the SAM. In *as1* mutants *KNAT1* is ectopically expressed at the base of the cotyledons. c, cotyledon, im, inflorescence meristem, s, sepal, p, petal, st, stamen, g, gynoecium, p1–p3, leaves of increasing developmental age. Scale bars, 25 μm.

In founder cells, *STM* is downregulated, allowing *AS1* to be expressed. *AS1* in turn downregulates *KNAT1* and *KNAT2*. Thus, *stm* mutant embryos fail to develop a meristem owing to misexpression of *AS1* in presumptive stem cells and their immediate derivatives, causing them to lose their undifferentiated meristematic state. In the *as1 stm-1* double mutant, lack of *AS1* allows meristem function in the absence of *STM*, potentially promoted by derepression of *KNAT1* and *KNAT2*. These *KNOX* genes are closely related to *STM*[7], although their ability to complement the *stm* phenotype is not known. In floral promordia *STM* has a function independent of *AS1*. The network of negative gene interactions between *AS1* and *KNOX* genes functions to distinguish between stem cells and founder cells within the SAM. This leads to a situation in which *STM* is not required for SAM formation in the absence of *AS1*. In contrast, several other genes known to interact with *STM*, including the *CLV* genes, *WUS* and *CUC2* (refs 23, 24, 25), are all expressed in regions of the SAM and are required for meristem function. Mutations in *CLV1*, *CLV3* and *WUS* show additive interactions with *as1*, demonstrating that *AS1* acts independently of these genes (not shown). This is consistent with *AS1* and *STM* acting in a parallel pathway to *WUS* and *CLV* to specify cell fate in the meristem[5,22].

AS1, *PHAN* and *RS2* all negatively regulate *KNOX* gene expression in organ primordia, demonstrating a degree of functional conservation in *Arabidopsis*, *Antirrhinum* and maize. In maize, *rs2* mutants show alterations along the leaf proximodistal axis, with proximal sheath and ligule tissues displaced distally into the leaf blade[14]. *as1* mutants show changes in the proximodistal and mediolateral axes, resulting in characteristic leaf asymmetry (Fig. 1). In *Antirrhinum*, lower leaves of *phan* mutants are broad and heart-shaped with prominent veins similar to those of *as1*. *phan* in addition affects the dorsoventral and proximodistal axes in a cold-sensitive fashion[10,12]. Upper *phan* leaves are radial and ventralized, and fail to grow out altogether at restrictive temperatures. In contrast, *as1* and *rs2* do not form radialized leaves. *Arabidopsis* and *Antirrhinum* are both eudicots with simple leaves, and fundamental aspects of leaf development are expected to be similar in the two species. The differences between *as1* and *phan* phenotypes may reflect allelic differences or functional divergence of these genes and their targets. Alternatively, they might be explained by modifiers in *Antirrhinum* that enhance *phan* in upper leaves. □

Figure 4 *as1* shows genetic interaction with *stm-1*. **a**, *as1* whole-plant phenotype. Rosette and cauline leaves are rounded and lobed. After 3–5 cauline leaves with associated secondary shoots, flowers form on the main inflorescence and lateral shoots. **b**, *stm-1* mutants showing cotyledons fused at the base and no vegetative shoot. **c**, *as1 stm-1* double mutant. Rosette is indistinguishable from *as1* single mutants. The main inflorescence and lateral shoots fail to produce flowers, but continue to form lateral shoots with subtending cauline leaves. **d**, *as1 stm-1* double mutant flower. Occasional flowers formed on double mutants typically have reduced petal and stamen number and no central carpel. Floral organs are sometimes mosaic (arrow).

Methods

Plant stocks and growth conditions

All alleles of *as1* (*magnifica*, *as1-1* and *as1-17*) and *stm* used in this study were obtained from the Arabidopsis Biological Resource Center (ARBC). Gene and enhancer trap lines were generated as previously described[26]. Plants were grown either on soil or on Murashige and Skoog salts media[26], supplemented with vitamins, with a minimum day length of 16 h. GUS staining was carried out as previously described[26].

Genetic analysis

as1 was mapped relative to *det2* by progeny testing the F2 plants from the cross *cp er as1 cer8* × *det2*. Out of 100 recombinants between *as1* and *cer8*, three carried the haplotype *cp er as1 det2*, placing *as1* 0.3 cM proximal to *det2*. A second cross between *hy1 as1* and ecotype Landsberg *erecta* identified recombinants proximal to *as1*. Molecular mapping of recombinants between *hy1* and *as1* was carried out using derived (this study) and previously identified CAPS markers (ARBC)[27]. To construct double mutants, plants homozygous for *as1-1* were crossed as males to plants heterozygous for *stm-1*. Double *as1-1 stm1* mutants segregated in the F2 progeny in the expected 1:15 ratio; percentage segregation for each phenotypic class were wild-type (55.8%): *as1* (17.4%): *stm-1* (21.2%): *as1 stm-1* (5.6%). The *stm-1* genotype of double mutants was confirmed by a PCR assay. For each DNA template a common primer GCCCATCATGACATCACATC was used in separate reactions with a primer, CTTTAAGCTCTCTATCCTCAGCTTG, designed to amplify the wild-type STM allele and a primer, CTTTAAGCTCTCTATCCTC AGCTTA, designed to amplify the mutant *stm-1* allele[17]. Standard PCR reaction conditions were used with an annealing temperature of 66 °C.

DNA and RNA analysis

DNA extraction and manipulation were as described previously[28]. Total RNA was purified using Trizol reagent (GibcoBRL). Following DNase treatment (Boehringer Mannheim) complementary DNA was synthesized using M-MuLV reverse transcriptase (New England Biolab) in 50 mM Tris-HCl (pH 8.3), 30 mM KCl, 8 mM $MgCl_2$, 10 mM DTT, 1 mM each of dATP, dCTP, dGTP, dTTP, 1 μM oligo dT, 50 units RNasin, 0.1 μg BSA and 100 units reverse transcriptase. RT–PCR reactions were performed with gene specific primers and products were subject to Southern hybridization using specific probes amplified or subcloned from each gene.

Cloning and sequencing

For complementation a 6-kb genomic fragment encompassing the *AS1* (At2g37630) locus was cloned into the vector pPZP112 (ref. 29) and transformed by *Agrobacterium* into plants. To sequence *as1-1* and *as1-17* alleles genomic DNA from homozygous plants was amplified with the primers ACATTGGAGACACCCAAATGA and CCCTGTTTGGTTT-CCAGAATA, encompassing the coding region of *AS1*. PCR products were sequenced with internal primers, using the dye terminator cycle sequencing (Applied Biosystems). TAIL-PCR[30] was used to determine the sequence disruption in the *magnifica* allele.

Scanning electron microscopy

Fresh material was mounted on silver tape (Electron Microscope Sciences) and viewed with an Hitachi S-3500N SEM using a beam voltage of 5 kV.

In situ hybridization

AS1 RNA was detected with a digoxigenin-labelled riboprobe complementary to part of the *AS1* transcript downstream of the conserved *MYB* domain (C-terminal 124 amino acids) using the method of ref. 21 (http://www.wisc.edu/genetics/CATG/ barton/protocols.html).

Received 4 June; accepted 23 October 2000.

1. Martienssen, R. & Dolan, L. in *Arabidopsis. Annual Plant Reviews* (eds Anderson, M. & Roberts, J.) 262–297 (Sheffield Academic Press, Sheffield, 1998).

2. Hudson, A. Development of symmetry in plants. *Annu. Rev. Plant. Physiol. Mol. Biol.* **51,** 349–370 (2000).
3. Jackson, D., Veit, B. & Hake, S. Expression of maize *KNOTTED1* related homeobox genes in the shoot apical meristem predicts patterns of morphogenesis in the vegetative shoot. *Development* **120,** 405–413 (1994).
4. Barton, M. K. & Poethig, R. S. Formation of the shoot apical meristem in *Arabidopsis thaliana*—an analysis of development in the wild type and in the *shoot meristemless* mutant. *Development* **119,** 823–831 (1993).
5. Clark, S. E., Jacobsen, S. E., Levin, J. Z. & Meyerowitz, E. M. The *CLAVATA* and *SHOOT MERISTEMLESS* loci competitively regulate meristem activity in *Arabidopsis*. *Development* **122,** 1567–1575 (1996).
6. Vollbrecht, E., Reiser, L. & Hake, S. Shoot meristem size is dependent on inbred background and presence of the maize homeobox gene, *knotted1*. *Development* **127,** 3161–3172 (2000).
7. Reiser, L., Sanchez-Baracaldo, P. & Hake, S. Knots in the family tree: evolutionary relationships and functions of *knox* homeobox genes. *Plant Mol. Biol.* **42,** 151–166 (2000).
8. Sinha, N. R., Williams, R. E. & Hake, S. Overexpression of the maize homeo box gene, *KNOTTED-1*, causes a switch from determinate to indeterminate cell fates. *Genes Dev.* **7,** 787–795 (1993).
9. Chuck, G., Lincoln, C. & Hake, S. *Knat1* induces lobed leaves with ectopic meristems when overexpressed in *Arabidopsis*. *Plant Cell* **8,** 1277–1289 (1996).
10. Waites, R., Selvadurai, H. R., Oliver, I. R. & Hudson, A. The *PHANTASTICA* gene encodes a MYB transcription factor involved in growth and dorsoventrality of lateral organs in *Antirrhinum*. *Cell* **93,** 779–789 (1998).
11. Timmermans, M. C., Hudson, A., Becraft, P. W. & Nelson, T. ROUGH SHEATH2: a Myb protein that represses *knox* homeobox genes in maize lateral organ primordia. *Science* **284,** 151–153 (1999).
12. Waites, R. & Hudson, A. *phantastica*: a gene required for dorsoventrality of leaves in *Antirrhinum majus*. *Development* **121,** 2143–2154 (1995).
13. Tsiantis, M., Schneeberger, R., Golz, J. F., Freeling, M. & Langdale, J. A. The maize *rough sheath2* gene and leaf development programs in monocot and dicot plants. *Science* **284,** 154–156 (1999).
14. Schneeberger, R., Tsiantis, M., Freeling, M. & Langdale, J. A. The *rough sheath2* gene negatively regulates homeobox gene expression during maize leaf development. *Development* **125,** 2857–2865 (1998).
15. Reidei, G. P. Non-mendelian megagametogenesis in *Arabidopsis*. *Genetics* **51,** 857–872 (1965).
16. Reinholz, E. *Arabidopsis thaliana* (L.) HEYNH. als Objekt fur genetische und entwicklungsphysiologische Untersuchungen. *Arabidopsis Inform. Service* **01S,** 24 (1965).
17. Long, J. A., Moan, E. I., Medford, J. I. & Barton, M. K. A member of the KNOTTED class of homeodomain proteins encoded by the *STM* gene of *Arabidopsis*. *Nature* **379,** 66–69 (1996).
18. Lincoln, C., Long, J., Yamaguchi, J., Serikawa, K. & Hake, S. A *knotted1*-like homeobox gene in *Arabidopsis* is expressed in the vegetative meristem and dramatically alters leaf morphology when overexpressed in transgenic plants. *Plant Cell* **6,** 1859–1876 (1994).
19. Dockx, J. *et al.* The homeobox gene *ATK1* of *Arabidopsis thaliana* is expressed in the shoot apex of the seedling and in flowers and inflorescence stems of mature plants. *Plant Mol. Biol.* **28,** 723–737 (1995).
20. Lin, X. *et al.* Sequence and analysis of chromosome 2 of the plant *Arabidopsis thaliana*. *Nature* **402,** 761–768 (1999).
21. Long, J. & Barton, M. K. Initiation of axillary and floral meristems in *Arabidopsis*. *Dev. Biol.* **218,** 341–353 (2000).
22. Endrizzi, K., Moussian, B., Haecker, A., Levin, J. Z. & Laux, T. The *SHOOT MERISTEMLESS* gene is required for maintenance of undifferentiated cells in *Arabidopsis* shoot and floral meristems and acts at a different regulatory level than the meristem genes *WUSCHEL* and *ZWILLE*. *Plant J.* **10,** 101–113 (1996).
23. Clark, S. E., Running, M. P. & Meyerowitz, E. M. *CLAVATA3* is a specific regulator of shoot and floral meristem development affecting the same processes as *CLAVATA1*. *Development* **121,** 2057–2067 (1995).
24. Mayer, K. F. *et al.* Role of *WUSCHEL* in regulating stem cell fate in the *Arabidopsis* shoot meristem. *Cell* **95,** 805–815 (1998).
25. Aida, M., Ishida, T. & Tasaka, M. Shoot apical meristem and cotyledon formation during *Arabidopsis* embryogenesis: interaction among the *CUP-SHAPED COTYLEDON* and *SHOOT MERISTEMLESS* genes. *Development* **126,** 1563–1570 (1999).
26. Sundaresan, V. *et al.* Patterns of gene action in plant development revealed by enhancer trap and gene trap transposable elements. *Gene Dev.* **9,** 1797–1810 (1995).
27. Li, J., Nagpal, P., Vitart, V., McMorris, T. C. & Chory, J. A role for brassinosteroids in light-dependent development of *Arabidopsis*. *Science* **272,** 398–401 (1996).
28. Springer, P. S., McCombie, W. R., Sundaresan, V. & Martienssen, R. A. Gene trap tagging of *PROLIFERA*, an essential *MCM2-3-5*-like gene in *Arabidopsis*. *Science* **268,** 877–880 (1995).
29. Hajdukiewicz, P., Svab, Z. & Maliga, P. The small, versatile pPZP family of *Agrobacterium* binary vectors for plant transformation. *Plant Mol. Biol.* **25,** 989–994 (1994).
30. Liu, Y. G., Mitsukawa, N., Oosumi, T. & Whittier, R. F. Efficient isolation and mapping of *Arabidopsis thaliana* T-DNA insert junctions by thermal asymmetric interlaced PCR. *Plant J.* **8,** 457–463 (1995).

Acknowledgements

We thank A. Groover, C. Kidner, E. Vollbrecht, M. Timmermans, J. Golz and D. Jackson for helpful discussions, Q. Gu, P. Springer, J. Li and J. Chory for help with mapping and T. Laux for wus-1 seed. We also thank T. Mulligan for plant care, and K. Schutz and D. McCombie for help with sequencing. This work was supported by a Human Frontiers Science Program postdoctoral fellowship to M.C., a Biotechnology and Biological Sciences Research Council studentship to R.B. and grant support from the National Science Foundation, Department of Energy and United States Department of Agriculture to R.M.

Correspondence and requests for materials should be addressed to R.M. (e-mail: martiens@cshl.org).